

# The vestibular drive for standing balance control is dependent on sensory cues of gravity

By

Anne I. Arntz

in partial fulfilment of the requirements for the degree of

**Master of Science**  
in Biomedical Engineering

at the Delft University of Technology,  
to be defended publicly on Thursday February 22, 2018 at 09:30 AM.

Thesis committee:	Dr. ir. A.C. Schouten,	TU Delft
	ir. M.L. van de Ruit,	TU Delft
	Dr. ir. D.A. Abbink,	TU Delft
	Dr. ir. P.A. Forbes,	Erasmus MC

An electronic version of this thesis is available at <http://repository.tudelft.nl/>.



## Abstract

By monitoring head movement and orientation in space, the vestibular system can evoke appropriate muscle responses in order to maintain standing balance. The present study investigates whether vestibular-evoked muscle responses are dependent on sensory cues of gravity by examining these responses across varying load and gravity conditions. Standing subjects were exposed to a stochastic electrical vestibular stimulus (EVS,  $\pm 5$  mA, 0-25 Hz) that induced a vestibular error signal, while vertical loading forces or vestibular signals of gravity were independently modified. A backboard structure limited subjects' whole-body rotation to the sagittal plane which corresponded with the EVS-evoked sway responses in anteroposterior direction, as the subject's head was rotated in yaw. Vestibular-evoked muscle responses were greatest when sensory cues of gravity matched the expected terrestrial force of gravity, and decreased when these cues were modified. The reduction was largest when both load- and vestibular-related cues of gravity were different from normal. Our results indicate that the vestibular drive for standing balance control is attenuated when sensory cues of gravity are not congruent to normal (i.e. terrestrial) expectations of standing balance and that the degree of attenuation is dependent upon the cumulative incongruity that arises from multiple sensory cues.

*Keywords:* vestibular system, balance control, gravity, electrical vestibular stimulation, vestibular-evoked response

## Introduction

Standing balance requires continuous motor corrections because the downward pull of gravity makes us inherently unstable. The vestibular system plays an important role in this process by continuously monitoring head movement and orientation in space and informing our nervous system to engage the muscles involved in balance. The generation of vestibular-evoked muscle responses occurs unconsciously and is proposed to operate on the principle of re-afference (von Holst and Mittelstaedt, 1950). According to this principle, the nervous system compares a sensory prediction (i.e. internal model) of the balancing motor commands with the actual sensory feedback, such that re-afferent signals (i.e. sensory signals from one's own action) and ex-afferent signals (i.e. sensory signals from external disturbances) can be extracted from the total sensory information. When correlation between the predicted and actual sensory information is highest, re-afferent information is cancelled and vestibular-evoked responses to external disturbances are largest (Héroux et al. 2015). Or in other words, vestibular-evoked responses are suppressed if the motor commands and sensory signals are not congruent; which occurs, for example, when standing subjects balancing in a robotic platform imperceptibly lose control of the platform (Luu et al. 2012). The nervous system is thought to use a model of the standing body's dynamics to predict the re-afference feedback (Héroux et al. 2015; Kuo, 1995; van der Kooij et al. 1999) and presumably, also accounts for a constant signal of gravity since our brain has adapted to living on Earth. Human behavioral and neurophysiological studies have shown that the nervous system possesses an internal representation of gravity to maintain accurate perceptions of self-motion (Laurens et al. 2013), generate appropriate oculomotor-reflexes (Merfeld et al. 1999; Angelaki et al. 2004; Laurens & Angelaki, 2011) and implement control policies during skilled movement (Gaveau et al. 2016). Whether an internal model of gravity also contributes to the re-afferent control of standing balance, however, remains unknown.

The sensory cues that inform the brain about gravity are derived from the somatosensory system, which senses forces (i.e. load) induced by gravity and from the vestibular system's otolith organs, which sense changes in head orientation within a gravitational field. Externally applied changes in body load (i.e. added or deducted weight) modify vestibular-evoked whole-body balance responses (Marsden et al. 2003), suggesting that load-related afferent feedback influences the vestibular drive to the muscles for the control of standing balance. But what would happen if gravity was independently removed such that only otolith-driven signals of gravity were absent? Whether load-related afferent feedback can provide sufficient sensory feedback related to the balance task to maintain a constant vestibular drive for standing balance control across gravity levels is currently unknown. Without gravity-driven otolith signals, the need for balance control would remain as the body is still subjected to a downward pull, and since muscle responses are dependent upon the relevance of their contribution to maintain balance (Forbes et al. 2016), vestibular drive for standing would remain. However, since according to the re-afference principle the sudden absence of gravity-related vestibular signals would create incongruent motor and sensory signals, vestibular-evoked muscle responses would perhaps be absent or diminished.

The aim of the current study is to examine the effect of gravity on the vestibular control of standing by independently varying the load-related afferent and gravity-related vestibular signals of balance. In our first experiment, we investigate whether vestibular-evoked muscle responses are modified under increasing vertical load conditions. By adding load to the subject, load-related afferent information is modified while a constant vestibular signal of gravity is maintained. Our second experiment is performed during parabolic flights to investigate whether vestibular-evoked muscle responses are modified under different gravitational conditions. Here, gravity-related vestibular signals are modified while maintaining a constant vertical load force on the body. By comparing the results of the different experimental conditions, the effects of load cues and gravity-related vestibular cues on the vestibular drive for standing balance control can be evaluated. For both experiments, vestibular-evoked balance responses were induced using electrical vestibular stimulation (EVS) (Nashner & Wolfson, 1974; Britton et al. 1993; Day et al. 1997; Dakin et al. 2007), which modulates the firing rate of vestibular afferents (Goldberg et al. 1984) to produce a craniocentric artificial vestibular error signal of head roll (Fitzpatrick and Day 2004; Peters et al. 2015). If, as we hypothesize, the re-afferent prediction of motor commands is dependent on a representation of gravity, we expect that vestibular-evoked muscle responses are decreased when sensory cues of gravity (i.e. load-related afferent and gravity-related vestibular signals) are modified. Knowing gravity's role in the vestibular control of standing balance will profoundly impact the understanding of the neural processes underlying standing balance and may help us understand and treat vestibular diseases and dysfunctionalities.

## Methods

### Participants

Twenty-one healthy subjects (*Experiment 1*: 16 subjects, mean age =  $24 \pm 4.2$  years, 10 men; *Experiment 2*: 6 subjects, mean age =  $38 \pm 8.3$  years, 5 men) with no known history of neurological disease or injury participated in this study. Subjects that participated in Experiment 2 completed both a training session under normal gravity conditions (*Experiment 2A*) and a flight session under variable gravity conditions (*Experiment 2B*) in the airplane. One subject participated in both experiments. Experiment 1 was approved

by the Erasmus Medical Center's Medical Review Ethics Committee and Experiment 2 by the University of Caen's Ethics Committee. The experiments were conducted in accordance with the Declaration of Helsinki. All subjects gave their written informed consent prior to participation.

### **Vestibular stimulation**

Stochastic EVS was delivered to the subjects in a bilateral bipolar electrode configuration via carbon rubber electrodes ( $\sim 15 \text{ cm}^2$ ). The electrodes were coated with Spectra360 electrode gel (Parker Laboratories, Fairfield, NJ) and secured over the mastoid processes with tape and an elastic headband. The skin over the mastoid processes was anaesthetized with Pliaglis cream [lidocaine and tetracaine] (Galderma, Lausanne, CH) to minimize non-vestibular cues related to the stimulus, e.g. cutaneous feeling under the electrodes. The stimuli were generated on a laptop with custom MatLab software (MathWorks, Natick, MA) and were sent to an isolated bipolar current stimulator (DS5; Digitimer, Hertfordshire, UK) via a data acquisition board (USB-6259; National Instruments, Austin, TX).

For both experiments, the electrical stimuli were designed as bandwidth limited stochastic signals (0-25 Hz, zero-mean low-pass filtered white noise, 25 Hz cutoff, zero lag, third-order Butterworth) with a peak amplitude of 5 mA (root mean square [RMS] 1.7 mA). In each experiment, the exact same stimulus was used for all trials. In Experiment 2, the stimulus lasted 20 seconds to fit within the different gravitational phases of the parabola (see *Experimental protocol; Experiment 2*). During the parabolic flights (i.e. Experiment 2B), the onset of the stimulation was automatically triggered by acceleration along the z-axis of the plane (i.e. g-level) in order to fit within each gravitational phase. During the micro-g phase, the stimulus was triggered when z-acceleration fell below 0.2 g, and during the hyper-g phase when z-acceleration exceeded 1.5 g. In the normal-g phase, stimulation was started 20 seconds after the second hyper-g phase of the parabola ended, i.e. when z-acceleration fell below 1.2 g. Offline examination of acceleration data assured that the 20 second stimulus occurred within the specific gravity phase for all trials. In Experiment 1, the stimulus was extended to 40 seconds in order to limit the overall time that subjects spent in loaded conditions (see *Experimental protocol; Experiment 1*) so as to avoid fatigue. In order to collect the same total amount of data across our two experiments, the number of trials for each condition in Experiment 1 was halved relative to Experiment 2.

### **Experimental set-up**

Two separate experiments were performed to study the effects of load and gravitational vestibular cues on the vestibular-evoked muscle responses. Experiment 1 assessed the influence of load cues on vestibular-evoked muscle responses under a constant gravitational load of 1 g. Experiment 2 assessed whether the presence and strength of a gravitational field influences the vestibular-evoked muscle responses. For both experiments, subjects maintained upright balance while being exposed to a stochastic EVS signal. Subjects stood barefoot on a force plate (BP400600HF; AMTI, Watertown, MA) with their feet 5 cm apart and their body secured to a backboard structure positioned immediately behind them (Fig. 1). The weight of the backboard structure was 10 kg with the center of mass at a height of  $\sim 0.7 \text{ m}$ . The backboard structure was supported by two bearings, such that the mass of the backboard only increased the subjects' inertia slightly ( $\sim 6.5 \%$ ). The backboard's axis of rotation passed through the approximate location of the ankle joints and limited whole-body sway to the sagittal plane only. This pivoting direction corresponds with the direction of EVS-evoked whole-body sway responses when the head is turned over

the shoulder (Lund and Broberg, 1983; Britton et al. 1993; Fitzpatrick et al. 1994). Angular limits of  $10^\circ$  anterior and  $6^\circ$  posterior from vertical prevented the subjects from falling forward or backward, respectively. Seatbelts across the chest and waist secured the subjects to the backboard. A laser distance sensor (optoNCDT-1401; Micro-Epsilon, Orteburg, DE) attached to the backboard was used to record whole-body sway angle.

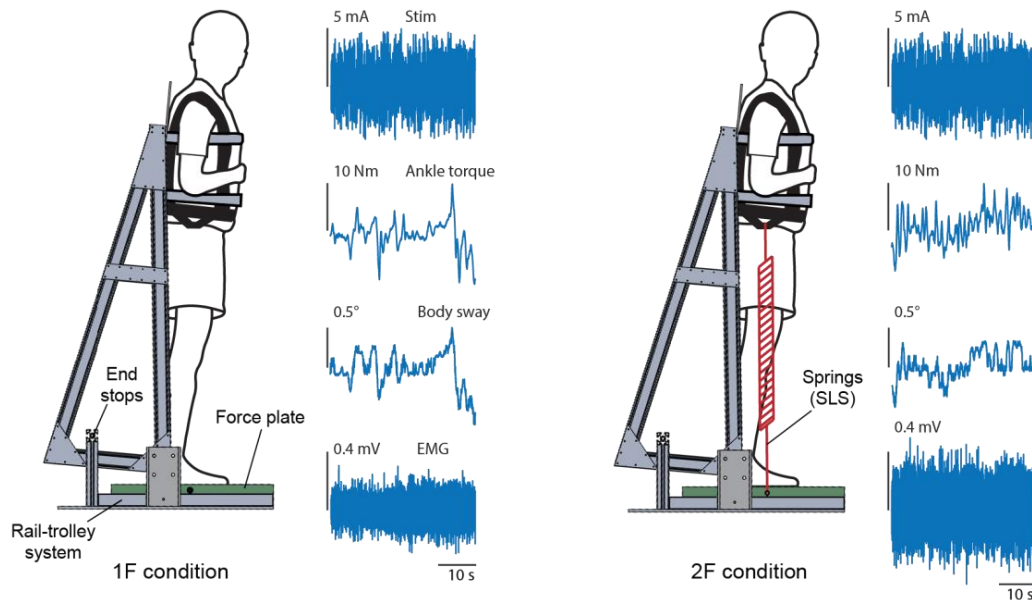


**Figure 1. Experimental setup.** The subject stood on a force plate and was strapped to a backboard setup that rotated in the sagittal plane about an axis that passed through the subject's ankles. End stops functioned as angular limits to prevent the subject-backboard system from falling forward or backward. The subject stayed upright in the slightly forward whole-body sway angle with normal 1 g body load or with added load. Raw data of the vestibular stimulus, ankle torque, whole-body sway angle and EMG activity of the right gastrocnemius are shown during a trial of Experiment 1 in the 1F (left), and in the 2F condition (right).

*Subject loading system.* To control vertical loading forces under varying gravitational levels (see *Experiment 1* and *Experiment 2*), subjects wore a subject loading system (SLS) that could provide additional vertical load. The SLS consisted of a body-harness (German Aerospace Center (DLR), Cologne, DE) and four springs. The body-harness was secured over the subject's shoulders and tightened at the waist. The springs were attached to the sides of the body-harness using straps located at the height of the hips (i.e. at the subject's approximate center of mass) and to a low-friction rail-trolley system secured to the floor. This rail-trolley system ensured that ground attachment of the springs moved with the center of mass of the subject such that the springs were always pulling vertically downwards. This way, the intrinsic dynamics of the subject (i.e. load-stiffness relationship, see *Appendix A*) would match conditions appropriate for each load and gravitational level. (More details of the body's dynamics with added load and the influence of a fixed/mobile spring attachment point are provided in *Appendix A*.)

### Experimental protocol

Prior to each experiment, a target whole-body sway angle was defined for each subject. This position was 3 degrees forward from their subjective zero angle, i.e. the position in which they could stand upright with minimal effort. For each trial, subjects were instructed to stand upright, lean forward to their target angle, cross their arms over their chest, and rotate their head axially to the left (i.e. leftward yaw). The head was

also rotated in extension such that the Reid plane was tilted up by 18° horizontally. This head position maximizes the postural responses to binaural bipolar EVS in the anterior-posterior direction (Cathers et al. 2005; Fitzpatrick and Day, 2004) along the line of action of the right gastrocnemius and soleus muscles. To guide the subjects to their appropriate body position before each trial, they were given a subject-specific visual target that was placed on the wall to their left. In Experiment 1, a laser pointer was attached to the subject's head and was used to align the head in the desired position. In Experiment 2, the subject was instructed to align their head visually by looking at a target placed ~1.5 m away on the aircraft wall. For safety reasons a head mounted laser could not be used in the aircraft. Just before the EVS was started, subjects closed their eyes. During each trial, verbal feedback was given to the subject about the whole-body sway angle and head position to help them maintain a similar position over all trials. (More details of the experimental set-up and protocol can be found in Appendix B.)

*Experiment 1.* Experiment 1 assessed three different load conditions to examine the influence of load cues on the vestibular control of balance. Subjects stood with cumulative load forces through the feet equivalent to 1, 1.5 and 2 times their own body weight (conditions 1F, 1.5F and 2F, respectively) by progressively increasing the tension in the springs of the SLS. Just before starting a trial, the subject was instructed to lean forward to their offset angle, point the laser to the mark and close their eyes (Fig. 1). For each condition (1F, 1.5F and 2F), subjects completed four 40-second trials, for a total of twelve trials per subject. The order of trial condition was randomized for each subject. This experiment was performed in the Department of Neuroscience at Erasmus Medical Center. The results from Experiment 1 were also used as a qualitative baseline dataset to check whether the smaller sample group of Experiment 2 showed similar trends.

*Experiment 2.* Experiment 2 was performed by six subjects during the 68th ESA Parabolic Flight Campaign in a modified A310 Zero-G airplane (Novespace, Mérignac, FR) and consisted of a training session (Experiment 2A) and a flight session (Experiment 2B). The training session was completed on-ground in the aircraft one day prior to each subject's participation in a parabolic flight (i.e. Experiment 2B; the flight session). The training session familiarized the subjects with the experimental protocol and provided baseline data for qualitative comparison to Experiment 1 and Experiment 2B. The experiment was performed for two different loading conditions – 1F and 2F – following a similar protocol as described for Experiment 1. A 20-second EVS stimulus was used to match the conditions used in Experiment 2B, resulting in eight trials for each loading condition per subject. The order of trial condition (1F and 2F loading) was randomized for each subject. For Experiment 2B, the A310 Zero-G airplane (Novespace, Mérignac, FR) carried out parabolic flight maneuvers (Fig. 2A) that produced periods of weightlessness (i.e. microgravity or 0 g) and increased gravity (i.e. hypergravity or 1.8 g) which modified gravity-related vestibular signals. Each parabola started with a pull-up and ended with a pull-out (hyper-g phases). The duration of the micro-g and hyper-g phases was about 21 seconds. Between each parabola the plane was in steady-flight (i.e. normal-g or 1 g) for approximately 100 seconds. The air pressure in the cabin was maintained at ~800 millibar during the parabolas, which corresponds to an altitude of about 2,000 meters. The temperature was controlled to be between 20°C and 25°C. Subjects participated in the experiment for 15 parabolic maneuvers and assessed four different trial conditions: 0G-1F, 1G-1F, 1.8G-1.8F and 1G-2F (Fig. 2B).

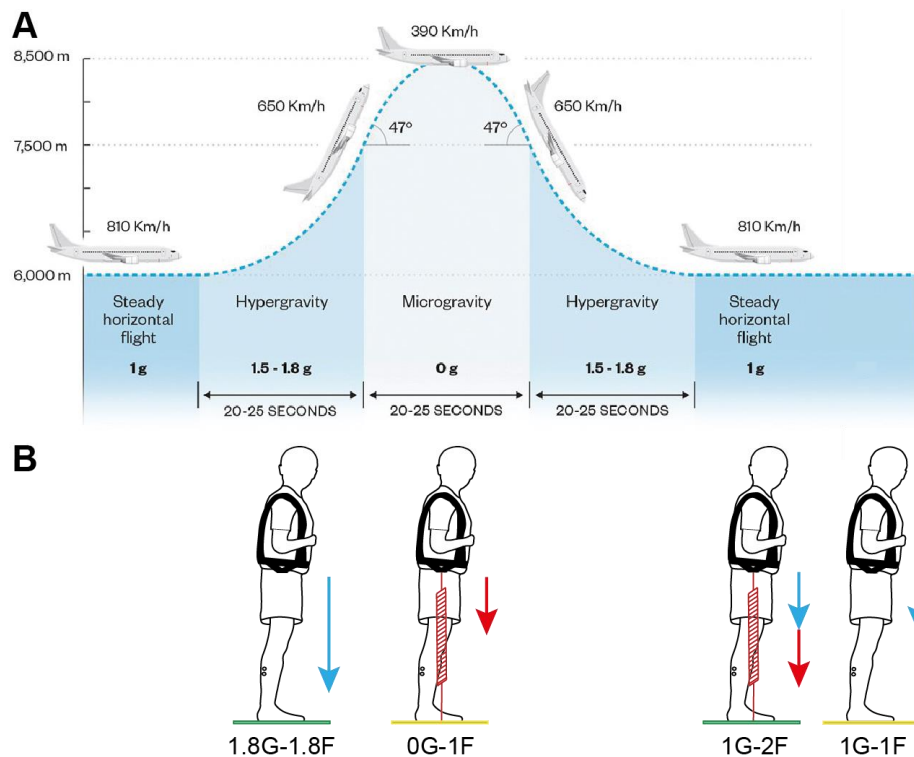


**Figure 2. Protocol of Experiment 2B. A)** Parabolic flight manoeuvre. Each parabola starts with a hyper-g phase that is followed by a micro-g phase and ends with a second hyper-g phase. In between each parabola, there is a flight break (i.e. steady flight) of approximately 100 sec. Source: Laboratory for Space and Microgravity Research Graphics: 5W Infographics; **B)** The four trial conditions that correspond with the phases of the parabolic manoeuvre shown in A. Blue arrows represent the load induced by gravity, red arrows represent the load induced by the subject loading system. Statistical comparisons were made between the results of the 0G-1F and 1G-1F conditions (yellow) and between the results of the 1.8G-1.8F and 1G-2F conditions (green).

During seven parabolas, subjects performed the 1G-1F and 1.8G-1.8F trials without additional spring loading in the normal-g and hyper-g phases, respectively. For measurements during hyper-g, only the first hyper-g phase (i.e. pull-up) was used. This phase generally reaches higher g-forces and has a more consistent gravity level compared to the second hyper-g phase (i.e. pull-out). During the remaining eight parabolas, subjects were spring loaded to perform the 0G-1F and 1G-2F trials in the micro-g and normal-g phase, respectively (Fig. 2B). The SLS load was set per subject to exert a force equal to their own weight, i.e. during the 0G-1F trials, the load on the subject's feet was equal to the load during 1G-1F trials, and during the 1G-2F trials, it was approximately equal to the load during 1.8G-1.8F trials. Due to the design of the SLS and strict timing of consecutive phases of the parabolic maneuvers, the SLS could not be reset in between phases to match both 1.8F loading in a steady flight phase (i.e. 1G-1.8F) and 1F loading in the micro-g phase (i.e. 0G-1F) to provide two comparisons in which load was equal while gravity differed. The current conditions enabled comparisons of the vestibular-evoked responses between 0G-1F and 1G-1F trials and between 1.8G-1.8F and 1G-2F trials. Within each comparison, load-related afferent cues were approximately equal while gravity-related vestibular cues varied, and will indicate whether gravity-driven otolith signals are relevant for the vestibular control of balance.

During Experiment 2B, unexpected plane accelerations due to turbulence caused some subjects to fall into the backboard end stops in the middle of a trial. When this occurred, the trial was removed from

further analysis. In addition, two subjects experienced motion sickness during the flight and skipped 1-3 parabolas. Despite this, all subjects performed a minimum of four trials (i.e. 80 seconds) per condition without falling into the end stops, which were used for further analysis. For subjects who performed more than four good trials, the four trials with the lowest mean variability of whole-body sway angle per condition were used.

### **Data recordings**

In all experiments, surface EMG was collected from the medial gastrocnemius (Gas) and soleus (Sol) muscles in the right leg using self-adhesive Ag-AgCl surface electrodes (BlueSensor M; Ambu®, Copenhagen, DK). The electrodes were placed on the skin along the length of the gastrocnemius and soleus muscles with an inter-electrode distance of 18 mm. The skin of the subject's right leg was shaved and cleaned with skin preparation gel (NuPrep; Weaver and Company, Aurora, CO) and alcohol (MediSwab; BSN Medical, Hamburg, DE) before the electrodes were secured. EMG was digitized at 2000 Hz (Porti7; TMSi, Oldenzaal, NL). Acceleration of the plane was measured with a 3-axis accelerometer (3D Accelerometer; TMSi, Oldenzaal, NL) and also digitized at 2000 Hz (Porti7; TMSi, Oldenzaal, NL). Vestibular stimuli, signals from the force plate and laser sensor data were digitized at 2000 Hz and recorded via a data acquisition board (USB-6259; National Instruments) using a custom MatLab script (MathWorks, Natick, MA). The two recording systems had separate internal clocks and received a trigger signal at the onset of the vestibular stimulus to facilitate synchronization of data.

### **Signal analysis**

Digitized EMG was high pass filtered offline using a non-causal sixth order Butterworth filter with a cut-off frequency of 30 Hz. EMG signals for each trial were time-locked to EVS onset using the shared trigger signal and full-wave rectified. Data was concatenated per condition per subject, producing a single data array for a subject's responses for each condition. Coherence and cumulant density functions were calculated for each subject with data from each condition to evaluate the correlation between the controlled electrical stimulus input and the rectified EMG of the two muscles (Dakin et al. 2014). Data from both experiments was cut into 1 second segments, yielding a frequency resolution of 1 Hz, before computing the auto-spectra and cross-spectrum for the EVS and EMG data. Coherence was defined as significant when exceeding the 95% confidence limit, as derived from the number of disjoint segments (Halliday et al. 1995). Cumulant density functions were estimated to provide a time domain measure of the relationship (i.e. cross-covariance) between the stochastic signal and the muscle responses and were used to assess the magnitude of the vestibular-evoked muscle response. Cumulant densities were calculated by taking the inverse Fourier transform of the cross-spectra (Halliday et al. 1995). To account for differences in EMG level between conditions, the cumulant density responses were normalized (between -1 and +1) by the product of the vector norms of the EVS input signal and EMG output signal (Dakin et al. 2010). After normalization, the magnitude of the evoked responses represents the relative correlation between the input and output signals rather than an absolute correlation. The cumulant density functions between EVS and the two recorded muscles exhibit a typical biphasic pattern, showing a short (50-70 ms) and a medium (100-120 ms) latency peak with opposing directions (Nashner and Wolfson, 1974; Britton et al. 1993; Fitzpatrick et al. 1994; Fitzpatrick and Day, 2004; Dakin et al. 2007; Dakin et al. 2011). For comparison across conditions, the peak-to-peak amplitude of the cumulant density

was extracted from each subject's response. When one of the peaks did not exceed the 95% confidence interval (Halliday et al. 1995), that peak was considered absent and set to zero, while the other peak's amplitude was still used in the analysis. Data was then averaged across all subjects to provide group data.

Changes in body load are known to modify the rate of vestibular-evoked reaction force development (Marsden et al, 2003). Therefore, we extracted the timing of the peaks, since an earlier peak would similarly indicate a more rapid development of a vestibular-evoked response. Timing was extracted from subjects' individual data for each condition and then averaged across all subjects.

### **Statistics**

To test the hypothesis that vestibular-evoked muscle responses will decrease when sensory cues of gravity are different from normal, peak-to-peak amplitudes of the cumulant density responses were compared between the various experimental conditions. For Experiment 1, the responses for the 1.5F and 2F conditions were compared to the 1F responses to evaluate the effect of load cues. The 1F and 2F responses of Experiment 2A were compared to these responses of Experiment 1 to identify whether the small sample group followed the same trends. To evaluate the effect of vestibular cues of gravity on vestibular-evoked responses in Experiment 2B, the responses for the 0G-1F condition were compared to the 1G-1F responses, and the 1.8G-1.8F responses to the 1G-2F responses. Preliminary analysis of the peak-to-peak amplitudes showed that the data was non-normally distributed, therefore significant changes between the responses of the various conditions were identified using the Wilcoxon Sign-Rank Test with a significance level of  $p < 0.05$  (SPSS, version 22, Chicago, IL). Finally, to examine any changes in general balance behavior across conditions, RMS muscle activity, vertical loading forces, estimated ankle torque, and whole-body sway angle (mean and mean-removed RMS) were compared. Note, mean whole-body sway angle was measured relative to each subject's subjective vertical. Preliminary analyses of these measures showed that the data was normally distributed, therefore the effect of load and gravity on these measures was identified using a repeated-measures general linear model (Experiment 1, three dependent groups, with load as factor) or a paired-samples t-test (Experiment 2, two dependent groups). If necessary, a Greenhouse-Geisser correction was used to deal with violations of sphericity. We expected that muscle activity and ankle torque would increase with load, while whole-body sway (mean and mean-removed RMS) would remain constant. Throughout this study, we reported means and standard deviations (SD) for normal data and medians and interquartile ranges (IQR) for non-normal data.

The effect of load and gravity on the timing of the peaks was analyzed using a repeated-measures general linear model when data was normally distributed (i.e. Experiment 1). If necessary, a Greenhouse-Geisser correction was used to deal with violations of sphericity. For non-normal data (i.e. Experiment 2) the Friedman Test was used.

## **Results**

### **Effect of load cues on vestibular-evoked muscle responses (Experiments 1 and 2A)**

During Experiments 1 and 2A, all subjects were able to balance themselves in all loading conditions without difficulty. Similarly, all subjects were able to stand slightly forward to their target angle in all loading conditions (Table 1). For Experiment 1, as expected, mean whole-body sway angle was not

affected by loading conditions ( $F_{(1.37,20.59)}=0.411$ ,  $p=0.592$ ). The increased vertical load during the 1.5F and 2F conditions influenced the mean-removed RMS whole-body sway (i.e. amount of sway) ( $F_{(2,30)}=7.650$ ,  $p=0.002$ ) and was, as expected, accompanied by increased gastrocnemius (84.4 and 128.6 %, respectively) and soleus (44.6 and 73.6 %, respectively) muscle activity (*Gas*:  $F_{(2,30)}=77.327$ ,  $p=0.000$ ; *Sol*:  $F_{(2,30)}=69.083$ ,  $p=0.000$ ) and ankle torque (86.9 and 142.0 %, respectively;  $F_{(1.21,18.08)}=156.074$ ,  $p=0.000$ ). Average vertical loading forces in the 1.5F and 2F conditions were equivalent to 145.9 and 187.3 % of the subjects' body load, respectively (Table 1).

For all subjects and in all conditions, EVS evoked significant muscle responses. Coherence and cumulant density estimates from all subjects are plotted together with the group mean for all loading conditions in Figure 3. For both muscles and for all conditions, the coherence showed significant EVS-EMG coupling at frequencies up to about 20 Hz. Similarly, EVS evoked cumulant density estimates with short and medium latency peaks exceeding the 95% confidence interval for all subjects. Vestibular-evoked muscle responses (coherence and cumulant density) were largest for the 1F condition and decreased by ~27-33 % in both muscles when load was increased to 1.5F (*Gas*:  $Z=-3.516$ ,  $p=0.000$ ; *Sol*:  $Z=-3.361$ ,  $p=0.001$ ) and by ~23-38 % when load was increased to 2F (*Gas*:  $Z=-3.309$ ,  $p=0.001$ ; *Sol*:  $Z=-3.154$ ,  $p=0.002$ ) relative to the 1F condition. Although vertical loading, muscle activity and ankle torque progressively increased with 2F, we saw no further decrease in the vestibular-evoked muscle response (Fig. 4).

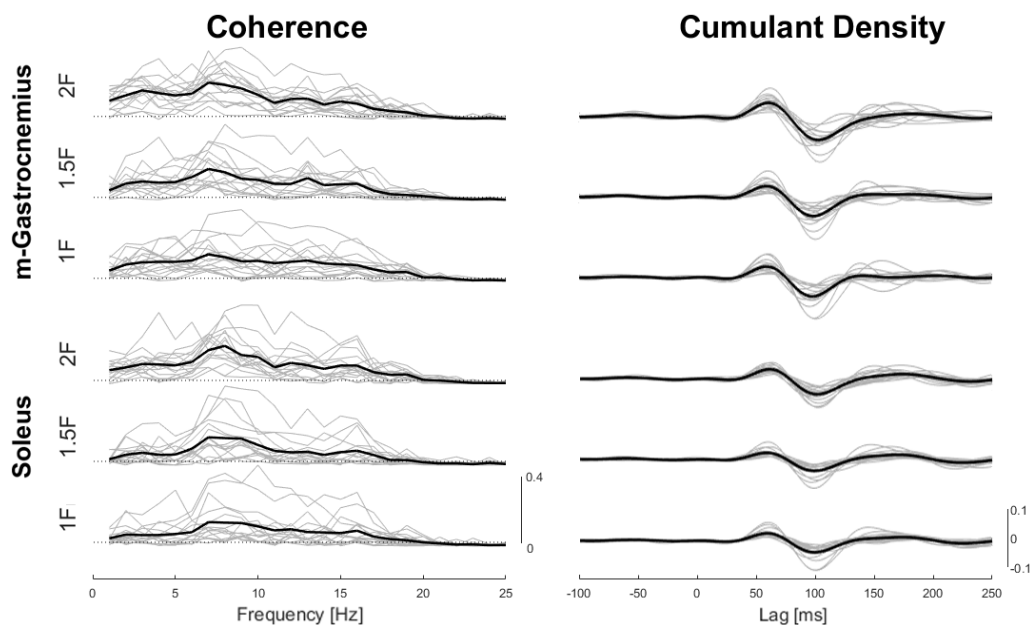


**Figure 3. Individual and group mean ( $n=16$ ) EVS-EMG coherence and cumulant density responses to electrical vestibular stimulation for the three load conditions of Experiment 1.** Dark bold lines are the group mean, grey thin lines are responses from the individual subject. For coherence, the 95% confidence limit is represented by the dotted line.

Timing of the short and medium latency cumulant density peaks were advanced in both muscles with additional load. During the 1.5F and 2F conditions, the short latency peaks occurred ~1.7-2.3 ms and ~1.4-2.4 ms earlier, respectively (*Gas*:  $F_{(2,30)}=11.244$ ,  $p=0.000$ ; *Sol*:  $F_{(2,30)}=18.056$ ,  $p=0.000$ ) while the medium latency peaks occurred ~2.5-4.6 ms and ~2.0-4.9 ms earlier, respectively (*Gas*:  $F_{(2,30)}=48.408$ ,  $p=0.000$ ; *Sol*:  $F_{(1.47,22.01)}=4.737$ ,  $p=0.028$ ), all relative to the normal 1F loading condition. A post hoc paired-samples t-

test showed no differences between the peak timings of the 1.5F and 2F conditions (*Gas*:  $t_{(15)}=-0.747$ ,  $p=0.466$ ;  $t_{(15)}=0.454$ ,  $p=0.656$ ; *Sol*:  $t_{(15)}=0.187$ ,  $p=0.855$ ;  $t_{(15)}=-0.486$ ,  $p=0.634$ , short and medium latency peaks respectively).

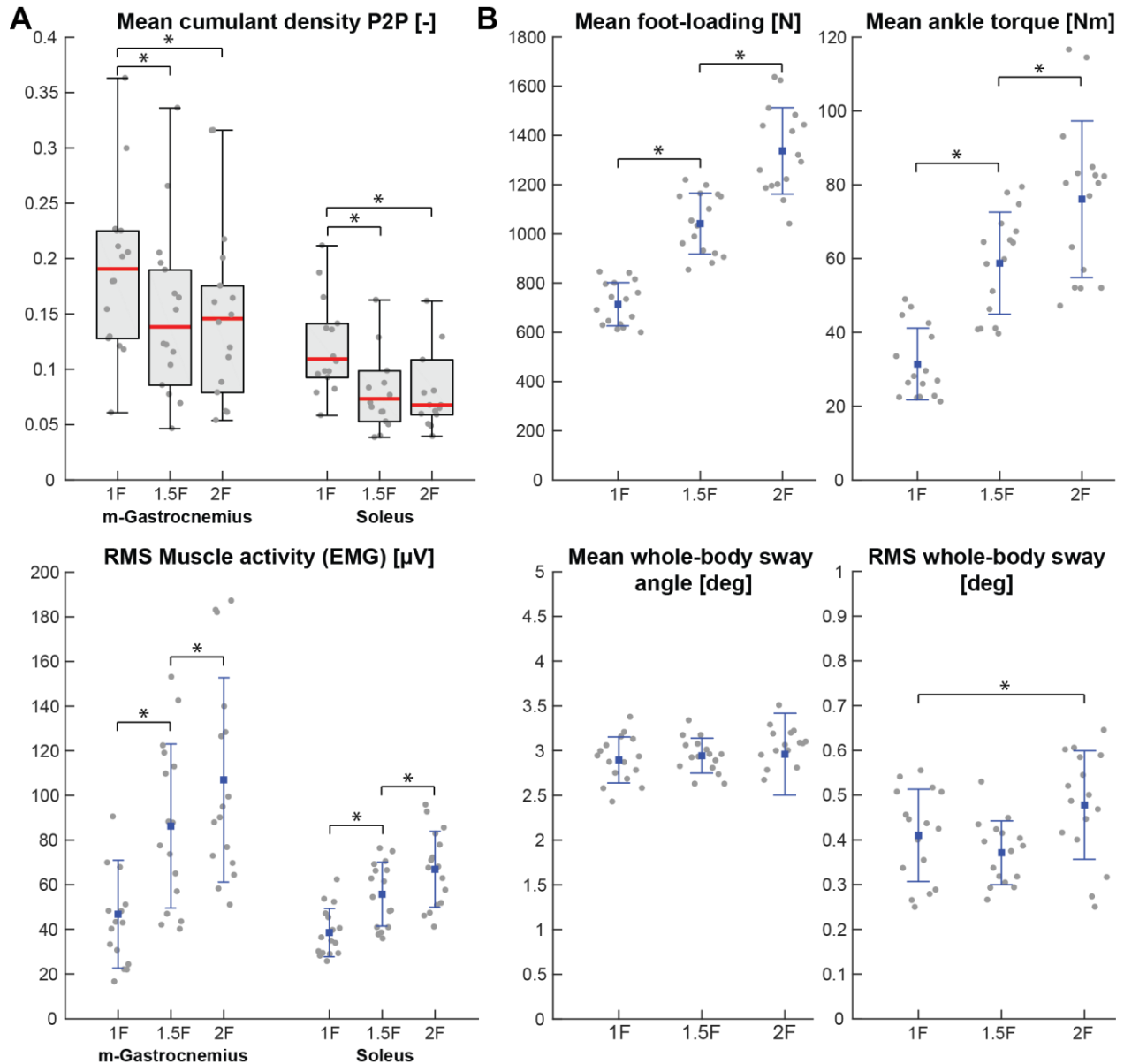


**Figure 4. Individual and group average ( $n=16$ ) data of Experiment 1. A)** Muscle-related outcome measures. Peak-to-peak (P2P) amplitudes of the cumulant density responses (top) and RMS of muscle activity (EMG) (bottom); **B)** Outcome measures of general balance behaviour including vertical loading forces, ankle torque and whole-body sway angle (mean and RMS). Individual subjects are plotted as grey dots. Group responses for normally distributed data were plotted with a mean (blue dots) and standard deviation (blue whiskers), while non-normally distributed data were plotted with a median (red line), 25 and 75 percentiles (grey box) and extreme data points (grey whiskers). Asterisks indicate significant differences between conditions.

Table 1. Group averaged absolute values of the measures of vestibular-evoked responses and general balance behaviour. For non-normally distributed data, median and interquartile range (IQR) are given while for normally distributed data mean and standard deviation (SD) are given. P2P = peak-to-peak, Gas = gastrocnemius muscle, Sol = soleus muscle.

		P2P amplitude		RMS EMG		Foot-loading (N)	Ankle torque (Nm)	Sway angle (°)	RMS angle (°)
		Gas	Sol	Gas	Sol				
		median ± IQR	median ± IQR	mean ± SD	mean ± SD				
Exp 1	1F	0,1906 ± 0,0972	0,1092 ± 0,0487	46,79 ± 24,16	38,54 ± 10,82	713,8 ± 87,8	31,44 ± 9,71	2,90 ± 0,26	0,41 ± 0,10
	1.5F	0,1383 ± 0,1042	0,0732 ± 0,0458	86,28 ± 36,78	55,74 ± 14,31	1041,7 ± 123,4	58,77 ± 13,82	2,94 ± 0,2	0,37 ± 0,07
	2F	0,1458 ± 0,0964	0,0676 ± 0,0497	106,97 ± 45,78	66,90 ± 17,01	1337,3 ± 175,6	76,08 ± 21,22	2,96 ± 0,46	0,48 ± 0,12
Exp 2A	1F	0,1636 ± 0,0835	0,1044 ± 0,0867	53,33 ± 23,09	40,27 ± 15,31	817,3 ± 117,6	40,06 ± 13,69	2,96 ± 0,09	0,58 ± 0,19
	2F	0,1319 ± 0,0893	0,0605 ± 0,0833	89,64 ± 31,31	69,11 ± 19,18	1517,2 ± 243	85,96 ± 24,78	3,05 ± 0,05	0,47 ± 0,14
Exp 2B	0G-1F	0,1176 ± 0,0460	0,0942 ± 0,0603	39,79 ± 28,28	43,57 ± 12,56	647,4 ± 165,5	36,91 ± 16,51	2,73 ± 0,99	1,28 ± 0,57
	1G-1F	0,1670 ± 0,1247	0,1216 ± 0,0951	64,85 ± 31,09	50,17 ± 9,86	795,3 ± 101,1	51,96 ± 18,07	2,07 ± 0,62	1,18 ± 0,81
	1.8G-1.8F	0,1150 ± 0,0743	0,1093 ± 0,0466	118,28 ± 34,99	98,87 ± 16,94	1325,4 ± 179,1	85,01 ± 17,29	-2,00 ± 0,67	3,08 ± 0,92
	1G-2F	0,1626 ± 0,0623	0,0928 ± 0,0371	92,91 ± 37,28	72,26 ± 12,66	1404,7 ± 259,3	85,21 ± 30,15	2,19 ± 0,46	0,70 ± 0,41

The six subjects who participated in the in-flight experiment showed similar balancing behavior during Experiment 2A (i.e. on-ground training) as subjects from Experiment 1, except for mean-removed RMS whole-body sway. Contrary to the results of Experiment 1, additional load for the 2F condition did not affect this measure ( $t_{(5)}=1.394$ ,  $p=0.222$ ) for the six subjects of Experiment 2. The additional load during 2F trials had no effect on mean whole-body sway angle ( $t_{(5)}=2.167$ ,  $p=0.082$ ), and showed the expected increase in muscle activity (Gas: 89.6 %,  $t_{(5)}=-4.573$ ,  $p=0.006$ ; Sol: 71.6 %,  $t_{(5)}=-11.452$ ,  $p=0.000$ ) and ankle torque (114.6 %,  $t_{(5)}=-8.368$ ,  $p=0.000$ ), similarly to Experiment 1. Vertical load force in the 2F condition was equivalent to 185.6 % of the subjects' body load (Table 1).

Significant muscle responses were also evoked in these six subjects by the EVS stimulus in both the 1F and 2F conditions. During the 2F load, the average peak-to-peak amplitude decreased by 19.4 % in the gastrocnemius muscle ( $Z=-2.201$ ,  $p=0.028$ ) and by 42.0 % in the soleus muscle ( $Z=-2.201$ ,  $p=0.028$ ) relative to the 1F peak-to-peak response (Fig 5, Table 1). Changes in peak latency timing also followed the trends of Experiment 1. With 2F loading, the short latency peak occurred  $\sim 1.3$ -2.5 ms earlier (Gas:  $t_{(5)}=3.658$ ,  $p=0.015$ ; Sol:  $t_{(5)}=1.263$ ,  $p=0.262$ ) and the medium latency peak occurred  $\sim 6.4$ -7.5 ms earlier (Gas:  $t_{(5)}=4.688$ ,  $p=0.005$ ; Sol:  $t_{(5)}=4.728$ ,  $p=0.005$ ), relative to the 1F condition.

Overall, the results of Experiments 1 and 2A indicate that vestibular-evoked muscle responses are largest in a normal 1 g environment, where load and vestibular cues of gravity are matched. Furthermore, vestibular-evoked muscle responses occur sooner with added load.

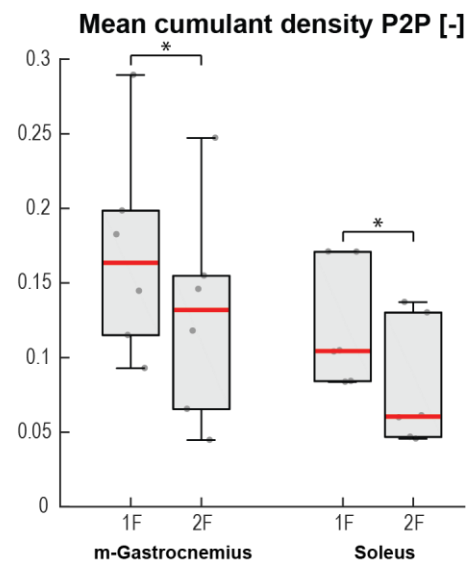


Figure 5. Individual and group average ( $n=6$ ) peak-to-peak amplitude of the cumulant density response of Experiment 2A. Peak-to-peak (P2P) amplitudes of the cumulant density responses are shown for both loading conditions. Individual subjects are plotted as grey dots. The median is represented by the red line and the 25 and 75 percentiles by the boxes. Extreme data points are indicated by the whiskers. Asterisks indicate significant differences

### Effect of gravity-related vestibular cues on vestibular-evoked muscle responses (Experiment 2B)

The increased difficulty to balance experienced by subjects during in-flight experiments compared to on-ground experiments was reflected in the high mean-removed RMS whole-body sway angle as well as the high variability in whole-body sway angle (mean and RMS) (Table 1). Despite the higher mean-removed RMS whole-body sway and variability, in-flight data of general balance behaviour showed similar trends for the effect of load (i.e. 1G-1F and 1G-2F comparison) as in Experiment 2A. However, for the 1G-1F condition in-flight, EVS did not evoke a short latency peak in the gastrocnemius' response for two subjects and in the soleus' response for 1 subject while in Experiment 2A it did. Consequently, the 1G-2F gastrocnemius' response only reduced by 2.6 % relative to the 1G-1F condition ( $Z=-1.153$ ,  $p=0.249$ ). The soleus' response followed the trend seen in Experiment 2A as the 1G-2F response reduced by 23.7 % relative to the 1G-1F condition ( $Z=-1.782$ ,  $p=0.075$ ), however, the change was not significant.

*Comparison 0G-1F/1G-1F condition.* During the micro-g phase of the parabola (i.e. 0G-1F condition), all subjects could balance without difficulty. Undesirably, load forces differed significantly between the 0G-1F and 1G-1F conditions (18.6 % difference;  $t_{(5)}=-3.575$ ,  $p=0.016$ ), as did mean whole-body sway angle (31.9 % difference;  $t_{(5)}=-2.884$ ,  $p=0.034$ ), gastrocnemius muscle activity (38.6 % difference;  $t_{(5)}=-4.931$ ,  $p=0.004$ ; *Sol*: 13.2 % difference;  $t_{(5)}=-1.558$ ,  $p=0.180$ ), and ankle torque (29.0 % difference;  $t_{(5)}=-4.458$ ,  $p=0.007$ ). Mean-removed RMS whole-body sway angle (i.e. amount of sway) did not statistically differ between conditions ( $t_{(5)}=0.279$ ,  $p=0.791$ ; 8.5 % difference) (Table 1, Fig. 6). Without the presence of gravity (i.e. 0G-1F condition), EVS evoked significant muscle responses in all subjects, except for one subject's short latency peak of the cumulant density response. Coherence showed reduced EVS-EMG coupling compared to the 1G-1F condition and similarly, cumulant density responses were decreased by ~22-30 % (*Gas*:  $Z=-1.992$ ,  $p=0.046$ ; *Sol*:  $Z=-1.782$ ,  $p=0.75$ ). Timing of the short and medium latency peaks was not different for both the gastrocnemius ( $Z=-0.535$ ,  $p=0.593$ ;  $Z=-0.135$ ,  $p=0.892$ , respectively) and soleus muscle ( $Z=-0.184$ ,  $p=0.854$ ;  $Z=-0.674$ ,  $p=0.500$ , respectively).

*Comparison 1.8G-1.8F/1G-2F condition.* During each parabola's hyper-g phase (i.e. 1.8G-1.8F condition), an unexpected longitudinal acceleration of the airplane pushed the subjects forward, making it difficult to maintain the desired whole-body sway angle without falling into the end stops. Consequently, the subjects were told to stand leaning forward at an angle without falling forward, in order to engage the muscles in an active balance task. As desired, load forces between the 1.8G-1.8F and 1G-2F conditions were statistically equal (5.6 % difference;  $t_{(5)}=-1.636$ ,  $p=0.163$ ), as was ankle torque (0.2 % difference;  $t_{(5)}=-0.017$ ,  $p=0.987$ ) (Table 1, Fig. 6). However, the other measures of general balance behavior differed significantly between the two conditions, i.e. mean whole-body sway angle (191 % difference;  $t_{(5)}=11.466$ ,  $p=0.000$ ), mean-removed RMS whole-body sway angle (340 % difference;  $t_{(5)}=7.752$ ,  $p=0.001$ ) and muscle activity (*Gas*: 21.4 % difference;  $t_{(5)}=5.484$ ,  $p=0.003$ ; *Sol*: 26.9 % difference;  $t_{(5)}=4.917$ ,  $p=0.004$ ), probably because of the plane accelerations during the hyper-g phase. EVS induced vestibular-evoked muscle responses in all subjects, however, for two subjects and for both muscles, the short latency peak did not exceed the 95% confidence limit. For the gastrocnemius muscle, coherence and cumulant density showed reduced responses for the 1.8G-1.8F condition compared to the 1G-2F condition (29.3 %;  $Z=-2.201$ ,  $p=0.028$ ), but for the soleus muscle an increase was observed (15.1 %;  $Z=-0.105$ ,  $p=0.917$ ). Timing of the short and medium latency peaks showed no change between conditions for both the gastrocnemius ( $Z=-$

1.604,  $p=0.109$ ;  $Z=-0.943$ ,  $p=0.345$ , respectively) and soleus muscle ( $Z=-1.095$ ,  $p=0.273$ ;  $Z=-1.625$ ,  $p=0.104$ , respectively).

The results of Experiment 2B indicate that vestibular-evoked muscle responses are decreased when the gravity-related vestibular signal is different from normal (i.e. 1 g) and that timing of the response is not influenced by vestibular signals of gravity.

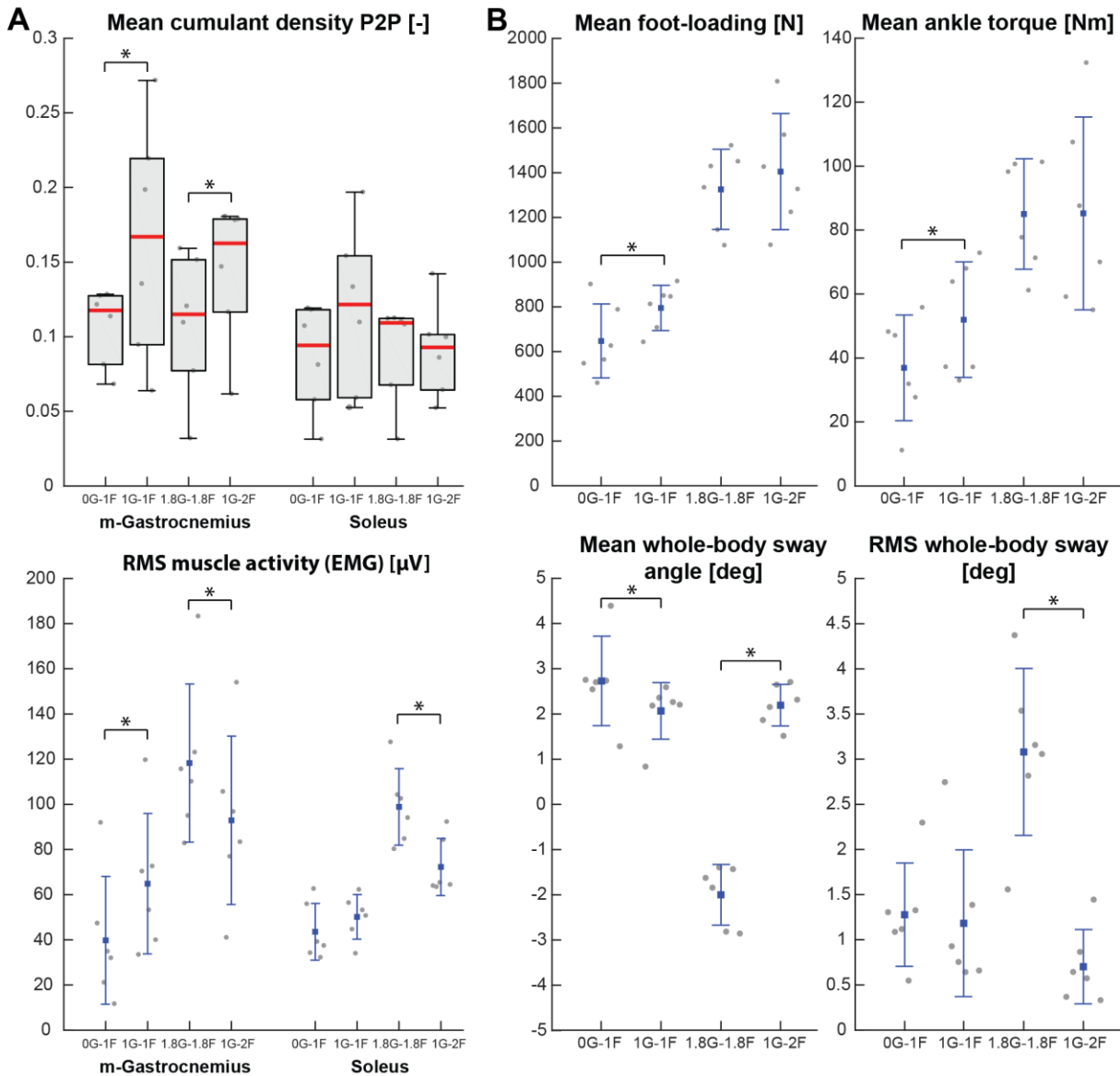


**Figure 6. Individual and group average ( $n=6$ ) data of Experiment 2B. A)** Muscle-related outcome measures. Peak-to-peak (P2P) amplitudes of the cumulant density responses (top) and RMS of muscle activity (EMG) (bottom); **B)** Outcome measures of general balance behaviour including vertical loading forces, ankle torque and whole-body sway angle (mean and mean-removed RMS). Individual subjects are plotted as grey dots. Group responses for normally distributed data were plotted with a mean (blue dots) and standard deviation (blue whiskers), while non-normally distributed data were plotted with a median (red line), 25 and 75 percentiles (grey box) and extreme data points (grey whiskers). Asterisks indicate significant differences between conditions.

## Discussion

The load- and vestibular-related sensory cues that respond to gravity inform the brain about the body's movement and orientation relative to the world, and evoke appropriate balance responses to external disturbances. The aim of the present study was to investigate the effect of these cues on vestibular-evoked muscle responses to an electrically induced vestibular error of head roll. When subjects balanced with added load and a constant 1 g vestibular signal, vestibular-evoked muscle responses decreased relative to responses during normal standing. Similarly, when the vestibular signal of gravity increased or decreased while the overall load was held constant, vestibular-evoked muscle responses also decreased. These results demonstrate that load- and vestibular-related sensory cues of gravity influence the vestibular drive for standing balance, and suggest that, according to the re-fference principle, changes in these sensory cues create incongruent sensory and motor signals, i.e. a mismatch between predicted and actual sensory feedback.

### **The flexible nature of vestibular-evoked muscle responses**

The presence of vestibular-evoked responses in appendicular muscles during standing balance is dependent upon the relevance of a muscle's contribution to compensate for a vestibular error (Fitzpatrick et al. 1994; Forbes et al. 2016; Luu et al. 2012). Therefore, the observation of vestibular-evoked muscle responses across our load and gravity conditions may not be surprising since the muscles were always engaged in and relevant to balancing the body against a downward pulling force. Under zero-g conditions, however, the otolith sensory cues relating to this downward pull were absent, limiting the available sensory information related to the constant downward load. Our results therefore suggest that sensory signals of load and balance other than the otolithic signal of gravity (e.g. somatosensory and/or dynamic vestibular signals) are capable of engaging the vestibular control of standing. In some ways, this is a counterpart to the observation that in balancing conditions without proprioceptive signals of ankle angle (i.e. sway referenced balance), vestibular-evoked responses continue to be observed (Luu et al. 2012; Forbes et al. 2016). More generally stated, these findings suggest that the vestibular control of balance can be engaged with a variable subset of sensory information related to standing.

Indeed, the availability of different sensory cues of balance, such as vision and somatosensory signals, can have a strong influence on vestibular-evoked responses (Britton et al. 1993; Lund & Broberg, 1983; Muise et al. 2012; Welgampola & Colebatch, 2001), and can provide some clue as where the modulation in our responses may originate from. Although the influence of vision was excluded by having subjects closing their eyes, our varying load conditions modified several somatosensory cues both within and across varying gravity levels. An increased load on the body is known to decrease sensitivity of cutaneous mechanoreceptors in the sole of the feet (Mildren et al. 2016), which in turn increases the vestibular-evoked muscle responses, at least when cooling the feet (Muise et al. 2012). Therefore, if changes in cutaneous feedback through foot-loading were the primary source of modulation of the vestibular control of balance, we would have predicted an increase in responses with increasing load instead of the decrease observed here. Nevertheless, such a prediction aligns with observations from Marsden et al. (2003), who indeed found a progressive increase in vestibular-evoked responses with increasing body load, and a progressive decrease in responses with decreasing body load. At first glance, our results seem to contradict these findings. However, Marsden et al. (2003) examined the rate of reaction force

development induced by an electrical vestibular stimulus instead of the muscle's response magnitude reported here. Although the correlation magnitude between EVS and EMG is not directly comparable to the development of ground reaction forces induced by EVS, the measure that perhaps relates closest to their study is the timing of the vestibular-evoked muscle response; the more rapid vestibular-evoked muscle response could produce a higher rate of force development. Indeed, our study showed that with additional loading, the response occurred sooner, though not progressively with more load. As Marsden et al. (2003) only found a progressive change for loads up to 150 % of the subject's body weight, we might have hit a threshold when loading up to 200 %. Changes in vestibular cues of gravity did not influence the timing of the response, suggesting that the speed of the vestibular drive to muscles is probably not dependent on sensory cues of gravity but rather on motor behavior. As such, an additional influencing factor on vestibular-evoked responses may be that an increased load on the body is accompanied by an increase in the excitability of the motoneurone pool (i.e. increased muscle activity) (Marsden et al. 2002; 2003), which could theoretically result in modulation of the vestibular-evoked muscle responses. However, increasing muscle activity did not always result in a change in the vestibular-evoked response (i.e. comparison 1.5F and 2F conditions), suggesting that the modulation is not primarily due to the excitability of the motoneurone pool. This aligns with observations from Marsden et al. (2002) who similarly demonstrated that changes in background muscle activity do not enhance nor deteriorate muscle responses to EVS.

Although there are many other motor or somatosensory cues (e.g. muscle proprioceptors or somatic graviceptors) of which the influence on vestibular-evoked responses is unknown, we suggest that the decreased muscle responses observed in this study are most likely to be due to a mismatch in the actual and predicted sensory feedback of the motor command.

#### **Load cues versus vestibular cues of gravity: a matter of (in)congruency**

The present experiments showed that vestibular-evoked muscle responses were fully facilitated when balancing under normal conditions, i.e. 1 g body load and 1 g vestibular load, and were decreased when these cues were modified. As vestibular-evoked responses are dependent upon congruent motor and sensory feedback signals (Luu et al. 2012), the observed decrease is most likely caused by an erroneous sensory feedback prediction of the motor behavior. Indeed, vestibular-evoked responses are decreased when sensory information is modified by electrically augmenting or reducing the vestibular sensory feedback signal with a head coupled perturbation (Héroux et al. 2015) such that the prediction is incongruent with the actual feedback. Given the observed reductions in vestibular-evoked responses in our study, we propose that the representation of the body's dynamics that underlie the feedback prediction (van der Kooij et al. 1999; Kuo, 2005; Héroux et al. 2015) is dependent upon the constant terrestrial force under which we have evolved. Consequently, when sensory cues of gravity are not congruent to normal expectations of standing balance, e.g. by changing the load on the body or otolith signals, an error will arise in the predicted sensory feedback.

In this study, a progressive increase in load under a constant 1 g vestibular load did not result in a progressive decrease of the vestibular-evoked response, suggesting that the vestibular drive is not dependent on the specific magnitude or direction of the incongruence of a specific cue. Moreover, when both body load and vestibular load were incongruent to the expectations of normal balance (i.e. 1.8G-

1.8F), vestibular-evoked responses in the gastrocnemius muscle decreased even further relative to the 1G-2F condition, in which only load cues were increased. These results suggest that the attenuation of the vestibular drive for standing balance control is dependent upon the cumulative incongruency that arises from multiple sensory cues.

Although vestibular-evoked responses in both muscles decreased with increasing load during Experiment 1 and 2A, we found no change in soleus muscle responses across all conditions during the flight. This is perhaps not surprising as the soleus muscle is known to be less sensitive to vestibular input than the gastrocnemius (Dakin et al. 2016). Nevertheless, a post hoc analysis of the magnitude of the evoked responses in the soleus showed a large effect size ( $r=0.51$ ) to detect a change in the response between the 0G-1F and 1G-1F condition, suggesting that with a bigger sample size a significant difference might have been found.

### **Limitations and recommendations**

The main limitation of the present study is that general balancing behaviors (particularly vertical load, mean and mean-removed RMS whole-body sway angle) during the flight (Experiment 2B) were not equivalent across the conditions that were compared. The differences in these measures mainly impeded the ability to make a direct comparison between the vestibular-evoked muscle responses and to extract the influence of gravity-driven otolith signals. For example, the vertical load forces in the 0G-1F condition were 18.6 % lower than the desired load of body weight under 1 g. According to the proposition that modified load cues decrease vestibular-evoked responses because of incongruent signals, we cannot exclude the possibility that the observed decrease in the 0G-1F condition was influenced by load cues being incongruent to normal expectations of standing balance. Though, since load cues in the 1.8G-1.8F and 1G-2F conditions were equal and the vestibular-evoked response was significantly reduced with increased vestibular load, we can still conclude that vestibular cues of gravity also modify the responses by causing incongruent feedback predictions when gravity is different from normal expectations. For future standing balance experiments in parabolic flights, we recommend to align the subject's sway direction with the lateral axis of the plane, so that unexpected plane accelerations will not interfere with the balancing task and influence the general balance behavior.

To find more evidence of the proposition that a terrestrial representation of the body's dynamics is used to predict the sensory feedback of motor actions, more trial conditions could be assessed with more variation in load and gravitational cues. For example, according to this proposition, changing load-related afferent cues by unloading the subject's body should have the same effect (i.e. direction and magnitude) on vestibular-evoked muscle responses as adding load to the body. Furthermore, vestibular cues of gravity can be modified on Earth by engaging subjects in a balance task while being positioned upside down or horizontally. In such balance set-ups, the otolith organs are still subjected to the gravitational pull, but in a different orientation than normal. We would again expect a decrease in vestibular-evoked muscle responses since otolith signals are incongruent to normal expectations of standing balance.

Additionally, to examine whether the representation of the body's dynamics can adapt to a new constant gravitational pull, astronauts would be valuable subjects. Before astronauts go to space, their representation is dependent on the terrestrial force of gravity and vestibular-evoked responses will be

fully facilitated. After a prolonged period in space (i.e. 0 g), their representation may be based on a weightless environment and we would expect a reduced or even an absent vestibular-evoked muscle response when they are back on Earth, as both load-related afferent and vestibular-related gravity cues will now be incongruent. Such an experiment would also be very interesting in persons with loss of otolith function; a baseline measure before otolithic function loss would show optimal vestibular-evoked muscle responses, then, an immediate loss of function would probably show a reduced response. Finally, after adaptation to the new normal situation without otolith function, vestibular-evoked responses might be back to their baseline level.

Furthermore, without modifying the sensory cues of gravity that were used in this study, one can manipulate the standing balance dynamics by modifying inertia of the subject's body without changing the load. As the internal model's representation of the body's dynamics is dependent upon the most common terrestrial dynamics, such an experiment would also result in incongruent motor and sensory signals and is therefore also expected to decrease vestibular-evoked muscle responses. In situations where both dynamics and sensory cues of gravity are changed, we expect an even further reduction of the response as the cumulative incongruency will be bigger.

## Conclusion

The present study showed that the vestibular drive for standing balance control was maintained across variations in load- and vestibular-related cues of gravity, though, attenuated when load was added or gravity-driven vestibular signals were altered. By modifying sensory cues of gravity, we decreased congruency between the predicted and actual sensory feedback. Our results provide evidence that the feedback prediction is dependent upon a 1 g representation of the body's standing dynamics, which results in an erroneous and incongruent prediction when sensory cues of gravity are different from normal and a subsequent decrease in the vestibular drive to muscles. In addition, our results suggest that the attenuation of the vestibular drive is dependent upon the cumulative incongruency that arises from multiple sensory cues, as vestibular-evoked responses were most attenuated when both the load- and vestibular-related cues of gravity were modified.

## Acknowledgements

I would like to thank, above all, my daily supervisor Patrick Forbes for his expertise, guidance and mentorship throughout the whole duration of this project. I know that this project has caused him many sleepless nights, but I also know that this has helped to improve the study in countless ways. Furthermore, I would like to thank Alfred Schouten for his supervision and valuable comments that contributed to the end result of this Thesis. I would like to thank the people from the VESTAND team with who I participated in the FlyYourThesis! Campaign for their support during the experiments. At last, I would like to thank the people at ESA Education for making this project possible and for their critical view during the preparation for the flights.

## Grants

This project was part of the FlyYourThesis!2017 Campaign of the European Space Agency (ESA). These experiments were funded by the ESA Education Office.

## References

- Angelaki, D., Shaikh, A., Green, A., & Dickman, J. (2004). Neurons compute internal models of the physical laws of motion. *Nature*, 560-564.
- Britton, T., Day, B., Brown, P., Rothwell, J., Thompson, P., & Marsden, C. (1993). Postural electromyographic responses in the arm and leg. *Exp Brain Res*, 141-151.
- Cathers, I., Day, B., & Fitzpatrick, R. (2005). Otolith and canal reflexes in human standing. *J Physiol*, 229-234.
- Dakin, C., Dalton, B., Luu, B., & Blouin, J. (2014). Rectification is required to extract oscillatory envelope modulation from surface electromyographic signals. *J Neurophysiol*, 1685-1691.
- Dakin, C., Héroux, M., Luu, B., Inglis, J., & Blouin, J. (2016). Vestibular contribution to balance control in the medial gastrocnemius and soleus. *J Neurophysiol*, 1289-1297.
- Dakin, C., Inglis, J., & Blouin, J. (2011). Short and medium latency muscle responses evoked by electrical vestibular stimulation are a composite of all stimulus frequencies. *Exp Brain Res*, 345-354.
- Dakin, C., Luu, B., van den Doel, K., Inglis, J., & Blouin, J. (2010). Frequency-specific modulation of vestibular-evoked sway responses. *J Neurophysiol*, 1048-1056.
- Dakin, C., Son, G., Inglis, J., & Blouin, J. (2007). Frequency response of human vestibular reflexes characterized by stochastic stimuli. *J Physiol*, 1117-1127.
- Day, B., Séverac Cauquil, A., Bartolomei, L., Pastor, M., & Lyon, I. (1997). Human body-segment tilts induced by galvanic stimulation: a vestibularly driven balance protection mechanism. *J Physiol*, 661-672.
- Fitzpatrick, R., & Day, B. (2004). Probing the human vestibular system with galvanic stimulation. *J Appl Physiol*, 2301-2316.
- Fitzpatrick, R., Burke, D., & Gandevia, S. (1994). Task-dependent reflex responses and movement illusions evoked by galvanic vestibular stimulation in standing humans. *J Physiol*, 363-372.
- Forbes, P., Luu, B., Van der Loos, H., Croft, E., Inglis, J., & Blouin, J. (2016). Transformation of vestibular signals for the control of standing in humans. *J Neurosci*, 11510-11520.
- Gaveau, J., Berret, B., Angelaki, D., & Papaxanthis, C. (2016). Direction-dependent arm kinematics reveal optimal integration of gravity cues. *eLife*, e16394.

- Goldberg, J., Smith, C., & Fernández, C. (1984). Relation between discharge regularity and responses to externally applied galvanic currents in vestibular nerve afferents of the squirrel monkey. *J Neurophysiol*, 1236-1256.
- Halliday, D., Rosenberg, J., Amjad, A., Breeze, P., Conway, B., & Farmer, S. (1995). A framework for the analysis of mixed time series/point process data: theory and application to the study of physiological tremor, single motor unit discharges and electromyograms. *Prog Biophys Mol Biol*, 237-278.
- Héroux, M., Law, T., Fitzpatrick, R., & Blouin, J. (2015). Cross-modal calibration of vestibular afference for human balance. *PLoS One*, e0124532.
- Kuo, A. (1995). An optimal-control model for analyzing human postural balance. *IEEE Trans Biomed Eng*, 87-101.
- Kuo, A. (2005). An optimal state estimation model of sensory integration in human postural balance. *J Neural Eng*, 235-249.
- Laurens, J., & Angelaki, D. (2011). The functional significance of velocity storage and its dependence on gravity. *Exp Brain Res*, 407-422.
- Laurens, J., Meng, H., & Angelaki, D. (2013). Computation of linear acceleration through an internal model in the macaque cerebellum. *Nat Neurosci*, 1701-1708.
- Lund, S., & Broberg, C. (1983). Effects of different head positions on postural sway in man induced by a reproducible vestibular error signal. *Acta Physiol Scand*, 307-309.
- Luu, B., Inglis, J., Huryn, T., Van der Loos, H., Croft, E., & Blouin, J. (2012). Human standing is modified by an unconscious integration of congruent sensory and motor signals. *J Physiol*, 5783-5794.
- Marsden, J., Blakey, G., & Day, B. (2003). Modulation of human vestibular-evoked postural responses by alterations in load. *J Physiol*, 949-953.
- Marsden, J., Castellote, J., & Day, B. (2002). Bipedal distribution of human vestibular-evoked postural responses during asymmetrical standing. *J Physiol*, 323-331.
- Merfeld, D. M., Zupan, L., & Peterka, R. J. (1999). Humans use internal models to estimate gravity and linear acceleration. *Nature*, 615-618.
- Mildren, R., Strzalkowski, N., & Bent, L. (2016). Foot sole skin vibration perceptual thresholds are elevated in a standing posture compared to sitting. *Gait Posture*, 87-92.
- Muise, S., Lam, C., & Bent, L. (2012). Reduced input from foot sole skin through cooling differentially modulates the short latency and medium latency vestibular reflex responses to galvanic vestibular stimulation. *Exp Brain Res*, 63-71.

- Nashner, L., & Wolfson, P. (1974). Influence of head position and proprioceptive cues on short latency postural reflexes evoked by galvanic stimulation of the human labyrinth. *Brain Res*, 255-268.
- Peters, R., Rasman, B., Inglis, J., & Blouin, J. (2015). Gain and phase of perceived virtual rotation evoked by electrical vestibular stimuli. *J Neurophysiol*, 264-273.
- van der Kooij, H., Jacobs, R., Koopman, B., & Grootenboer, H. (1999). A multisensory integration model of human stance control. *Biol Cybern*, 299-308.
- von Holst, E., & Mittelstaedt, H. (1950). Das reafferenzprinzip. *Naturwissenschaften*, 464-476.
- Welgampola, M., & Colebatch, J. (2001). Vestibulospinal reflexes: quantitative effects of sensory feedback and postural task. *Exp Brain Res*, 345-353.

## Appendix A – Standing body's dynamics

Load-stiffness curves are used to characterize the body's dynamics of standing balance as they provide information about the amount of torque that is needed to stand in a certain angle (Fig. 1). The subject loading system was designed to match the intrinsic load-stiffness relationship of the standing body. The subjects that performed Experiment 1 additionally completed four trials with 2F load (i.e. 2 times body weight) while the attachment point of the springs was fixed on the ground. The attachment point was determined so that the springs were pulling straight down when the subjects leaned 4° forward from vertical (i.e. ~3° forward from the average subjective zero angle). This configuration changed the load-stiffness characteristics as can be seen in the red dotted line in Figure 1.

In the 2F-fixed condition, vertical load forces, mean whole-body sway angle and the RMS sway angle were approximately equivalent to the 2F condition (see Table 1). EMG and ankle torque, however, differed from the 2F condition, those were more equal to the 1.5F condition. EVS did induce vestibular-evoked muscle responses in the 2F-fixed condition. The responses were even further attenuated relative to the other conditions (Fig. 2). Relative to the 2F condition, the response of the soleus muscle in the 2F-fixed condition was significantly decreased ( $Z=-2.637$ ,  $p=0.008$ ). For the gastrocnemius, only a trend was visible ( $Z=-1.241$ ,  $p=0.215$ ).

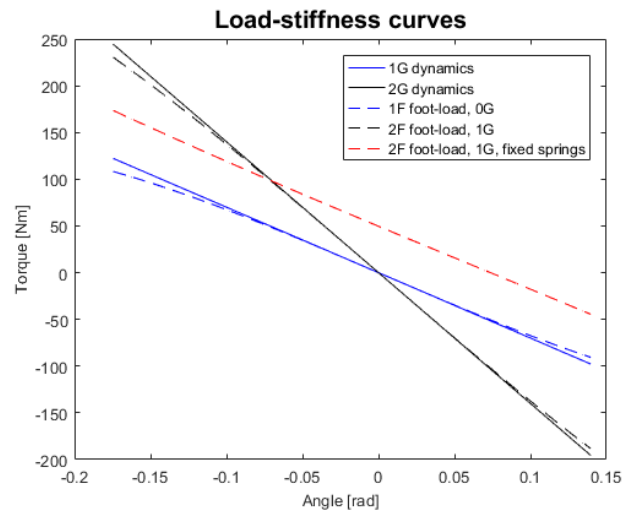


**Figure 1. Load-stiffness curves for different load conditions.** The lines show the load-stiffness curves for a person of 75 kg with the center of mass height at 0.98 m. The 1G and 2G dynamics are based on the weight of the subject, while for the 1F-0G and 2F-1G the force of (mobile) springs is taken into account. The graph shows that a mobile spring attachment resembles the inherent load-stiffness curves of the standing body dependent on body load. The fixed attachment point of the springs (dotted red line) shows a load-stiffness curve parallel to a 1F load condition, but with an offset. This does not resemble the dynamics of a real 2G body load.

*Table 1. Group average absolute values of Experiment 1.*

	P2P amplitude		RMS EMG		Foot-loading (N)	Ankle torque (Nm)	Sway angle (°)	RMS angle (°)
	Cas	Sol	Cas	Sol				
	<i>median ± IQR</i>	<i>median ± IQR</i>	<i>mean ± SD</i>	<i>mean ± SD</i>	<i>mean ± SD</i>	<i>mean ± SD</i>	<i>mean ± SD</i>	<i>mean ± SD</i>
<i>1F</i>	0,1906 ± 0,0972	0,1092 ± 0,0487	46,79 ± 24,16	38,54 ± 10,82	713,8 ± 87,8	31,44 ± 9,71	3,96 ± 0,38	3,99 ± 0,37
<i>1.5F</i>	0,1383 ± 0,1042	0,0732 ± 0,0458	86,28 ± 36,78	55,74 ± 14,31	1041,7 ± 123,4	58,77 ± 13,82	4,01 ± 0,37	4,03 ± 0,37
<i>2F</i>	0,1458 ± 0,0964	0,0676 ± 0,0497	106,97 ± 45,78	66,90 ± 17,01	1337,3 ± 175,6	76,08 ± 21,22	4,03 ± 0,55	4,06 ± 0,54
<i>2F-fixed</i>	0,1233 ± 0,0790	0,0621 ± 0,0407	92,78 ± 39,52	59,49 ± 15,50	1338,9 ± 171,6	57,95 ± 13,11	4,08 ± 0,4	4,10 ± 0,40

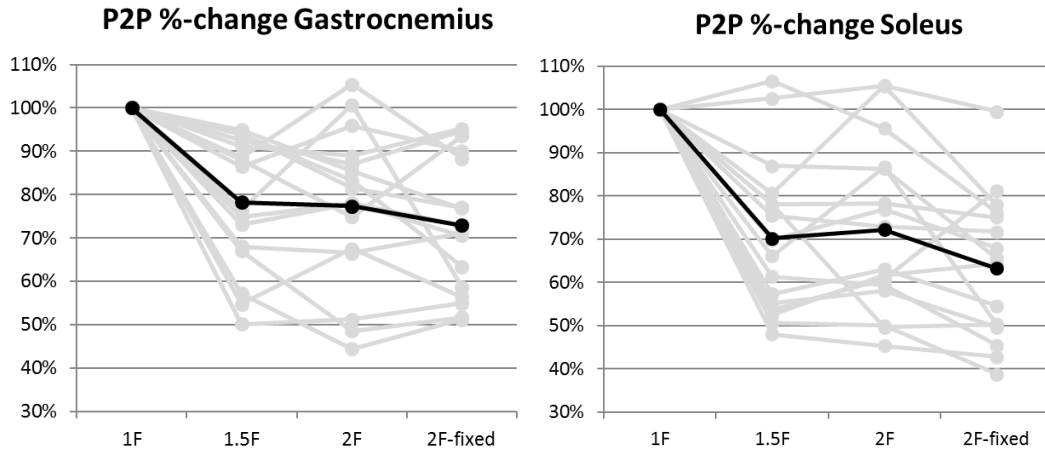


**Figure 2.** Peak-to-peak percentage change relative to the normal 1F condition for the four conditions of Experiment 1. Grey lines represent individual subjects ( $n=16$ ), the black line shows the mean percentage change.

In the 2F-fixed condition, vestibular-evoked muscle responses showed the biggest reduction relative to responses for normal standing. This reduction can be explained by the re-afference principle, since in this condition both load cues and the body's dynamics were incongruent to the internal representation. The nervous system downregulates the vestibular drive for balance control even more compared to a situation in which only load cues are incongruent to the expectations.

## Appendix A – Standing body’s dynamics

Load-stiffness curves are used to characterize the body’s dynamics of standing balance as they provide information about the amount of torque that is needed to stand in a certain angle (Fig. 1). The subject loading system was designed to match the intrinsic load-stiffness relationship of the standing body. The subjects that performed Experiment 1 additionally completed four trials with 2F load (i.e. 2 times body weight) while the attachment point of the springs was fixed on the ground. The attachment point was determined so that the springs were pulling straight down when the subjects leaned 4° forward from vertical (i.e. ~3° forward from the average subjective zero angle). This configuration changed the load-stiffness characteristics as can be seen in the red dotted line in Figure 1.

In the 2F-fixed condition, vertical load forces, mean whole-body sway angle and the RMS sway angle were approximately equivalent to the 2F condition (see Table 1). EMG and ankle torque, however, differed from the 2F condition, those were more equal to the 1.5F condition. EVS did induce vestibular-evoked muscle responses in the 2F-fixed condition. The responses were even further attenuated relative to the other conditions (Fig. 2). Relative to the 2F condition, the response of the soleus muscle in the 2F-fixed condition was significantly decreased ( $Z=-2.637$ ,  $p=0.008$ ). For the gastrocnemius, only a trend was visible ( $Z=-1.241$ ,  $p=0.215$ ).

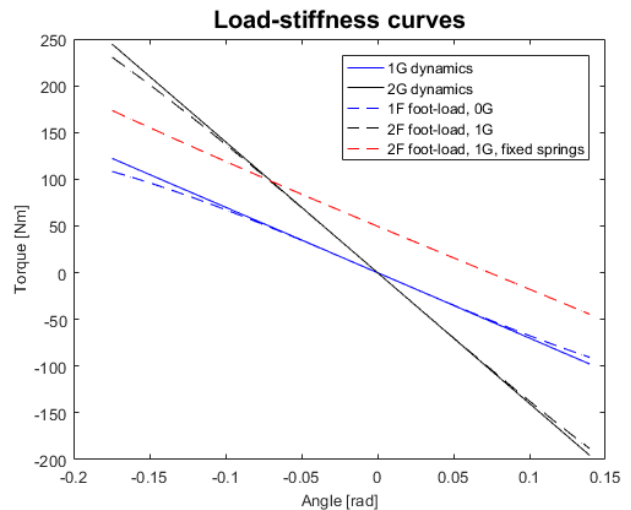


**Figure 1. Load-stiffness curves for different load conditions.** The lines show the load-stiffness curves for a person of 75 kg with the center of mass height at 0.98 m. The 1G and 2G dynamics are based on the weight of the subject, while for the 1F-0G and 2F-1G the force of (mobile) springs is taken into account. The graph shows that a mobile spring attachment resembles the inherent load-stiffness curves of the standing body dependent on body load. The fixed attachment point of the springs (dotted red line) shows a load-stiffness curve parallel to a 1F load condition, but with an offset. This does not resemble the dynamics of a real 2G body load.

*Table 1. Group average absolute values of Experiment 1.*

	P2P amplitude		RMS EMG		Foot-loading (N)	Ankle torque (Nm)	Sway angle (°)	RMS angle (°)
	Gas	Sol	Gas	Sol				
	<i>median ± IQR</i>	<i>median ± IQR</i>	<i>mean ± SD</i>	<i>mean ± SD</i>	<i>mean ± SD</i>	<i>mean ± SD</i>	<i>mean ± SD</i>	<i>mean ± SD</i>
1F	0,1906 ± 0,0972	0,1092 ± 0,0487	46,79 ± 24,16	38,54 ± 10,82	713,8 ± 87,8	31,44 ± 9,71	3,96 ± 0,38	3,99 ± 0,37
1.5F	0,1383 ± 0,1042	0,0732 ± 0,0458	86,28 ± 36,78	55,74 ± 14,31	1041,7 ± 123,4	58,77 ± 13,82	4,01 ± 0,37	4,03 ± 0,37
2F	0,1458 ± 0,0964	0,0676 ± 0,0497	106,97 ± 45,78	66,90 ± 17,01	1337,3 ± 175,6	76,08 ± 21,22	4,03 ± 0,55	4,06 ± 0,54
2F-fixed	0,1233 ± 0,0790	0,0621 ± 0,0407	92,78 ± 39,52	59,49 ± 15,50	1338,9 ± 171,6	57,95 ± 13,11	4,08 ± 0,4	4,10 ± 0,40

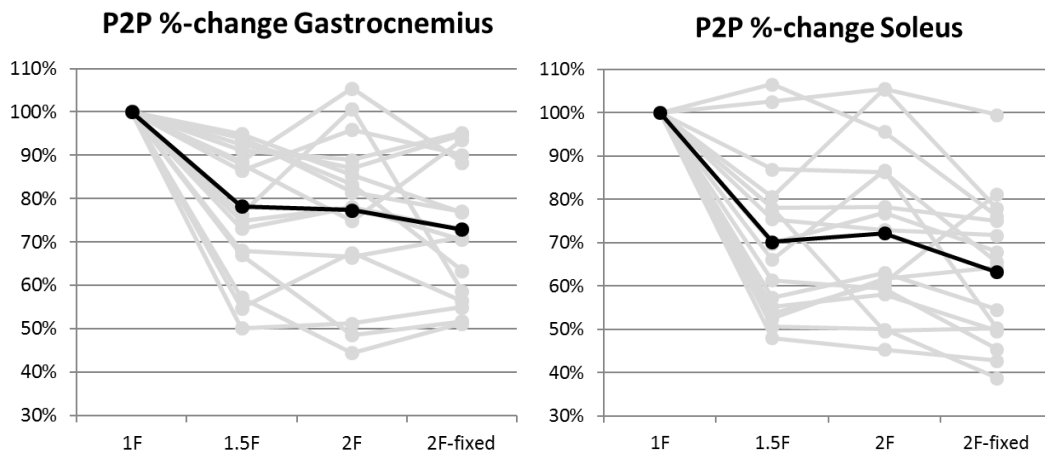


**Figure 2. Peak-to-peak percentage change relative to the normal 1F condition for the four conditions of Experiment 1.** Grey lines represent individual subjects (n=16), the black line shows the mean percentage change.

In the 2F-fixed condition, vestibular-evoked muscle responses showed the biggest reduction relative to responses for normal standing. This reduction can be explained by the re-afference principle, since in this condition both load cues and the body's dynamics were incongruent to the internal representation. The nervous system downregulates the vestibular drive for balance control even more compared to a situation in which only load cues are incongruent to the expectations.

# Appendix B – Experimental Safety Data Package for Parabolic Flight Campaign

Authors: A.I. Arntz & D.A.M van der Putte

Format of the document was provided by Novespace

# The contribution of gravity to self-motion perception and standing balance responses evoked by electrical vestibular stimulation

## VESTAND

### 1. Points of Contact

#### Principal Coordinator:

First and last name	<i>Maarten Frens</i>	<i>Patrick Forbes</i>
Office phone number:	<i>+31 (0) 107 043 561</i>	
Mobile phone number:	<i>+31640609067</i>	<i>+31631917511</i>
Email:	<i>m.frens@erasmusmc.nl</i>	<i>p.forbes@erasmusmc.nl</i>
Name and address of the Laboratory:	<i>Erasmus MC, Dept. Neuroscience, Rotterdam</i>	<i>Erasmus MC, Dept. Neuroscience, Rotterdam</i>

#### Technical Coordinator:

First and last name	<i>Anne Arntz</i>
Office phone number:	<i>...</i>
Mobile phone number:	<i>+31630012473</i>
Email:	<i>annearntz93@gmail.com</i>
Name and address of the Laboratory:	<i>Erasmus MC, Dept. Neuroscience, Rotterdam</i>

## 2. Tables of Changes

### List of Changes since last Flight Campaign

Campaign #	Date	List of Main Changes Since Last Flight Campaign
Fly Your Thesis! 2017	2016-2017	First participation

### List of Changes of the ESDP

ESDP Revision	Revision Date	Modified §	Description of Changes
0	24-07-2016	all	Initial issue of the document
1	09-01-2017	all	Updated every section of the ESDP
2	31-05-2017	3.2 4.1 & 4.2  6.1 7 8 9	Experimental procedure changed Some experimental equipment is changed, therefore the system set-up is also changed Cabin layout is changed Adjusted to include all changes in experimental equipment Racks 2 and 3 are changed New overview of procedure
3	04-10-2017	3.2 3.3 4.1 & 4.2  6.1 7.1 8 9 11	Updated and more detailed Added stimulation protocol Some experimental equipment is changed, therefore the system set-up is also changed Orientation of rack #2 is changed Some equipment is added Rack 2 (chair) is changed significantly and some adjustments have been made to rack 3 (backboard) More detailed procedure + subject training Updated
4	23-10-2017	3.2  6.1 8 9	Protocol slightly changed because of new orientations experiment 1 Cabin lay-out is changed Rack 2 (chair) is changed again Updated the procedures during the flights
5	24-11-2017	3  4.2 8 9 10	For exp1, stim periods are changed, accordingly, Figure 1 is changed Backup laptop is listed Added photos specifications for the racks and included backboard (rack 3) calculations Chapter 9 is updated Adjusted hazard reports based on Novespace comments
6	28-11-2017	4.2  6 7 8.3	Added a head positioning subsystem that described products that we bring in flight to check the head angle of the subjects Updated rack weight and dimensions Added info on laptop batteries and added power references Added force plate structural integrity and updated linear loading
7	1-12-2017	4.2 5 6 8 Appendix C	Added details about silicium Added silicium to the list Added photos of set-up is plane Added combined set-up linear loading Exemption request laser

## 3. Experiment Overview

### 3.1 Objectives:

The scientific objective of our research is to determine how gravity, whether absent (micro-g), normal (1g) or elevated (hyper-g), contributes to perceptual and standing balance responses evoked by artificial vestibular stimulation, and the context driven modulation of these responses that normally occur. To this end we want to perform two experiments:

**Experiment 1.** In the first experiment we want to examine the effect of gravity on the perceived rotation/translation and on eye movements induced by electrical vestibular stimulation in healthy volunteers.

**Experiment 2.** In the second experiment, we want to examine the effect of gravity on standing balance control identified by random noise electrical vestibular stimulation in healthy volunteers.

### 3.2 Overview experimental procedure:

Electrically evoked vestibular contributions to perception and posture will be investigated in six different subjects during the three days of the parabolic flight campaign in normal, hyper and microgravity. In each of the flights, we will measure two subjects in two different experiments: a) during experiment 1, we will examine perceptual responses to electrical vestibular stimulation by recording eye movements and verbal reports during head-straight and head-down trials, and b) during experiment 2, we will examine postural responses to electrical vestibular stimulation during spring-loaded and non-loaded trials. The experiments will be performed simultaneously so each subject will do both experiments for 15 parabolas. During the mid-flight breaks, the subjects will be switched to the other experiment. To counterbalance for confounding factors, the order of experimental trials is different for the two subjects per flight. In Figure 1, the entire procedure is shown for both subjects. The colours indicate the phases of the parabola during which experiments will be performed.

The entire experimental procedure can be divided into four different periods, of which two will be performed during the parabolic maneuvers.

#### Period 0

##### *Preparation before take-off*

This phase entails getting the subjects and the equipment ready for the experiments. On ground, before the morning meeting, the skin behind the ear of the subjects will be covered with an anaesthetic cream (Pliaglis) to numb the skin. After 45 minutes, the Pliaglis film is removed and subsequently, gel (Spectra360) coated stimulation electrodes will be placed on those places and fixed with tape and a headband. In the meantime, surface EMG electrodes will be placed over the planter-flexor muscles (i.e. limb muscles) of the subjects. Therefore, the skin will be cleaned (i.e. scrubbed) with NuPrep first. At last, the subjects have to insert a marked scleral lens in their left eye. Both subjects will put on and tighten the loading harness prior to getting onto the plane.

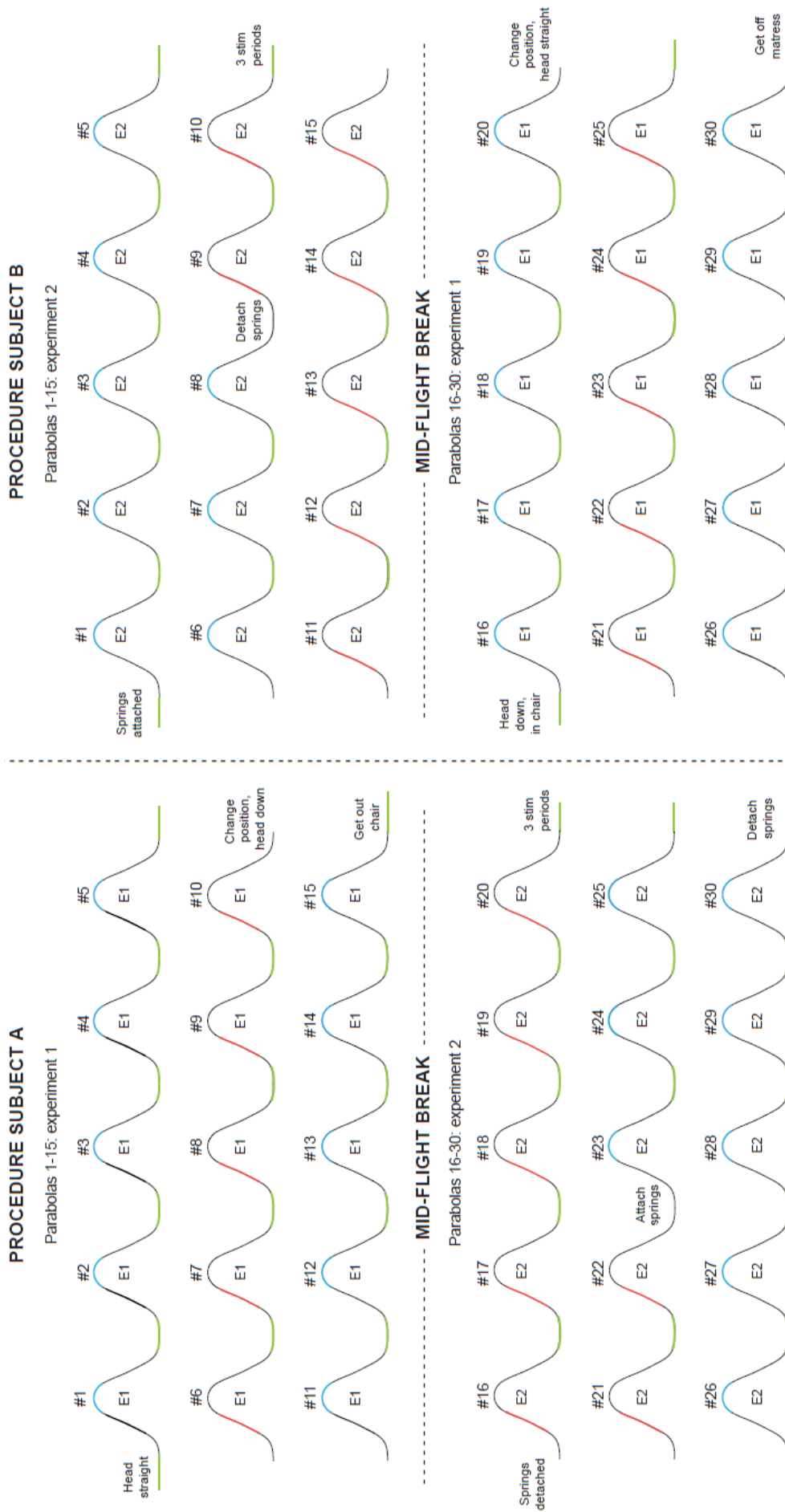


**Figure 1:** Experimental procedure. Left: procedure shown for subject 1, right: procedure shown for subject 2. After fifteen parabolas, the subjects will be switched to the other experiment. E1 and E2 represent experiment 1 and experiment 2, respectively. The blue parts are micro-g phases, the red parts are hyper-g phases and green parts are normal-g phases during which experiments will be performed.

### *Preparation in-flight before first parabola*

In flight, before the parabolas, the measurement equipment has to be turned on. Subject A will put on the recording goggles (EyeSeeCam) and the helmet, sit down in the chair and buckle the seatbelts. The eye recording system will then be adjusted for recording and subsequently calibrated. The stimulation electrodes will be connected to the stimulator through insulated wires and the subject will be lying down on the mattress restrained in the head straight position (see chapter 9 for more detailed procedure on this). The earphones with the microphone attached will be worn by the subject. For experiment 2, the subject will be secured against the backboard with two seatbelts and the EVS and EMG electrodes will be connected to the stimulator and the amplifier, respectively. The springs will be attached to the harness and appropriately tensioned. At the end of phase 0, everything should be ready to start experiment 1 with subject A and experiment 2 with subject B.

### **Period 1 (parabolas 1-15)**

#### *Experiment 1 – Head-straight trials (parabolas 1-10)*

Throughout these parabolas subject A will be in the head-straight position with the head slightly pitched up relative to their body. The subject will be lying on the foam mattress next to the chair and will lie on their side. A cushion will be put on top of the subject and belts will secure both the cushion and subject to the mattress and the floor. The helmet will be secured to the horizontal beam. Throughout the experiments, the EyeSeeCam will record eye movements. Furthermore, the subject will be instructed to report their perception via the earphones and they will verbally report the motion (s)he perceives as a result of the stimulation. Instructions for performance of the experiment and information about the timing of the stimulation will also be played to the subject via the earphones. The playing of the recorded instructions are triggered by the beginning of the normal-g phase or the ending of the stimulation. The stimulation is applied during the normal-g phase before each parabola, the zero-g phase during parabola 1-5 and the first hyper-g phase during parabola 5-10. The stimulation is triggered by the gravitational acceleration level as explained in section 5.1.1 and lasts for 20 seconds. During the stimulation, the subject will be exposed to a 0.4 Hz sinusoidal stimulus that will reach an amplitude of 4 mA. After the stimulation, the subject will be asked to verbally report the motion (s)he perceives.

#### *Experiment 1 – Head-down trials (parabolas 11-15)*

The stimulation paradigm is the same as in head-straight trials. The only difference is that for these parabolas the head will be supported in head-down position. Throughout these parabolas subject A will sit in the head-down position with the head slightly pitched up. The head is supported by a helmet that is fixed to the vertical profile in front of the chair. The chair on which the subject is seated will be covered with memory foam to minimize non-vestibular sensory inputs. A back cushion will be placed to support the subject in the restraints. The subject's feet are placed on memory foam that is attached to the ground. The subject will be secured to the chair using seat belt straps wrapped in foam. Stimulation for this condition will occur in the normal-g phase before each parabola and during the zero-g phase.. The procedure (measurements, etc.) during the parabolas is the same as during the head-up trials.

#### *Experiment 2 - spring-loaded trials (parabolas 1-8)*

During these trials, the experiment will be performed during the normal-g and zero-g phases while the springs are attached to the harness of the subject. For the experiment, the subject stands on the force plate with his/her body rotated 3° anterior from his/her subjective zero angle, this maximizes the EMG response evoked by the stimulation. During the normal-g and zero-g phases, subjects will be exposed to a 20 second stochastic stimulus (0-25 Hz bandwidth, peak amplitude 5 mA) that is triggered by the gravitational acceleration level as explained in section 5.1.1. During the hyper-g phases, the subject is attached to the springs but no measurements are done. The subject can lean into the endstops of the

backboard to be supported and crouch a bit. Prior to entering the zero-g phase, the subject will be instructed/helped to lean slightly forward so that (s)he is ready for another trial during the zero-g phase. After the zero-g phase, the subject can lean into the endstops of the backboard and crouch again to complete the second hyper-g phase. Once back in the normal-g phase, the subject will stand in the correct position again in order to start a the loaded-normal-g trial. During the measurements, the subjects will look over their left shoulder, have their head pitched slightly up and have their eyes closed. One experimenter will instruct the subject to stand in this position before every trial.

#### *Experiment 2 - non-loaded trials (parabolas 9-15)*

During these trials, the experiment is performed during the first hyper-g and normal-g phases, without spring loading. The other features of the experiment as well as the electrical stimulus are the same as in the spring-loaded trials. During the zero-g phase the subjects are prevented from floating by the seatbelts. During the second hyper-g phase the subjects can lean into the backboard to be supported.

### **Period 2 (Mid-flight break)**

The mid-flight break between parabolas 15 and 16 will be used to change the subjects from experiment. The stimulators are disengaged to make sure that the subjects cannot receive any stimulation while switching experiments.

For the subject that started with experiment 2, the seatbelts are unbuckled and the EVS and EMG wires are disconnected. The subject is instructed to move over to the set-up of experiment 1. The preparations are the same as described in Period 0 except the subject will now start in head-down position.

For the subject of experiment 1, the seatbelts are unbuckled and the helmet, the goggles and the microphone are removed. Then, the insulated wires for EVS are disconnected from the rubber electrodes. The subject is instructed to move over to the set-up of experiment 2. The preparations are the same as described in Period 0 except the subject will start with the springs being detached.

### **Period 3 (parabolas 16-30)**

#### *Experiment 1 – Head-down trials (parabolas 16-20)*

Procedures are the same as described in “Head-down trials” in Period 1.

#### *Experiment 1 – Head-straight trials (parabolas 21-30)*

Procedures are the same as described in “Head-straight trials” in Period 1, except that stimulation now occurs during the hyper-g phase of parabolas 20-25 and during the zero-g phase of parabolas 25-30.

#### *Experiment 2 - non-loaded trials (parabolas 16-22)*

Procedures are the same as described in “Non-loaded trials” in Period 1.

#### *Experiment 2 - spring-loaded trials (parabolas 23-30)*

Procedures are the same as described in “Spring-loaded trials” in Period 1.

## **3.3 Stimulation protocol**

Ideally, the stimulation protocol will be carried out automatically based on input from the accelerometer. This will be checked during parabola 0. For experiment 1 and experiment 2, the timing of the stimulation depends on the trial, as explained in 3.2.

We will use one software script that accounts for the number of parabolas and the trial order so that the stimulation conditions are switched automatically to the correct combination of trials for experiment 1 and 2. In the automated scenario, the only thing the experimenter needs to do is manually start the stimulation before the zero parabola when the “One minute” announcement is given.

In case of automated stimulation, 20 seconds of stimulation is activated when the acceleration level indicates the following g-levels (z-axis):

Normal-g phase: 20 seconds after  $g < 1.1$  is reached  
Hyper-g phase:  $g > 1.5$   
Zero-g phase:  $g < 0.2$

In the event that the automatic trigger via the accelerometer does not work, stimulation can be started manually for every parabola-phase. First, the experimenter must specify the current parabola so that the software uses the correct combination of stimulation for the experiments. The experimenter can then deliver the stimuli per phase of each parabola: button '1' is pressed for normal-g phases, button '2' is pressed for hyper-g phases and button '3' is pressed for zero-g phases. The buttons will be pressed according to the pilot announcements of "*one minute*", "*pull-up*" and "*injection*". When the buttons are pressed, 20 seconds of stimulation is started after 1 second to account for transition phases. An overview of the manual control actions is given in Figure 2.

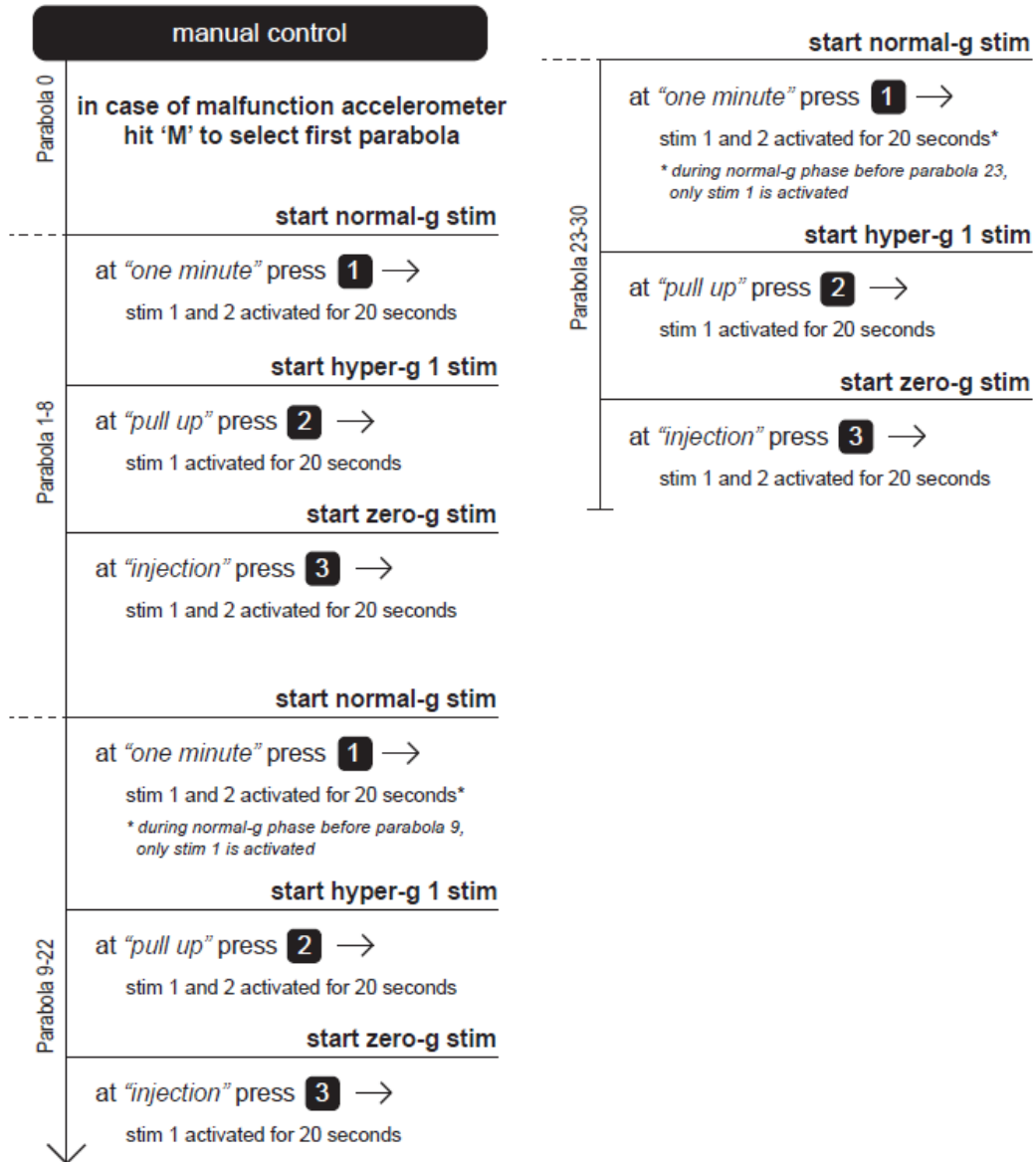
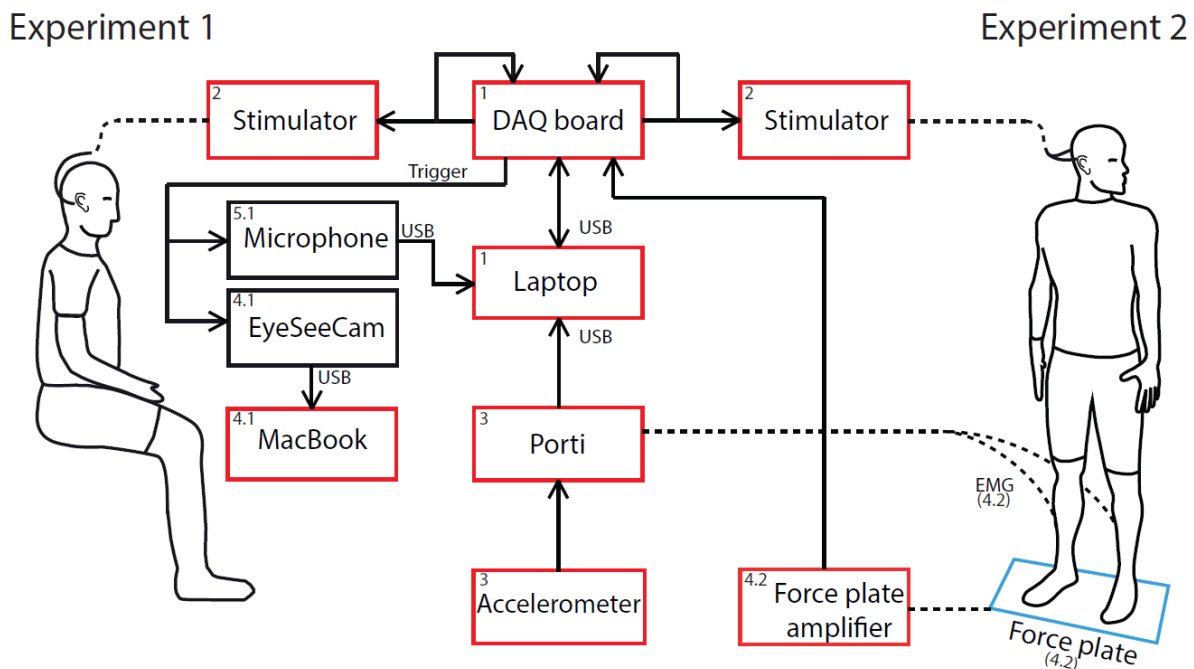


Figure 2: Actions for manual control of experiments

## 4. Description of the Experimental Equipment in Flight

### 4.1 System Description

The set-up of the systems is shown in Figure 3. Experiment 1 and 2 partly use the same equipment as can be seen. The numbers in Figure 3 refer to the different subsystems which are described in the following sub-section. A subsystem designated with a single number is used in both experiments, subsystems with #.1 are used in experiment 1 and with #.2 in experiment 2. The color coding of the blocks refer to the rack on which that subsystem is located. Information about the racks is given in chapter 8.



**Figure 3:** System overview of experiments 1 and 2. Numbers refer to a subsystem and colors refer to a rack, red is rack 1 and blue is rack 3. All lines represent physical cables. The dotted lines coming from the stimulators and the limbs (experiment 2, EMG) are insulated wires, connecting the stimulator and amplifier to electrodes.

### 4.2 Subsystems

Experiments 1 and 2 both use five subsystems, of which three are used for both experiments. In total we will use 7 subsystems for the experiments, these are listed and explained below.

#### 1. Data acquisition system

The first subsystem is a data acquisition system that consists of a data acquisition (DAQ) board (National Instruments USB-6259), a fan-out board (National Instruments, BNC-2090A) and a laptop (HP Pavilion), see Table 1. The laptop and DAQ board will be used to trigger/control other subsystems and to save the data. The DAQ board sends the stimulation signals from the laptop to the stimulators. These signals will be recorded back on the DAQ board as a control of the sent signals. At the same time, a trigger signal is sent to the camera (subsystem 4.1) and the amplifier (subsystem 3) for synchronization purposes. We will only use one DAQ board and one laptop to run both experiments simultaneously.

We will take an extra backup laptop in case we have problems with the HP. This is a Dell Vostro and is also listed in Table 1. Note that we will either use HP or Dell, not both.

Table 1. DAQ system

Component	Power	Mass	Dimensions	Connector	Certification
National Instruments USB-6259 Mass Term	Powered by adapter; 100-240V-AC/ 11-30 V DC 20 Watt	0.816 kg	188 x 171 x 45 mm	USB to laptop, 32 analog inputs, 4 analog outputs and 48 digital in-/outputs	IEC 61010-1, CE
National Instruments BNC Connector Block 2090A	Powered by NI USB-6259 (5V DC)	0.7 kg	44 x 483 x 97 mm	22 BNC connectors	IEC 61010-1, CE
HP Pavilion Touchsmart 15-N006ED	Powered by adapter 65W AC	2.28 kg	22.6 x 385.6 x 258 millimeters.	Not applicable	CE
HP Power adapter R33030	100-240V AC	0.18 kg	44 x 30 x 96 mm	Not applicable	CE
Dell Vostro 14 5468	Powered by adapter 45 W (19.5 V, 2.31 A)	1.6 kg	34 x 24 x 1.8 cm	Not applicable	CE

## 2. Stimulation system

The second subsystem consists of two electrical stimulation devices (Digitimer DS5, see Table 2) which are used in combination with two gel coated (Spectra 360 electrode gel, Parker Laboratories, Fairfield, NJ) rubber electrodes per stimulator. The electrodes will be taped over the mastoid processes (behind the ears) of each subject through which the stimulator will deliver sinewave electrical stimuli to evoke a ‘virtual’ perception of motion in experiment 1 and random noise to evoke a muscle response in experiment 2. The current controlled signal will be sent by the laptop, via the DAQ board to the stimulator. We will use two stimulators, one for experiment 1, and one for experiment 2.

The stimulation signal will be automated by the gravitational acceleration level (subsystem 3). For hyper-g phases, the stimulation signal is sent when acceleration is higher than 1.5g. For the zero-g phases, the stimulation signal is sent when acceleration is lower than 0.07g. For normal-g phases, the stimulation signal is sent 40 seconds after 1.05g is reached.

Table 2. Stimulator component

Component	Power	Mass	Dimensions	Connector	Certification
Digitimer DS5 (2 pieces)	100V, 120V, 200V or 240V (externally selected), 47-63Hz, 35VA	4 kg (approx.) per stimulator	225 x 100 x 255 (w x h x d)	Multiple sockets	EN-60601, CE

### 3. Amplifier system

The third subsystem consists of a 32-channel amplifier (TMSi Porti) and an accelerometer (TMSi). The separate components of this system, including the accelerometer, are summarized in Table 3. Figure 4 illustrates how the different components of the amplifier are connected. For the safety recommendations of the amplifier see attachment “1\_Porti\_Manual”, page 5-9.

The amplifier will be connected to the laptop to store, among others, acceleration and EMG data. The acceleration data will trigger the stimulation in both experiments. The Porti receives a signal from the DAQ board at the instant that EVS is delivered, to be able to synchronize the incoming data (force plate data, EMG data, acceleration data). We need only one amplifier and one accelerometer to record and trigger both experiments.

Table 3. Amplifier components

Component	Power	Mass	Dimensions	Connector	Certification
TMSi Porti 32 channel set-up	By TMSi SUP3 power supply	0.75 kg	158 mm x 112 mm x 73 mm	Fiber optic cable connecting to Fusbi	IEC-60601-1, IEC 60601-1-2, CE
TMSi SUP5 Power Supply	100-240V to 10V DC	0.4 kg	98 x 98 x 46 mm	To be specified	IEC-60601-1, IEC 60601-1-2, CE
TMSi Fusbi signal converter	No power consumption	0.1 kg	55 mm x 112 mm x 26mm	USB to laptop	IEC-60601-1, IEC 60601-1-2, CE
TMSi 3D Accelerometer	Powered by TMSi Porti	0.015kg	13x10x5 mm + 1,5m cable	Connected to TMSi Porti	IEC-60601-1, IEC-60601-1-2

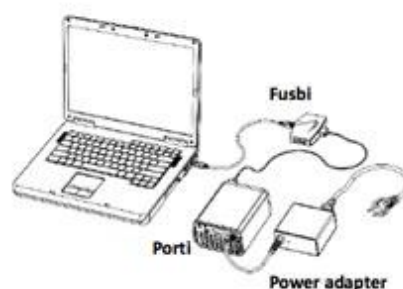


Figure 4: Connection of all TMSi components

#### 4.1 Eye-movement recoding system

During experiment 1, eye movements as a result of EVS will be recorded with an EyeSeeCam (Micromedical Technologies, Chatham). The system consists of an infrared camera with infrared lights to capture the eye. The camera and lights are placed on a swimming-like goggles. The frame of the goggles is covered with custom-made blinders so that external (visible) light cannot reach the eyes. The right eye cover has a hole we tape shut during measurements, but we remove the tape when we are moving the subject to a different position to allow the subject to see something. We will only capture the left eye, and so the left cover includes a plastic filter that only allows infrared light to pass through. The left cover also has a hole that allows it to be vented from time to time if needed. We will use a pump that blows a small amount of clean air onto the cover if the inside gets foggy. It will be taped shut during measurements. This setup allows for the subject to receive no visual information, while the camera can still capture the eye movements. The goggles can be seen in Figure 5. The glass on the outside of the goggles is covered with a see-through tape to prevent it from shattering. On the inside of the left eye cover we will tape silica packages to prevent water vapor to condense on the plastic IR filter.



**Figure 5:** Out- and inside of the EyeSeeCam goggles (shown without camera)

The subjects will wear a scleral lens (Microlens), a hard contact lens that vaults over the cornea. The surface of the lens is covered with markings to allow for accurate tracking of eye movements during the experiments (see Figure 6 for the prototype in use). Because of this lens, the torsional eye-movements can be tracked. The recordings from the camera will be saved and analyzed on a separate laptop (MacBook Air, Apple). At the instant that the stimulation for experiment 1 is started, a signal sent by the DAQ board will be recorded by the camera system to indicate the start of the stimulation on the video recording.



**Figure 6:** Prototype of the marked scleral lens in use

To calibrate the eye, a white sheet is spanned at approx. 1,5 meters away from the subject. The EyeSeeCam has an own integrated calibration program that we will use. Five infrared (visible) calibration points will shine from the calibration sheet and the subject is asked to look at the different points in a certain order. The infrared LEDs are powered by a battery.

Table 4. Camera system

Component	Power	Mass	Dimensions	Connector	Certification
EyeSeeCam (Micromedical Technologies)	5VDC Powered by laptop	0,072 kg		USB to laptop	Medical CE
MacBook Air (Apple)	45W (14.85V 3.05A) Powered by power supply	1,35 kg	325 x 227 x 17 mm	Not applicable	CE
MacBook Air Power supply	100-240 V-AC			Not applicable	CE
Scleral lens	Not applicable	Not important	Not important	Not applicable	Medical CE
5 Infrared LEDS integrated in a foam board	9V Battery	Negligible	56 x 56 cm	Not applicable	None
Silica packets	Not applicable	Negligible	Negligible	Not applicable	See Safety Datasheet
5 Infrared LEDS integrated in a foam board	9V Battery	Negligible	40 x 40 cm	Not applicable	None
Air pump / blower	Not applicable	Negligible	5 x 5 cm	Not applicable	CE

At this moment, the marked scleral lens is still a prototype and thus not certified. Separately, they are medically certified. The lens company works together with the ink company to make the lenses work and have them certified. However, this will probably not be ready at the time of the parabolic flight campaign.

#### 4.2 Muscle activity recording system

During experiment 2, muscle activity (EMG) and exerted forces and moments to the ground in reaction to GVS are measured by self-adhesive surface EMG electrodes (Ambu) and a force plate (AMTI, see Table 5). EMG surface electrodes attached the subject's lower right limb will transmit ongoing muscle activity signals to the 32-channel amplifier for recording (subsystem 3). The measured muscle activity of the plantar flexion muscles will be correlated to the electrical vestibular stimulation. The force plate signals will also be recorded on the same 32-channel amplifier, via a signal conditioner.

To check the position of the subject, a laser distance sensor is mounted to the backboard structure so that it moves with the backboard and thus the subject, see Figure 7. The output of this sensor is converted to the angle of the backboard.



**Figure 7:** Laser distance sensor attached to the backboard

*Table 5. Force plate and laser distance sensor*

<b>Component</b>	<b>Power</b>	<b>Mass</b>	<b>Dimensions</b>	<b>Connector</b>	<b>Certification</b>
AMTI High Frequency Force Platform	10V maximum	18.2 kg	600 x 400 x 83 mm	Connected to the AMTI signal conditioner	CE
AMTI signal conditioner Gen5	120-240 VAC, 50/60 Hz	2 kg	260x210x40 mm	Connected to the TMSi Porti	IEC-60601-1
OptoNCDT 1401-100 laser distance sensor (Micro-Epsilon)	11..30 VDC, max. 150 mA	0.1 kg (without cable)	65 x 50 x 20 mm	BNC cable to DAQ board	CE, DIN EN ISO 9001: 2000

### 5.1 Voice recording system

During experiment 1, subjects will verbally report their perceived motion in reaction to the vestibular stimulation. Their report is recorded with a simple voice recording system that consists of a small microphone (see Table 6) plugged into the laptop and taped next to the subjects mouth. Subjects will be asked to indicate their perceives motion after each stimulation period. Subjects will be trained on the ground prior to the flights on how to properly report the perception of motion (see Chapter 9).

The voice recording system will record continuously during the flight. We may decide to end the recording in the mid-flight break and start a new recording at the beginning of parabola 16.

*Table 6. Microphone*

<b>Component</b>	<b>Power</b>	<b>Mass</b>	<b>Dimensions</b>	<b>Connector</b>	<b>Certification</b>
Apple earbuds with build-in microphone	Powered by laptop (1-10V DC)	32 gr	Not applicable	3.5 mm jackplug to laptop	CE

## 5.2 Subject loading system

The subject loading system (not indicated in figure 3) consists of a body harness attached to two custom made springs on each side of the subject that will be secured to a rail-trolley system, attached to the baseplate. The springs are similar to the setup used in previous parabolic flights by Ritzmann et al. (2015) from the institute of Sport and Sport Science, University of Freiburg, Germany (see Experiment Record No. 9381 and attachment 2 “2\_Ritzmann\_2015”) and will be designed to generate a pulling force equal to the weight of the subject (i.e. 1-g foot loading). During experiment 2, the springs provide a downward force during zero-g to keep the load on the feet and ankles of the subject equal to normal-g conditions and during normal-g to be able to compare the load to hyper-g, while allowing freedom of movement in anteroposterior direction. The harness and springs are designed to avoid stabilizing effects in the horizontal plane. The springs are connected to the harness through heavy duty straps, which can be adjusted per subject to replicate the 1g loading expected for each subject. On the other end, the springs are connected to the rail-trolley system. The rail-trolley system allows the attachment point of the springs to moves together with the subject so that the springs are always pulling straight down. In this way, the load-stiffness curve of the standing body is comparable to normal 1-g conditions. In Figure 8, this rail-trolley system is shown. The components of the system are indicated in Table 7. The subject wearing the harness, will be strapped onto a backboard to limit the range of motion. This backboard set-up is discussed in Chapter 8.

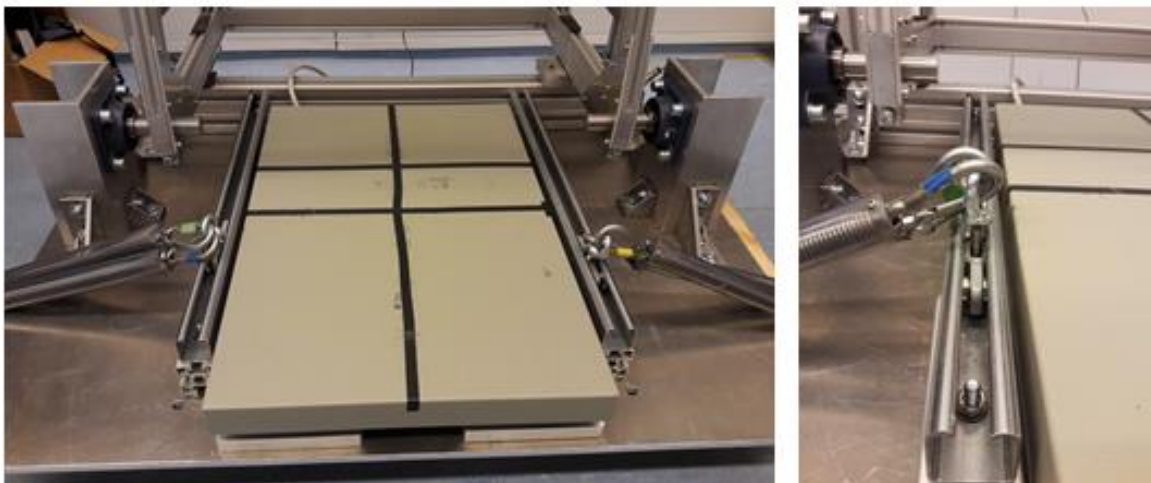


**Figure 8:** Rail-trolley system for spring attachment

The springs are covered in plastic tubes to make sure nothing can get stuck in there. Additionally, in case of spring shattering, the plastic tubes make sure that the metal pieces cannot go anywhere.

The trolleys to which the springs are attached can hold 100 kg each (200kg total). Since all subjects will be under 100 kg., this is definitely enough.

The straps that connect the springs to the harness have a wear load of 2500 N each.

*Table 7. Harness and spring system specifications*

Component	Power	Mass	Dimensions	Connector	Certification
DLR body harness	Not applicable	To be specified	Not important	Not applicable	
Heavy duty straps to	Not applicable	To be specified	Not important	Not applicable	CE

Freiburg University, Custom made springs	Not applicable	ca. 4kg g (1000g each)	length ca. 250mm (350mm when stretched)	Not applicable	None
Carabiner	Not applicable	To be specified	Not important	Not applicable	CE
Rail-trolley system	Not applicable		560 x 35 x 80 mm (l x w x h)	Not applicable	CE

The springs are loaned from Freiburg University and the harness is loaned from DLR.

## 5. Description of the In-Flight Products

Products Used for In-Flight Operations					
Name of Pure Products and/or Solution <sup>(1)</sup>	Existing MSDS (Yes/No)	IATA Class/Division <sup>(2)</sup>	IATA Group <sup>(2)</sup>	Total Quantity per Flight	PRODUCT Containment Means
NuPrep Skin Prep Gel (Weaver, Aurora, Colorado)	Yes	Not regulated	n/a	2 tubes	Tube
Spectra 360 electrode gel (Parker Laboratories, Fairfield, NJ)	Yes	Not regulated	n/a	2 tubes	Tube
Carbon rubber electrodes (Uni-Patch, Wabasha, USA)	No			4	Backpack
Self-adhesive Ag/AgCl Ambu Blue Sensor M surface EMG electrodes (Ambu, Ballerup, Denmark)	No			50	Backpack
Adhesive tape (Durapore)	Yes	Not regulated	n/a	1 roll	Backpack
Skin Cleansing Swabs, saturated with 70% v/v Isopropyl Alcohol (Medi-Swab)	Yes	Not regulated	n/a	4 swabs	Backpack
Fixomull stretch adhesive tape (BSN medical)	Yes	Not regulated	n/a	1 roll	Backback
Elastofix (BSN medical)	No			1 box	Box
Desi-Dry Silica Packets	Yes		n/a	2 packets	Inside the eye tracking goggles

(1) If you use solutions based upon the pure chemicals above, please mention them and mention the concentrations.

(2) Information available in chapter 14 of MSDS.

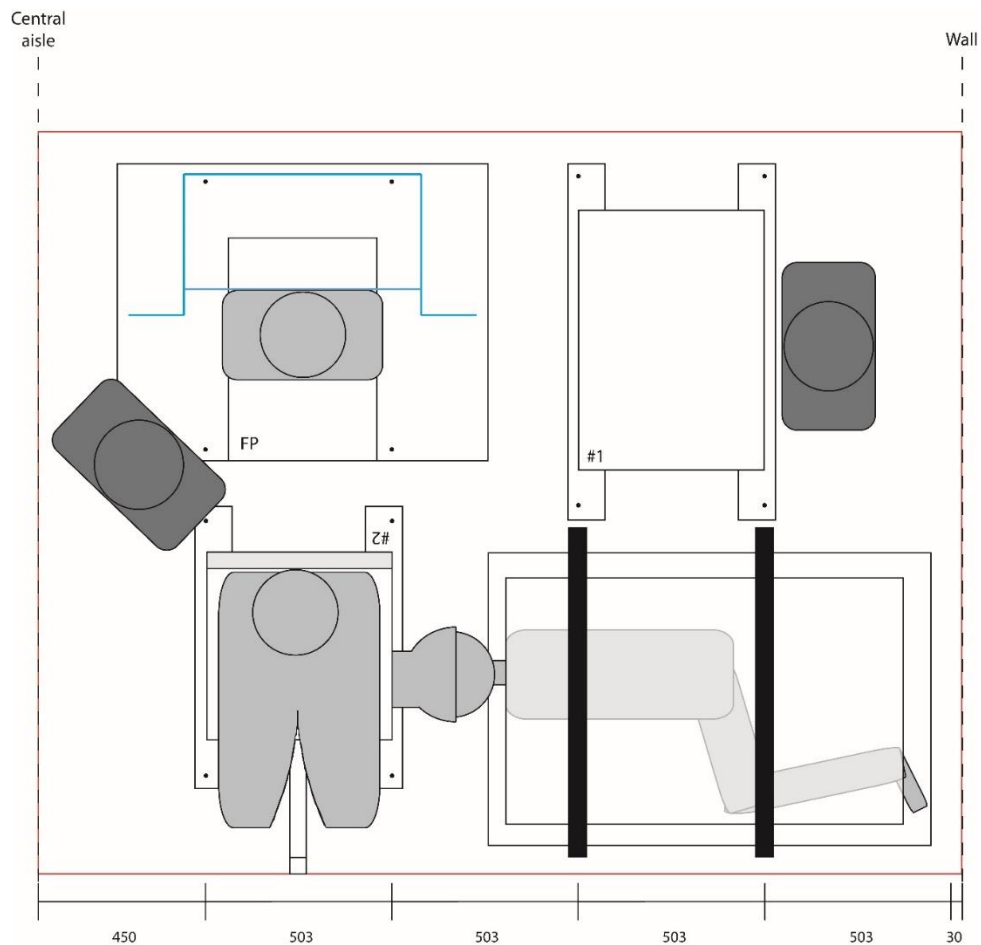
The electrodes for electrical stimulation and EMG measurement will be fixed on the subjects before the flight. If everything goes well, the electrodes will be fixed for the whole flight and we will not need the products listed above. Nevertheless, backup electrodes, gel and tape will be brought on board in the event any electrodes need to be reapplied.

All products are stored in their own containment means. In the flights, they will be kept in a backpack (second containment means).

## 6. Technical Specification of the Experiment

### 6.1. Cabin Layout

#### Top view of cabin layout



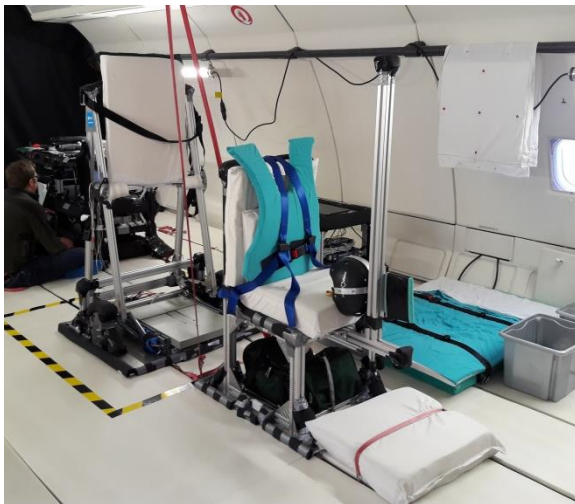
In the cabin layout shown above, the red box represents an area of 2 x 2,49 meters (i.e. the area we can use). The subjects are depicted in light grey; the subject in rack #2 is seated for experiment 1, the subject in rack #3 stands on the force plate for experiment 2. The experimenters are depicted in dark grey; one experimenter will be standing or kneeling behind rack #1 with all the equipment, the other experimenter will keep an eye on the subjects. The cabin layout shows the 3 racks that we will need for our experiments.

1. Rack 1 holds all measurement equipment of experiment 1 and 2. The rack will be 700x500x600mm with a light intermediary shelf at 300 mm from the ground and a lower shelf. Subsystems with a red block around it in Figure 2 are installed on this rack. The rack design is discussed in more detail in chapter 8.
2. Rack 2 functions as a chair for the subject of experiment 1. The base of the chair is a 500x500x430mm rack to which a backrest is attached together. The chair has an additional vertical and horizontal profile to which the helmet can be clamped. With this helmet, the subjects' heads are restrained.

- Rack 3 contains the force plate, subject loading system and backboard structure (blue in the cabin layout drawing) for experiment 2. All elements will be mounted on a baseplate which will be 800x1000x10mm.

Attachment points of the racks with base bars and the baseplates are shown as little black dots. Cockpit direction may be to either side for our experiments.

The photos below show the set-up in the plane.



**Cabin Side**

For our experiment, the side on which we will be located does not matter. If the experiment is swapped from one side to the other, everything should be mirrored over the axis of the central pathway to the cockpit. This way, rack 3 will remain situated next to the central aisle, to allow the subject to stand fully upright during experiment 2.

**Location in the Cabin**

Location in the cabin	Front	Middle	Rear
Right	X	X	X
Left	X	X	X

**6.2. Flight Crew**

	Flight #1	Flight #2	Flight #3	Flight #4
Flight Operator(s)	2	2	2	Not applicable
Test subject(s) <sup>(1)</sup>	2	2	2	Not applicable
Total number of seats	4	4	4	Not applicable

(1) Only for biomedical experiments involving test subjects

**6.3. Overall Rack Weight and Dimensions**

Rack Number	Weight (kg)	Length – X axis (mm)	Width – Y axis (mm)	Height – Z axis (mm)
-------------	-------------	----------------------	---------------------	----------------------

#1	63	980	590	610
#2	41	1000	590	1550
#3	75	850	1000	1600

#### 6.4. Power Supply

The equipment that need to be powered externally are the laptops, the DAQ-board, the two electrical stimulators, SUP5 (power supply of 32-channel amplifier), the force plate conditioner and the laser sensor.

Aircraft Power Source	Theoretical Power Consumption (W)	Measured Nominal/Peak Power consumption (W)	Location of Novespace Electrical Power Block	Main Fuse Value (A)
#1	220W	85W/85W	On rack 1	TBD

#### 6.5. Vent-line Connection

Connection to vent-line	No
Nature of the evacuated product(s)	-
Max. temperature of the evacuated product(s)	-
Max. flow rate of the evacuated product(s)	-
Max pressure of the evacuated product(s)	-
Type of pipe to connect the vent-line	-

#### 6.6. Nuisances and Sensitivities

##### Experiment Nuisances

Noise:	No
Odors:	No
Vibrations:	No
Electromagnetic fields:	No
Wireless comm. System:	No
Others:	No

##### Experiment Sensitivities

Noise:	No
Odors:	No
Light:	No
Vibrations:	Yes: Strong vibrations might interfere with the force plate measurements
Electromagnetic fields:	Yes: Strong electromagnetic pulses might interfere with the EMG signal
most sensitive axis(es) to g variation	x-axis, this will influence the balance of our subjects
Others:	No

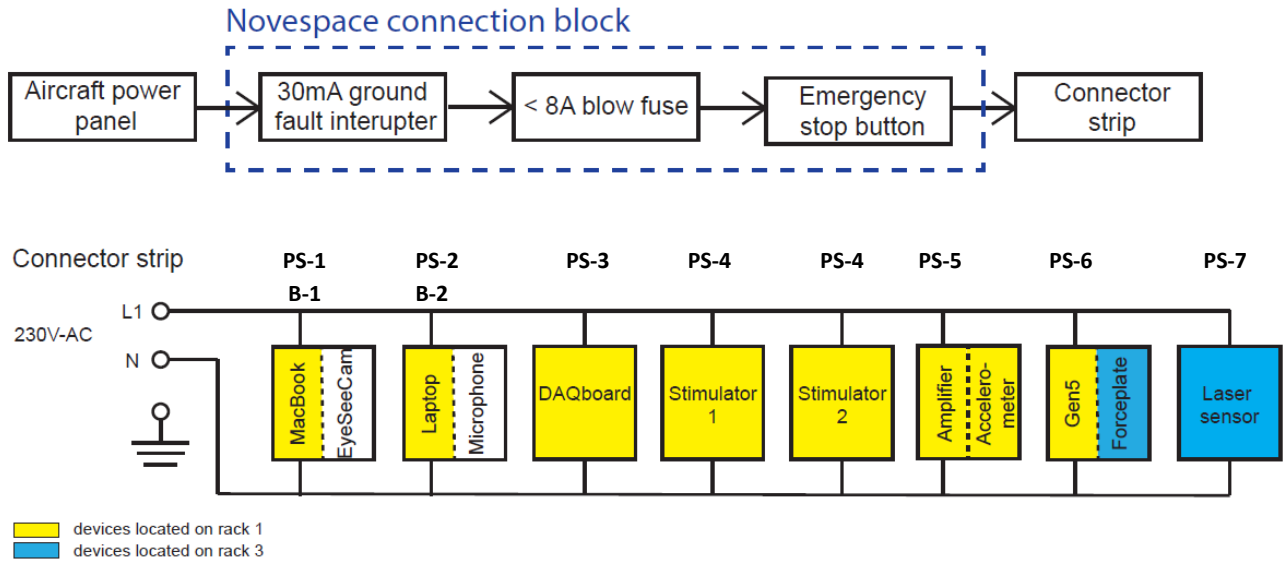
#### 6.7. Specific In-Flight Requirements

We don't have specific in-flight requirements.

## 7. Electrical System

### 7.1. Electrical block diagram

Below, the electrical block diagram is shown. We will make use of the Novespace connection block.



As the block diagram shows, eight devices need a power source coming from the aircraft (2x stimulator).

### 7.2. Power supplies and Converters

Power Supplies Reference	Input / Output voltage	List of Equipment	Equipment Purchased with its Power Supply <sup>(1)</sup> (Yes/No)	Min. Output Wire Gauge (mm <sup>2</sup> ) <sup>(2)</sup>	Output Fuse Protection (A) <sup>(2)</sup>
PS-2	120-230V-AC/19.5V-DC	<ul style="list-style-type: none"> <li>Dell Laptop</li> </ul>	Yes	N/A	N/A
PS-1	100-240V-AC/	<ul style="list-style-type: none"> <li>MacBook Air</li> </ul>	Yes	N/A	N/A
PS-3	100-240V-AC/12V-DC	<ul style="list-style-type: none"> <li>DAQ-board</li> </ul>	Yes	N/A	N/A
PS-5	100-240V-AC/10V-DC	<ul style="list-style-type: none"> <li>32-channel amplifier</li> </ul>	Yes	N/A	N/A
PS-4	100-240V-AC/±10V-DC	<ul style="list-style-type: none"> <li>Electrical stimulator</li> </ul>	Yes	N/A	N/A
PS-6	120-240V-AC/15V-DC	<ul style="list-style-type: none"> <li>Force-plate</li> </ul>	Yes	N/A	N/A
PS-7	240V-AC/24 VDC	<ul style="list-style-type: none"> <li>Laser sensor</li> </ul>	No	0.2	0.5

(1) Reply "YES" if the power supply is dedicated to the equipment and purchased with it (example: laptop). Reply "NO" if the power supply and the related powered equipment are purchased separately (example: laboratory power supply, multipurpose power supply....)

(2) To be completed if the power supply and the related powered equipment are purchased separately, otherwise enter "N/A".

### 7.3. Batteries

Battery Reference	Voltage (V)	Capacity (Ah / Wh)	Powered Equipment	Technology (LiPo, NiCad, NiMH, ...)	Purchase Date <sup>(1)</sup>	Check if Part of Recall Program (Yes/No) <sup>(2)</sup>
-------------------	-------------	--------------------	-------------------	-------------------------------------	------------------------------	---

B-2	19.5 V	42 Wh	Dell Laptop	3-cells lithiumion	21-11-2017	No
B-1	14.85 V	54 Wh	MacBook Air	LiPo	12-2016	No

(1) Applicable for laptop, UPS and other heavy-duty battery

(2) Applicable for laptop only

#### 7.4. Electrical Item Verification Checklist

Item of Verification	Yes – No – N/A – Date
Presence of an emergency pushbutton capable of turning off the complete hardware <sup>(1)</sup>	N/A
Emergency push button switches off both phase and neutral of the power line <sup>(1)</sup>	N/A
Presence of Ground Fault Interrupter (GFI) rated at max. 30mA <sup>(1)</sup>	N/A
Measurement of experiment power consumption <sup>(2)</sup>	85 W 27/11/2017
Check of experiment conductive surface grounding	27/12/2017
Absence of accessible powered conductive surface	Yes
Availability of technical documentation of all electrical equipment	Yes
Check that wires, power supplies are tightly secured.	Yes

(1) State "n/a" if the Novespace power plug is used to connect the experiment to the aircraft power panel

(2) Report measured values from chapter §0

## 8. Structure

As indicated in Chapter 6, we will build three experimental racks.

### Rack #1: Equipment rack

*Description:* Rack 1 will hold most systems that we use for the experiments. These are:

- Laptop + adapter (<3,5 kg) (top shelf)
- MacBook Air + adapter (<2,5 kg) (top shelf)
- 2 stimulators (4 kg per stimulator) (lower shelf)
- DAQ board + fan-out board (0,816 kg + 0,7 kg) (middle shelf)
- Amplifier + accelerometer (1,265 kg total) (middle shelf)
- Force plate conditioner (2 kg) (middle shelf)

Photos of the rack are given in Figure 9 (note that in the drawing the base bars are too small and miss the brackets parallel to the y-axis). The placement of the equipment on the rack is shown in Figure 10.

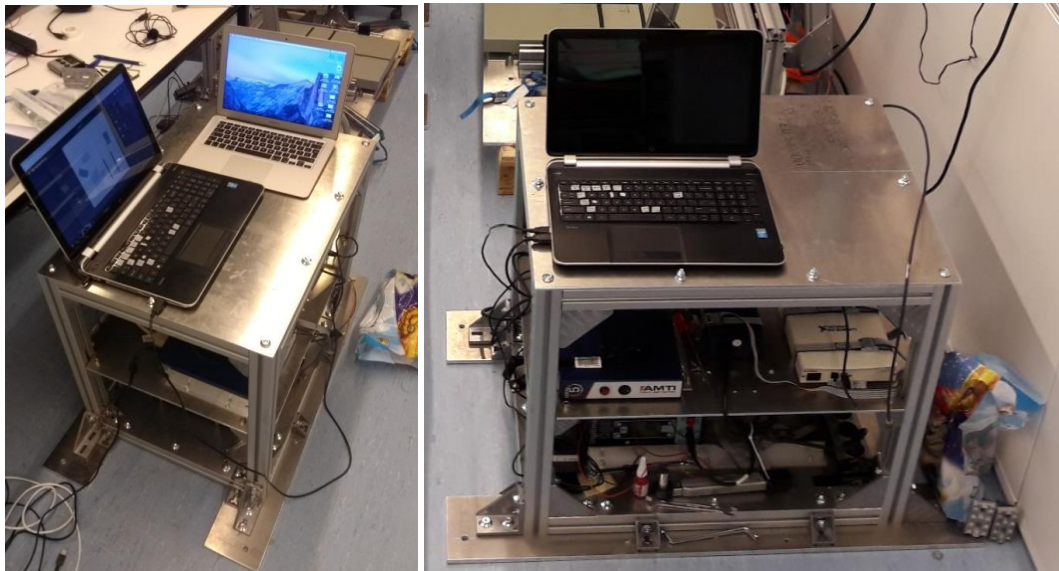


Figure 9: Photos of rack 1

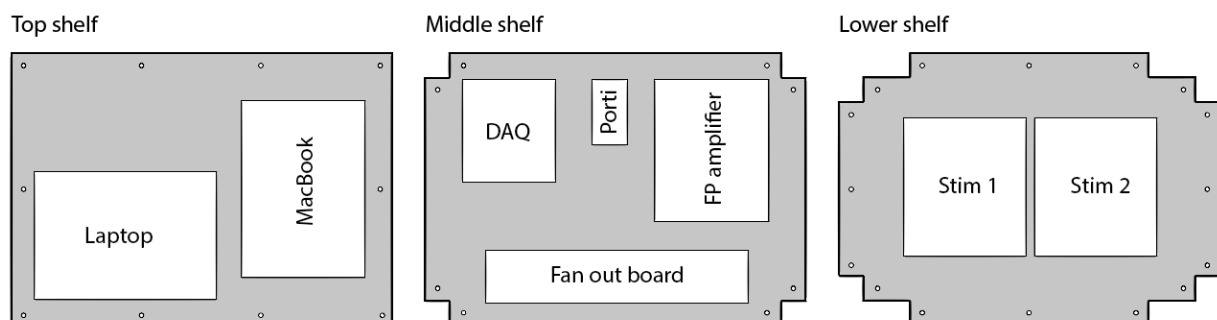


Figure 10: Lay-out rack 1

*Specifications:*

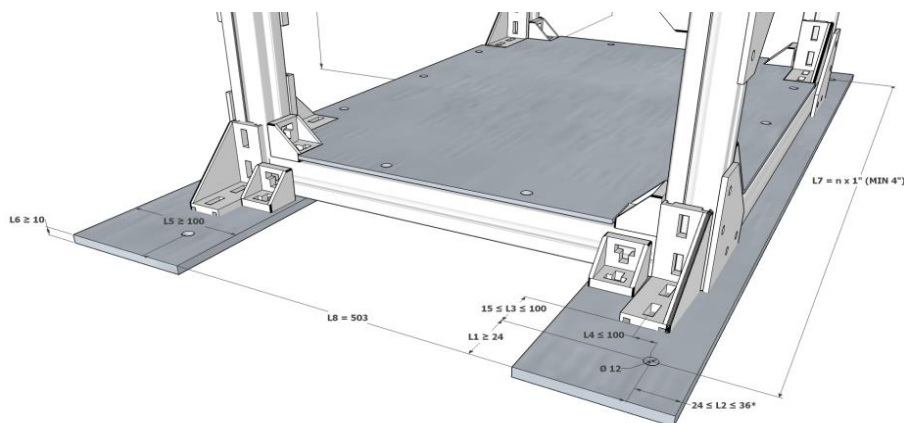
- The rack will be a standard primary structure with dimensions 700x500x600mm and 3 light shelves (one at 45mm, one at 300mm and one at 600mm). The rack will be connected to two base bars, which connect to the seat tracks.
- Straps are used as equipment blocking in the z-direction with a wear load of 1500 N

*Characteristics of the Rack*

Strut profile brand name	Bosch Rexroth
Strut profile reference	www.boschrexroth.com
Strut profile cross-section	45 x 45 mm
Base plate/bars aluminum ultimate strength	275 - 350 MPa
Confirm that a torque wrench has been used for tightening the primary structure bolts, in accordance with the recommendations of the strut profile provider	Yes
Confirm that thread locking compound has been used on primary structure bolts	Yes

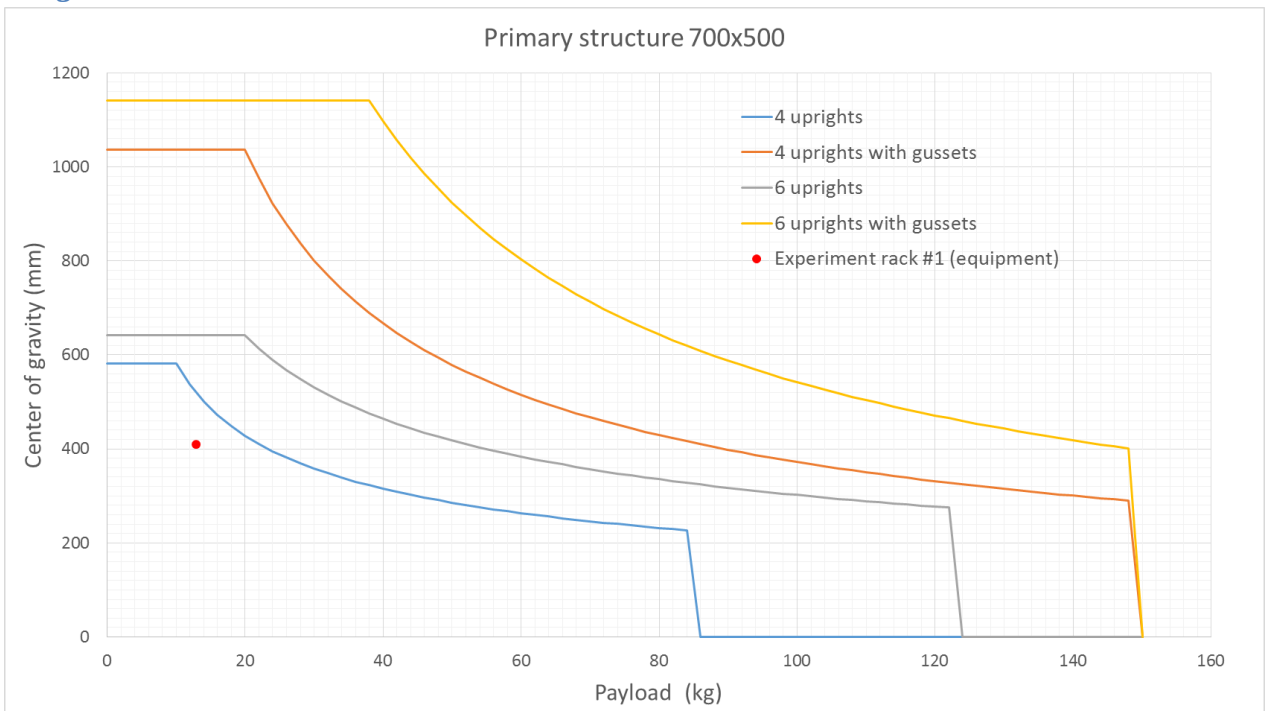
Table summarizing the weight distribution in the rack:

Experiment rack #1 (equipment)				
	Item	COG (mm)	Structural mass (kg)	Payload (kg)
Participating to bending	Primary structure: 700mm X ; 500mm Y ; 600mm Z	300	20,2	0,0
	Top shelf (700 x 500 x 5 mm, light)	600	5,5	3,5
	Middle shelf (700 x 500 x 5 mm, light)	300	0,0	8,3
Not participating to bending	Base bars (2 bars of 980 x 135 x 10 mm)	0	7,4	0,0
	Lower shelf (700 x 500 x 5 mm)	45	5,5	8,0
Total mass (kg)			38,6	19,8
			58,4	
Experiment rack CoG (mm)			249,2	
<b>Bending payload mass +10% (kg)</b>			<b>13,0</b>	
<b>Bending CoG +10% (mm)</b>			<b>409,2</b>	



L1:	32.8 mm	$L1 \geq 24 \text{ mm}$
L2:	43.5 mm	$24 \leq L2 \leq 36 \text{ mm}$
L3:	15 mm	$15 \leq L3 \leq 100 \text{ mm}$
L4:	24 mm	$L4 \leq 100 \text{ mm}$
L5:	135 mm	$L5 \geq 100 \text{ mm}$
L6:	10 mm	$L6 \geq 10 \text{ mm}$
L7:	$36 * 25.4 \text{ mm} = 914.4 \text{ mm}$	$L7 \geq 4 * 25.4 \text{ mm}$
L8:	503 mm	$L8 = 503 \text{ or } L8 = 1006 \text{ mm}$

**Margins**



**Linear Loading**

Insert here a figure or a table showing status of the linear loading:

Quick Linear Load Assessment	Value	Unit
Total mass of the experiment rack + 10% (kg)	64	Kg
Total number of attachment points	4	-
Height of CoG + 10% (mm)	274	mm
Is the CoG centered in XY plane? (see GDL)	YES	-
Has the experiment more than two attachment points on 530mm/X?	NO	-
Minimum Pitch between fixation points /X	503	mm
<b>Status</b>	<b>Ok</b>	-

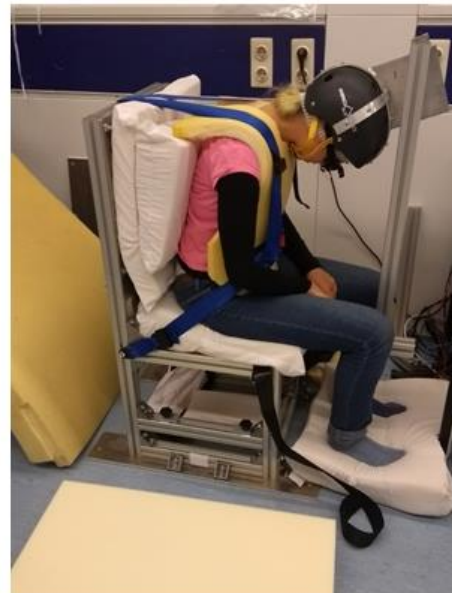
## Rack #2: Chair for experiment 1

*Description:* Rack 2 needs to hold a subject with a maximum weight of 100 kg. The heavy shelf functions as the seat and is covered with memory foam. From this seat-part, a horizontal beam extends with a vertical beam attached to it. The location of this vertical beam can be adjusted by sliding across the horizontal profile to suit the subject. The subject will wear a helmet with an aluminum fin that will be clamped onto this profile to stabilize the head in head down position. A backrest is attached to this primary standard structure with brackets, under a 90° angle. The backrest is also covered with a thin layer of memory foam. Below the backrest, another horizontal profile will be attached. The height of this profile can be adjusted to suit the subject by sliding in-between the vertical beams. The helmet will be clamped onto this profile to stabilize the head in the head straight position. Seat belts that will secure the subject are mounted to the back of the chair, see Figure 11 for photos of this set-up. The fin on the helmet will be covered by a foam cover while subjects are unrestrained or when the helmet is not worn to prevent any injury due to collision with the fin. The standard primary structure of the rack will be connected to two base bars that connect to the seat tracks.

**Figure 11:** Subject seated in the chair. Right: helmet is clamped to the vertical beam to support head-down position. Left:



helmet is clamped to the horizontal profile to support head-straight position.



### *Specifications:*

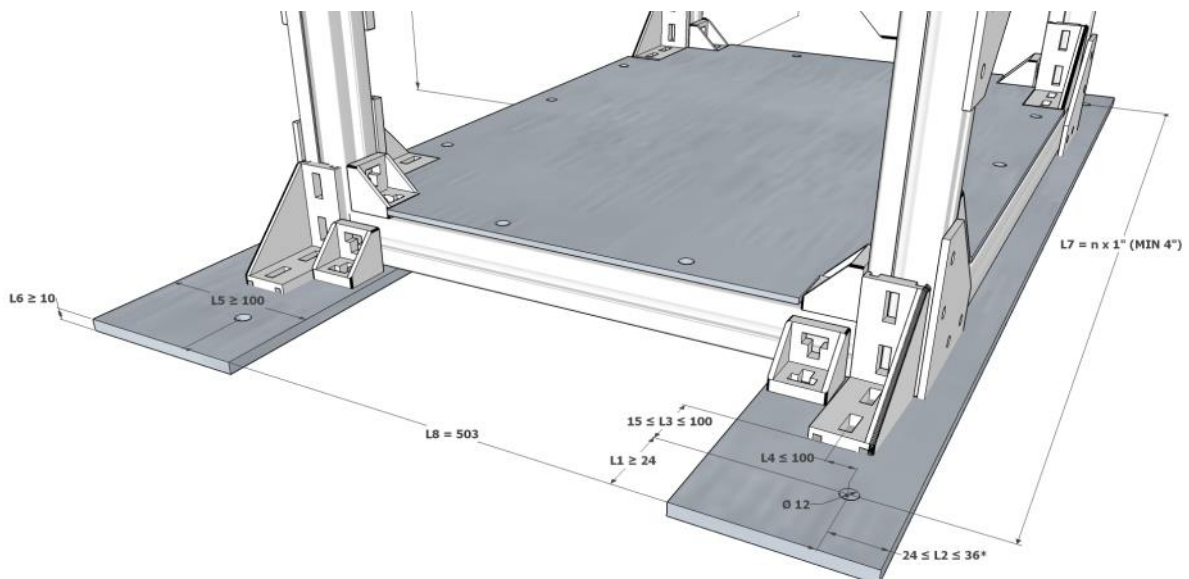
- The seat part of the chair will be a standard primary structure of 500x500x430mm with one heavy shelf on top.
- The dimensions of the base bars are: 770 x 135 x 10 mm

### Characteristics of the Rack(s)

Strut profile brand name	Bosch Rexroth
Strut profile reference(s)	www.boschrexroth.com
Strut profile cross-section(s)	45 x 45 mm
Base plate/bars aluminum ultimate strength	275 - 350 MPa
Confirm that a torque wrench has been used for tightening the primary structure bolts, in accordance with the recommendations of the strut profile provider	Yes
Confirm that thread locking compound has been used on primary structure bolts	Yes

Table summarizing the weight distribution in the rack:

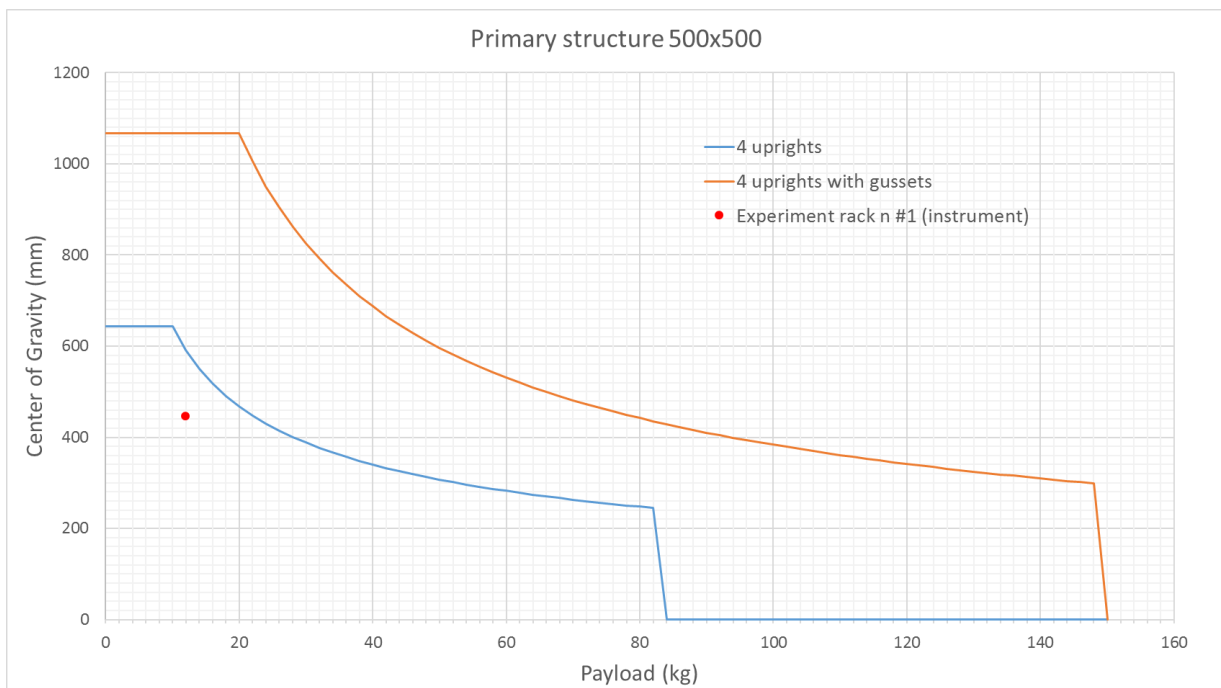
Experiment rack n #1 (instrument)				
	Item	COG (mm)	Structural mass (kg)	Payload (kg)
Participating to bending	Primary structure: 500mm X ; 500mm Y ; 430mm Z	215	16,0	0,0
	Top shelf (500x500x5mm) + extending profiles	430	3,4	2,6
	Payload top shelf with higher CoM	755	0,0	8,3
Not participating to bending	Base bars (2 bars of 770x135x10mm)	0	5,7	0,0
Total mass (kg)			25,1	10,9
			36,0	
Experiment rack CoG (mm)				341,5
<b>Bending payload mass +10% (kg)</b>				<b>12,0</b>
<b>Bending CoG +10% (mm)</b>				<b>445,9</b>



L1:	29.4 mm	$L1 \geq 24 \text{ mm}$
L2:	43.5 mm	$24 \leq L2 \leq 36 \text{ mm}$
L3:	15.6 mm	$15 \leq L3 \leq 100 \text{ mm}$
L4:	24 mm	$L4 \leq 100 \text{ mm}$
L5:	135 mm	$L5 \geq 100 \text{ mm}$
L6:	10 mm	$L6 \geq 10 \text{ mm}$
L7:	$28 * 25.4 \text{ mm} = 711.2 \text{ mm}$	$L7 \geq 4 * 25.4 \text{ mm}$
L8:	503 mm	$L8 = 503 \text{ or } L8 = 1006 \text{ mm}$

### Margins

Insert here a figure or a table showing the margins:



### Linear Loading

Insert here a figure or a table showing status of the linear loading:

Quick Linear Load Assessment	Value	Unit
Total mass of the experiment rack + 10% (kg)	40	Kg
Total number of attachment points	4	-
Height of CoG + 10% (mm)	376	mm
Is the CoG centered in XY plane? (see GDL)	YES	-
Has the experiment more than two attachment points on 530mm/X?	NO	-
Minimum Pitch between fixation points /X	503	mm
<b>Status</b>	<b>OK</b>	-

### Rack #3: Baseplate and backboard structure for experiment 2

*Description:* Rack 3 consists of a 800x1000x10mm baseplate that holds the force plate and the backboard structure (see drawing in Figure 13). The backboard structure is connected to the baseplate via bearing supports and can therefore swivel in forward and backward direction. A bumper structure is mounted to the baseplate to prevent the subject from falling and limits the movement from the backboard structure to 6° backward and 10° forward. The subjects will be secured to the backboard with two seatbelts. At both sides of the force plate a rail is placed through which a trolley will be able to move. In Figure 14, the experimental set-up is shown. When the springs are not in use (also during take-off and landing), they will be fixed to the baseplate with Velcro. During take-off and landing, the backboard is secured in the backward position with two straps.

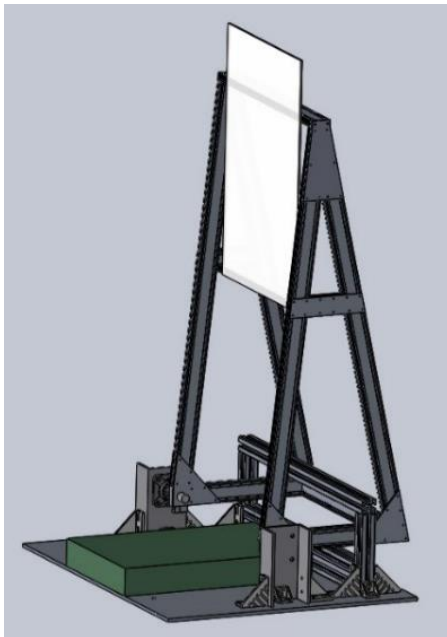


**Figure 13:** Rack 3, this rack functions as baseplate for the force plate and for a backboard structure



**Figure 14:** Photo of rack 3 with force plate and rail trolley system

### Forceplate structural integrity

The mechanical characteristics of our force plate (AMTI 400600HF-1000) are as follows:

<b>BP400600HF SERIES SPECIFICATIONS</b>	<b>1000</b>
<b>Fx, Fy Capacity, lb, (N)</b>	500 (2225)
<b>Fz Capacity, lb, (N)</b>	1000 (4450)
<b>Mx Capacity, in*lb, (Nm)</b>	11800 (1300)
<b>My Capacity, in*lb, (Nm)</b>	7900 (900)
<b>Mz Capacity, in*lb, (Nm)</b>	5900 (700)
<b>Fx, Fy Natural Frequency, Hz</b>	470
<b>Fz Natural Frequency, Hz</b>	780
<b>Fx, Fy Sensitivity, <math>\mu\text{V}/[\text{V}^*\text{lb}]</math>, (<math>\mu\text{V}/[\text{V}^*\text{N}]</math>)</b>	3.0 (0.67)
<b>Fz Sensitivity, <math>\mu\text{V}/[\text{V}^*\text{lb}]</math>, (<math>\mu\text{V}/[\text{V}^*\text{N}]</math>)</b>	0.75 (0.17)
<b>Mx Sensitivity, <math>\mu\text{V}/[\text{V}^*\text{in}^*\text{lb}]</math>, (<math>\mu\text{V}/[\text{V}^*\text{Nm}]</math>)</b>	0.158 (1.394)
<b>My Sensitivity, <math>\mu\text{V}/[\text{V}^*\text{in}^*\text{lb}]</math>, (<math>\mu\text{V}/[\text{V}^*\text{Nm}]</math>)</b>	0.201 (1.776)
<b>Mz Sensitivity, <math>\mu\text{V}/[\text{V}^*\text{in}^*\text{lb}]</math>, (<math>\mu\text{V}/[\text{V}^*\text{Nm}]</math>)</b>	0.369 (3.268)
<b>Height, in, (mm)</b>	3.25 (82.5)
<b>Weight, lb, (Kg)</b>	40 (18.2)
<b>Top Plate Material</b>	composite

Therefore, in case of a 9g forward acceleration, the safety factor (SF) for our forceplate structural integrity is:

$$SF = \frac{M_x \text{Capacity}}{\text{Weight} \times 9 \times g} = \frac{2225}{18.2 \times 9 \times 9.81} = 1.38$$

This safety factor is considered satisfactory for an equipment weighing less than 20kg, especially considered that the  $M_x$ Capacity figure provided by the datasheet is already likely to include a safety factor of its own.

### ***Force plate/baseplate fixation***

The force plate (18.2kg) is one solid structure and is connected to the baseplate with 4 countersunk M10 class 8.8 bolts, able to withstand a shear load of 27840N each.

The resulting safety factor would therefore be:

$$SF = \frac{\text{Max shear load} * 4}{\text{Weight} \times 9 \times g} = \frac{27840 * 4}{18.2 \times 9 \times 9.81} = 4.33$$

### Backboard calculations

With this set-up, the subjects always have to face the back side of the plane. For this configuration, calculations are performed to check the strength of the backboard structure.

#### Specifications:

- The backboard structure is made from 20x60 mm Bosch-Rexroth profiles and the bumper structure from 45x45 mm Bosch-Rexroth profiles. The backboard plate itself is a 6 mm thick polycarbonate and is covered with 25 mm thick foam.
- The baseplate is 800x1000x10 mm.
- All non-straight angles of the triangle structure are strengthened with 5 mm thick aluminum plates with an ultimate strength of 275-350 MPa
- The triangle structure is 1.57 m high and 0.64 m wide
- The weight of the total triangle structure (incl. plates and brackets) is 10 kg
- Calculations are done with a mass of 15 kg to include a safety factor
- Backward position is 6° back and forward position is 10° forward ( $\theta = 6^\circ$  or  $10^\circ$ )
- The force plate is one solid structure and is connected to the baseplate with 4 countersunk M10 class 8.8 bolts
- The straps that are used to hold that backboard during take-off and landing have a wear load of 1500 N.
- The straps that are used for spring connection have a wear load of 2500 N.

#### Force calculations emergency landing

The force calculations are done for the following situation:

- During emergency landing (7.3g down, 9g backwards, 3g sideways), so without subject
- Structure is fastened in backward position (leaning against bumper)

① The location of the center of mass (CoM) is determined for a backward position (in upright position, values for  $l_1$  and  $l_2$  are given by SolidWorks). A is the position of the bearing, the drawings are from a side view.

Parameters:

$$l_1 = 0.15m; l_2 = 0.62m$$

$$l_3 = \sqrt{l_1^2 + l_2^2} = 0.638$$

$$\alpha = \tan^{-1}(l_1/l_2) = 13.6^\circ$$

$$l_4 = \sin(\alpha + \theta) \cdot l_3 = 0.21$$

$$l_5 = \cos(\alpha + \theta) \cdot l_3 = 0.60$$

② Forces in the x-z-plane are calculated. (The drawing is simplified, only the triangle structure is shown, the backboard plate is not. Drawing is a side view in the x-z plane, A is the bearing.)

Parameters:

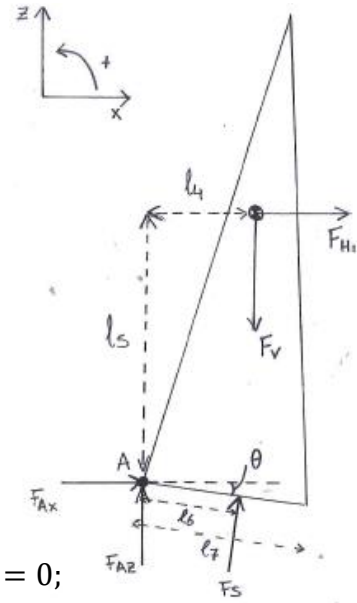
$$\begin{aligned}
 l_4 &= 0.21 \text{ m} & \theta &= 6^\circ \\
 l_5 &= 0.60 \text{ m} & m &= 15 \text{ kg} \\
 l_6 &= 0.25 \text{ m} & F_v &= m \cdot g \cdot 7.3 = 1074 \text{ N} \\
 l_7 &= 0.44 \text{ m} & F_{H1} &= m \cdot g \cdot 9 = 1324 \text{ N}
 \end{aligned}$$

Determine  $F_S$  (force on the bumper structure):

$$\begin{aligned}
 \Sigma M_A &= 0; \\
 -F_v \cdot l_4 - F_{H1} \cdot l_5 + F_S \cdot l_6 &= 0; \\
 F_S &= \frac{F_v \cdot l_4 + F_{H1} \cdot l_5}{l_6} = 41780 \text{ N}
 \end{aligned}$$

Determine forces at A:

$$\begin{aligned}
 \Sigma F_x &= 0; & \Sigma F_z &= 0; \\
 F_{H1} + F_{Ax} + F_S \cdot \sin \theta &= 0; & -F_v + F_{Az} + F_S \cdot \cos \theta &= 0; \\
 F_{Ax} &= -F_{H1} - F_S \cdot \sin \theta = -1761 \text{ N} & F_{Az} &= F_v - F_S \cdot \cos \theta = -3081 \text{ N}
 \end{aligned}$$



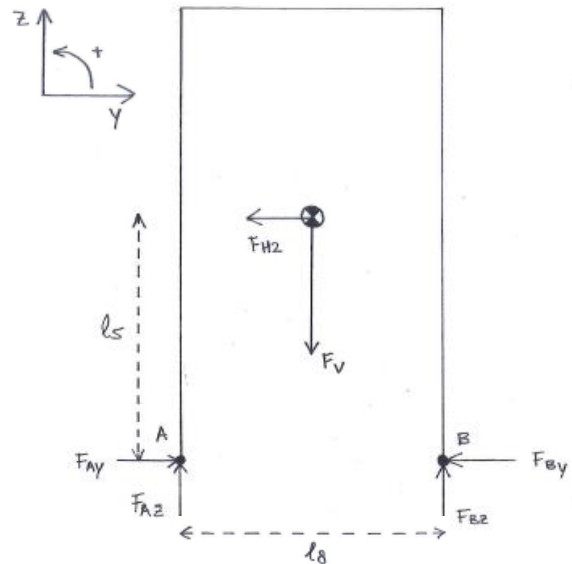
N.B. These calculated forces are supported by two bearings and bumper points so they should be divided by 2 when doing stress calculations!

③ Forces in the y-z-plane are calculated.

Parameters:

$$\begin{aligned}
 l_5 &= 0.60 \text{ m} & m &= 15 \text{ kg} \\
 l_8 &= 0.62 \text{ m} & F_v &= m \cdot g \cdot 7.3 = 1074 \text{ N} \\
 & & F_{H2} &= m \cdot g \cdot 3 = 441.5 \text{ N}
 \end{aligned}$$

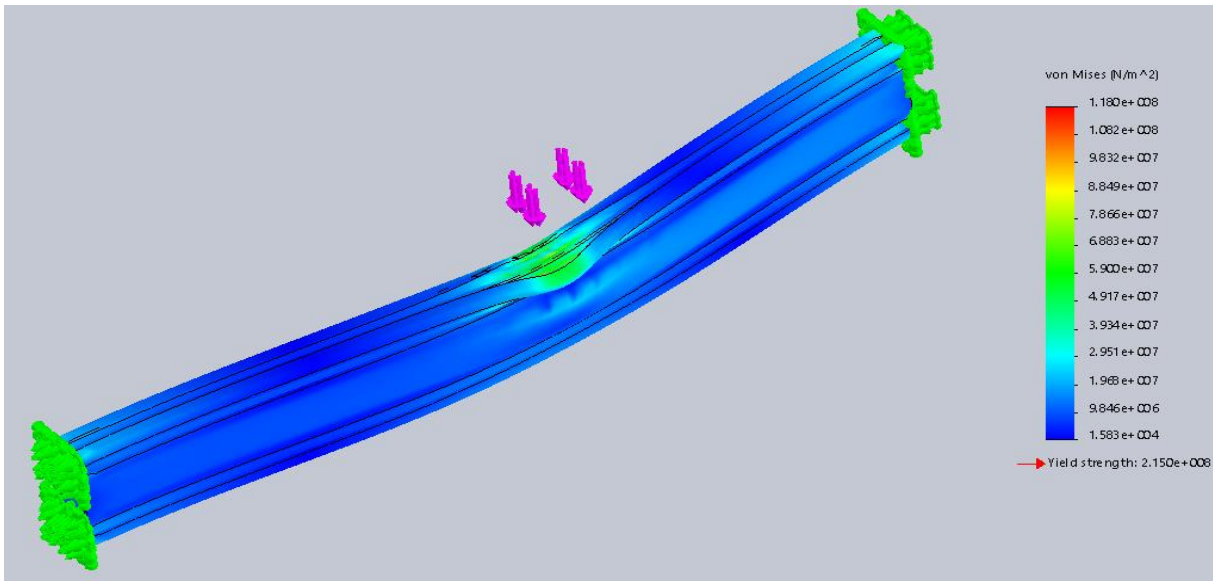
We did not solve the forces at the support ourselves. We run the structure (simplified!) with the loads through a software (SkyCiv) which gave us much lower values for the reaction forces, moments and shear forces than the situation above (point 2). Of course, the force in y direction during an emergency landing is much lower than in the x direction. Therefore, we are confident that the structure will also withstand this situation.



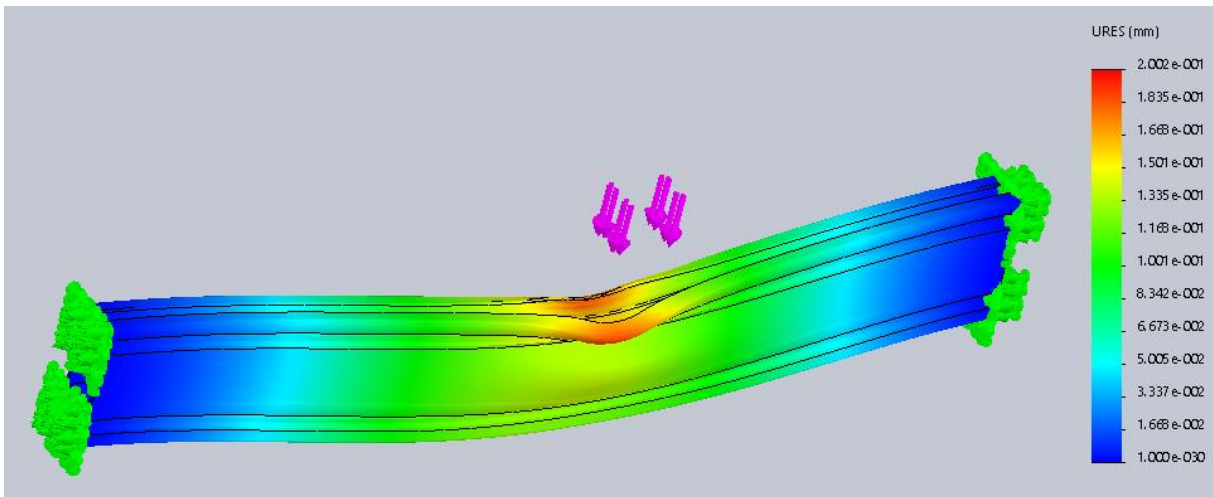
④ Stresses in the beams are calculated.

We performed a stress analysis in Solidwork to compute the maximum stresses on the beam that bumps into the bumper structure. This is the location where the highest forces and stresses will originate. To do this, we specified that the beam is rigidly fixed at both ends and we applied a force of 2100N (approx. half of  $F_S$ ) to the place where the beam hits the bumper. As can be seen from the

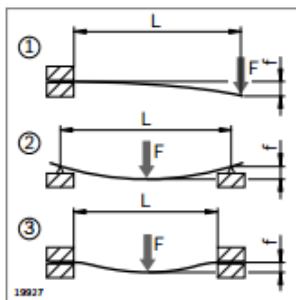
figure, the highest stress in the beam is equal to 118 N/mm<sup>2</sup>, which is below the Yield strength which is 195 N/mm<sup>2</sup> for strut profiles according to Bosch Rexroth.



In the drawing below the displacement looks big but that is just an exaggeration. In the following figure the displacements can be seen (maximum displacement of 0,20 mm).



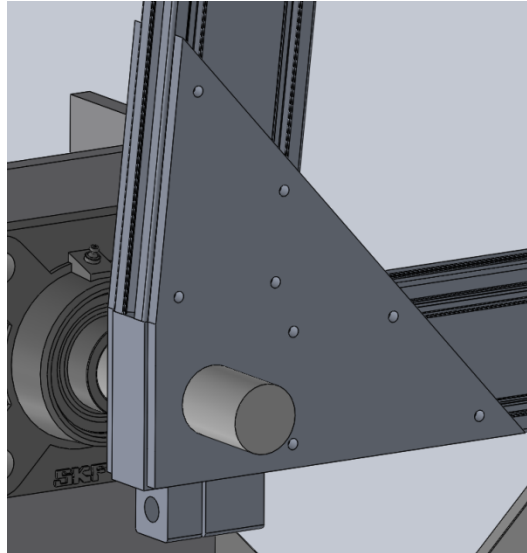
When calculating the maximum occurring bending stress using the formula provided by Bosch Rexroth (see figure below), the bending stress is only 92.75 N/mm<sup>2</sup>. Note that Solidworks gives the total stress in the beam, including bending and shear stress. Also, our set-up is more stiff than illustrated in the 2<sup>nd</sup> situation of the figure.



$$\sigma_{\ominus} = \frac{(m' \times g \times L + F) \times L}{4 W \times 10^3}$$

### ⑤ Bearing connection

We use a bearing of SKF with a diameter of 25 mm (SKF FY25TF). To make sure that the bearing is connected well to the structure, we use a solid aluminum block through which the shaft of the bearing runs, so that we do not have to drill a big hole in the profiles. This block is connected to the profiles with 5 mm thick aluminum plates covering all the surfaces, see SolidWorks model in the figure below.



### Force calculations subject

The force calculations are done for the following situation:

- a subject is leaning against the backboard structure in backward position ( $6^\circ$ ) during hyper-g ( $2g$ ) (see ⑥)
- a subject is leaning forward ( $10^\circ$ ) with the backboard structure during hyper-g, the bumper stops the subject from further forward movement (not the intention but may happen if subject loses balance, see ⑦)
- the weight of the subject is 100 kg max. and the mass of the structure = 10 kg. This makes the total mass 110 kg. To include a safety factor of 1.5, calculations are done for a mass of 165 kg.

⑥ Forces in the x-z plane are calculated for a subject leaning  $6^\circ$  backwards against the backboard during hyper-g. The center of mass of a subject is estimated at a height of 0.9 meter relative to the bearing height. (The drawing is simplified, only the triangle structure is shown, the backboard plate is not. Drawing is a side view in the x-z plane, A is the bearing.)

Parameters:

$$l_6 = 0.25 \text{ m}$$

$$m = 165 \text{ kg}$$

$$l_9 = 0.9 \text{ m}$$

$$F_p = m \cdot g \cdot 2 = 3237,3 \text{ N}$$

$$\theta = 6^\circ$$

Determine  $F_S$  (force on the bumper structure):

$$\Sigma M_A = 0;$$

$$-F_p \cdot l_9 \cdot \sin \theta + F_S \cdot l_6 = 0;$$

$$F_S = \frac{F_p \cdot l_9 \cdot \sin \theta}{l_6} = 1241 \text{ N}$$

Determine forces at A:

$$\Sigma F_x = 0;$$

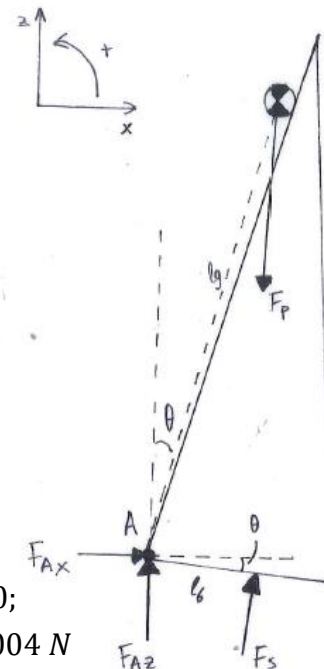
$$F_{Ax} + F_S \cdot \sin \theta = 0;$$

$$F_{Ax} = -F_S \cdot \sin \theta = -130 \text{ N}$$

$$\Sigma F_z = 0;$$

$$-F_p + F_{Az} + F_S \cdot \cos \theta = 0;$$

$$F_{Az} = F_p - F_S \cdot \cos \theta = 2004 \text{ N}$$



N.B. These calculated forces are supported by two bearings and bumper points so they should be divided by 2 when doing stress calculations!

The forces  $F_S$ ,  $F_{Ax}$  and  $F_{Az}$  are all lower than the forces calculated for the emergency landing situation (see ②) so stress calculations for this situation are not needed (i.e. we are confident that the structure can hold the subject during hyper-g in a backward position).

⑦ Forces in the x-z plane are calculated for a subject leaning  $10^\circ$  forward with the backboard during hyper-g.

Parameters:

$$l_6 = 0.25 \text{ m} \quad m = 165 \text{ kg}$$

$$l_9 = 0.9 \text{ m} \quad F_p = m \cdot g \cdot 2 = 3237,3 \text{ N}$$

$$\theta = 10^\circ$$

Determine  $F_S$  (force on the bumper structure):

$$\Sigma M_A = 0;$$

$$F_p \cdot l_9 \cdot \sin \theta - F_S \cdot l_6 = 0;$$

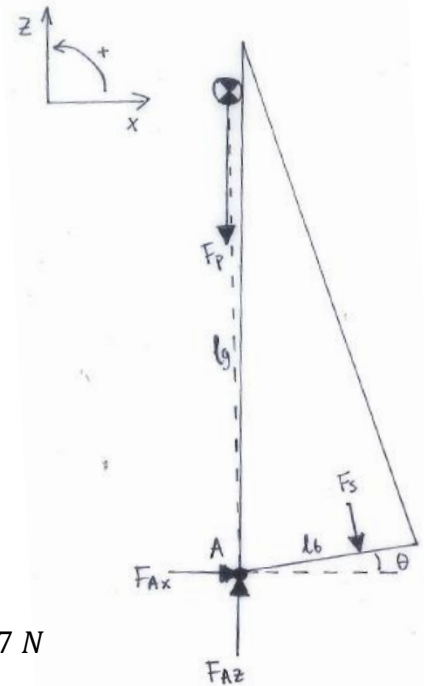
$$F_S = \frac{F_p \cdot l_9 \cdot \sin \theta}{l_6} = 2061 \text{ N}$$

Determine forces at A:

$$\Sigma F_X = 0; \quad \Sigma F_Z = 0;$$

$$F_{Ax} + F_S \cdot \sin \theta = 0; \quad -F_p + F_{Az} - F_S \cdot \cos \theta = 0;$$

$$F_{Ax} = -F_S \cdot \sin \theta = -358 \text{ N} \quad F_{Az} = F_p + F_S \cdot \cos \theta = 5267 \text{ N}$$



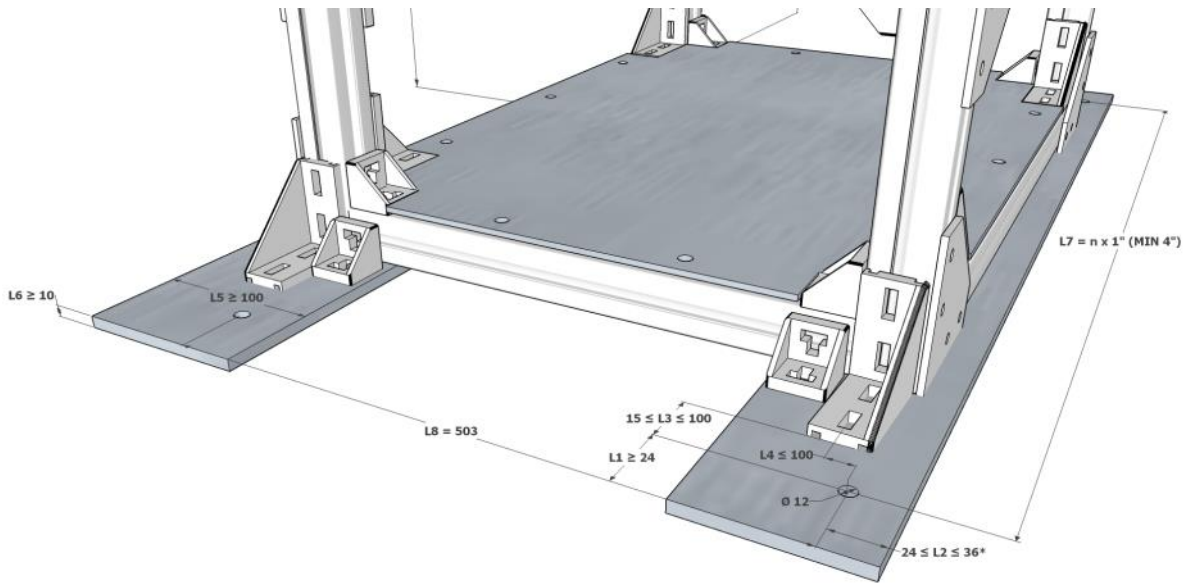
N.B. These calculated forces are supported by two bearings and bumper points so they should be divided by 2 when doing stress calculations!

In this situation,  $F_S$  is lower than in ② but the force in  $F_{Az}$  is significantly higher. Each bearing should withstand a vertical load of  $5267/2 = 2633 \text{ N}$ . For the bearing itself this is not a problem (can withstand static loads up to 7.8 kN, see <http://www.skf.com/group/products/bearings-units-housings/bearing-units/ball-bearing-units/y-bearing-flanged-units/y-brg-square-flanged-units/index.html?designation=FY%2025%20TF>) so we need to make sure that the connection of the shaft block (see ⑤) with the profiles is strong enough. With aluminum plates of 5 mm thick at both sides of each connection block, we are confident that the structure is strong enough to take these loads.

The brackets holding the upper bar of the bumper can also handle the loads induced by the backboard structure ( $F_S$ ) (maximum load that one 45x45 bracket can take is 3000N).

**Characteristics of the Rack(s)**

Strut profile brand name	Bosch Rexroth
Strut profile reference(s)	www.boschrexroth.com
Strut profile cross-section(s)	45 x 45 mm for bumper 20 x 60 mm for frame
Base plate/bars aluminum ultimate strength	275 - 350 MPa
Confirm that a torque wrench has been used for tightening the primary structure bolts, in accordance with the recommendations of the strut profile provider	Not yet, but will do
Confirm that thread locking compound has been used on primary structure bolts	Not yet, but will do



L1:	69,8 mm	$L1 \geq 24$ mm
L2:	248,5 mm	$24 \leq L2 \leq 36$ mm
L3:	Not applicable	$15 \leq L3 \leq 100$ mm
L4:	Not applicable	$L4 \leq 100$ mm
L5:	1000 mm	$L5 \geq 100$ mm
L6:	10 mm	$L6 \geq 10$ mm
L7:	26*25.4 mm	$L7 \geq 4*25.4$ mm
L8:	503 mm	$L8 = 503$ or $L8 = 1006$ mm

**Linear Loading**

Insert here a figure or a table showing status of the linear loading:

Quick Linear Load Assessment	Value	Unit
Total mass of the experiment rack + 10% (kg)	83	Kg
Total number of attachment points	4	-
Height of CoG + 10% (mm)	164	mm
Is the CoG centered in XY plane? (see GDL)	YES	-
Has the experiment more than two attachment points on 530mm/X?	NO	-
Minimum Pitch between fixation points /X	503	mm
<b>Status</b>	<b>Ok</b>	-

**Linear Loading of combined set-up**

Due to the layout of the experiment there can never be more than 2 fixation points over 21"; calculating the linear loading between the racks is not necessary.

## 9. Procedures for Ground and In-Flight Operations

### Procedures on the day of the flight

For an overview of the experimental procedure during the parabolas, please look back to Figure 1. This figure indicates during which phases of the parabolas measurements will be performed.

### Scenarios

There are two different scenario's regarding the experimental procedure; one automatically controlled procedure and one manually controlled procedure. The automatically controlled procedure is the one we will use if the accelerometer functions as it should. However, in the event the accelerometer does not provide the right data, we will switch to manual control of the experiments. See Chapter 3.3 for more details. The on ground procedure before flight, the procedures in flight before and after the parabolas and the procedure during the flight breaks are the same for both scenarios.

### Operator proceedings

During the parabolic maneuvers, the two operators (i.e. members of VESTAND team) have specific tasks:

- Operator 1 is responsible for the experimental equipment, checking the recordings, intervening with the stimulation if necessary (i.e. when a subject feels sick) and ensures that the subject of experiment 1 verbally reports the perceived motion after each stimulation period.
- Operator 2 is primarily responsible for implementing the conditions and assistance for experiment 2 (i.e. instructing subject to stand, orient, close eyes, etc., as well as positioning subject, attaching/detaching the springs, and releasing/attaching seatbelts). Operator 2 also looks after both subjects by making sure they are doing fine.

The proceedings of the operators during all phases of the flight are described in the following tables. General notes:

- All words in *italic* between quotation marks are the announcements that the pilots make
- Subject A starts with experiment 1, subject B starts with experiment 2
- All text in orange indicate actions in case of manual control

Period 0: On ground – Pre flight	
<ul style="list-style-type: none"> <li>• In the afternoon before each flight day, the beams of the chair for experiment 1 for helmet attachment are set to the right location for the first subject of the day.</li> <li>• On the flight day, at 7.30 AM, before the morning meeting, one operator applies Pliaglis cream to the mastoid processes of both subjects to locally anaesthetize the skin.</li> <li>• The already shaved skin region (done during training) of the subjects' right leg is cleaned with NuPrep and an alcohol tissue, and subsequently the self-adhesive electrodes are placed and secured with skin tape.</li> <li>• At 8.15 AM (after morning briefing), one operator pulls of the dried Pliaglis from the skin of the subjects. The other operator covers the rubber electrodes with gel and prepares 16 pieces of tape.</li> <li>• When the Pliaglis is removed, the operators will place the rubber electrodes and fix them with tape and a head band.</li> <li>• Subject B will put on a harness; an operator will help with tightening it. (The harness of subject B is stored in the galley)</li> <li>• Both subjects will insert a marked scleral lens in their left eye with the assistance of an operator.</li> </ul>	
<b>Time needed</b>	60 minutes, this includes waiting time during the morning meeting
Period 0: In flight – Before first parabola	

<ul style="list-style-type: none"> <li>• Subjects take off their shoes, socks and flight suit and the operators take off their shoes. All this clothing is given to Novespace to store in the galley</li> <li>• Operator 1 starts with turning on all electrical equipment and getting it ready for the experiments (turn on laptops and DAQ board and start software, turn on amplifier, stimulators, force plate and laser sensor). Operator 1 already runs the MatLab script</li> <li>• Operator 1 then releases straps that secured the backboard in backward position and springs that are secured to the baseplate with Velcro</li> <li>• Operator 2 will start with preparing the subject for the experiment 1:             <ul style="list-style-type: none"> <li>- The earphones with microphone are attached to the subject.</li> <li>- The EyeSeeCam goggles are placed on the subject’s head</li> <li>- The helmet is placed on the subject’s head</li> <li>- The insulated wires are connected to the rubber electrodes.</li> <li>- The subject is seated in the chair to perform the calibration</li> <li>- The camera is adjusted with direct feedback from the MacBook, so that the eye is in focus.</li> <li>- Eye movements are calibrated: operator 2 spans the calibration sheet while operator 1 runs the software and tells the subject what to do</li> <li>- ESC: Operator 1 selects ‘Recording’ after calibration.</li> <li>- The subject is correctly positioned on the foam mattress next to the chair, a cushion is placed on the subject, then the belts are tightened</li> <li>- The fin of the helmet is clamped onto the horizontal beam when the subject is in the right position (head pitched up 18.8°)</li> <li>- Check the position of the microphone, earphones, camera and electrodes.</li> </ul> </li> <li>• Once the software is up and running, operator 1 will prepare the subject for experiment 2:             <ul style="list-style-type: none"> <li>- EMG electrode check to see if the electrodes are still in place</li> <li>- The subject is secured to the backboard by attaching and tightening the two seat belts</li> <li>- The insulated wires are connected from the stimulator to the rubber electrodes</li> <li>- The EMG cables are connected from the amplifier to the surface electrodes and operator 1 checks to see if EMG responses are well measured. If not, the electrode placement will be adjusted</li> <li>- The springs are attached to the harness</li> <li>- When operator 2 is finished with subject A, (s)he helps with tensioning the springs appropriately. Operator 1 will look at the force plate feedback on the laptop and tells operator 2 what to do</li> <li>- When the springs are tensioned correctly, the subject can lean into the endstops and crouch during parabola 0.</li> </ul> </li> <li>• Operator 1 disengages the stimulators</li> <li>• During parabola 0, operator 1 checks the recordings of the accelerometer to see if it measures the acceleration correctly. If it is not, (s)he switches to manual control mode and indicates the start of parabola 1</li> </ul>	
<b>Time needed</b>	15 minutes

	Period 0:	Parabola 0
<b>Normal 1</b>	•	Operator 1, at “10”, starts the eye recording
<b>Hyper 1</b>	•	Operator 1 checks the recordings of the accelerometer to see if it measures the acceleration correctly.
<b>Micro</b>	•	Operator 1 checks the recordings of the accelerometer to see if it measures the acceleration correctly.
<b>Hyper 2</b>	•	Operator 1 checks the recordings of the accelerometer to see if it measures the acceleration correctly.
<b>Normal 2</b>	•	If accelerometer doesn’t work, operator 1 switches to manual mode by hitting button ‘p’
	•	Operator 1, at “steady flight” hits button ‘5’ to enter Normal 2 mode and start stim.
	•	Operator 2, at “steady flight”, instructs subject B to place feet in correct position and rise up. (S)he helps subject B to lean forward
	•	Operator 1, with laser feedback, instructs subject B to stand in correct position and to close eyes

Period 1: Parabola 1-5	
<b>Normal 1</b>	<ul style="list-style-type: none"> <li>Operator 1, at "10", stops and starts the eye recording</li> <li>Operator 2, at "10", instructs subject B to place feet in correct position and lean backward and/or crouch</li> </ul>
<b>Hyper 1</b>	<ul style="list-style-type: none"> <li>Operator 1, in second hyper-g phase, hits button ' 2' (manual control only).</li> </ul>
<b>Micro</b>	<ul style="list-style-type: none"> <li>Operator 1, at "injection", hits button '3': stimulation for <a href="#">exp. 1 and 2</a> is started after 3 seconds (manual control only)</li> <li>Operator 2, at "injection", instructs and helps subject B to stand in correct position and to close eyes</li> <li>Operator 1, at "injection", gives feedback about the angle of subject B</li> <li>Operator 2, at "pull-out", instructs subject B to lean back and crouch. If needed, the upper seat belt is released</li> </ul>
<b>Hyper 2</b>	<ul style="list-style-type: none"> <li>Operator 1, in second hyper-g phase, hits button ' 4' (manual control only)</li> </ul>
<b>Normal 2</b>	<ul style="list-style-type: none"> <li>Operator 1, at "steady-flight", hits button 5, stimulation for <a href="#">exp. 1 and 2</a> is started after 20 seconds (manual control only)</li> <li>Operator 2, at "steady flight", instructs subject B to place feet in correct position and rise up. (S)he helps subject B to lean forward</li> <li>Operator 1, with laser feedback, instructs subject B to stand in correct position and to close eyes</li> <li>ONLY IN PARABOLA 5: Operator 1, after stim, stops the eye recording</li> <li>ONLY IN PARABOLA 5: Operator 2, after stim, releases the tension in the springs</li> <li>ONLY IN PARABOLA 5: Operator 2, at "1 minute", tensions the springs up to the mark and adjusts with feedback from operator 1</li> </ul>

Period 1: Parabola 6-7	
<b>Normal 1</b>	<ul style="list-style-type: none"> <li>Operator 1, at "10", stops and starts the eye recording</li> <li>Operator 2, at "10", instructs subject B to place feet in correct position and lean backward and/or crouch</li> </ul>
<b>Hyper 1</b>	<ul style="list-style-type: none"> <li>Operator 1, at "pull-up", hits button '2': stimulation for <a href="#">exp. 1</a> is started after 1 second (manual control only)</li> </ul>
<b>Micro</b>	<ul style="list-style-type: none"> <li>Operator 1, at "injection", hits button '3': stimulation for <a href="#">exp. 2</a> is started after 3 seconds (manual control only)</li> <li>Operator 2, at "injection", instructs and helps subject B to stand in correct position and to close eyes</li> <li>Operator 1, at "injection", gives feedback about the angle of subject B</li> <li>Operator 2, at "pull-out", instructs subject B to lean back and crouch. If needed, the upper seat belt is released</li> </ul>
<b>Hyper 2</b>	<ul style="list-style-type: none"> <li>Operator 1, in second hyper-g phase, hits button ' 4' (manual control only).</li> </ul>
<b>Normal 2</b>	<ul style="list-style-type: none"> <li>Operator 1, at "steady-flight", hits button 5, stimulation for <a href="#">exp. 1 and 2</a> is started after 20 seconds (manual control only)</li> <li>Operator 2, at "steady-flight", releases tension in springs, detaches springs from harness and attaches them to baseplate with Velcro.</li> </ul>

Period 1: Parabola 9	
Normal 1	<ul style="list-style-type: none"> <li>Operator 1, at "10", stops and starts the eye recording</li> <li>Operator 2, at "10", instructs subject B to stand in correct position and to close eyes</li> <li>Operator 1, at "10", gives feedback about the angle of subject B</li> </ul>
Hyper 1	<ul style="list-style-type: none"> <li>Operator 1, at "pull-up", hits button '2': stimulation for <a href="#">exp. 1 and 2</a> is started after 1 second (manual control only)</li> </ul>
Micro	<ul style="list-style-type: none"> <li>Operator 1, at "injection", hits button '3': stimulation for <a href="#">exp. 1</a> is started after 3 seconds (manual control only)</li> <li>Operator 2, at "injection", instructs subject B to lean back, relax and support themselves</li> </ul>
Hyper 2	<ul style="list-style-type: none"> <li>Operator 1, in second hyper-g phase, hits button '4' (manual control only)</li> </ul>
Normal 2	<ul style="list-style-type: none"> <li>Operator 1, at "steady-flight", hits button 5, stimulation for <a href="#">exp. 1 and 2</a> is started after 20 seconds (manual control only)</li> <li>Operator 2, at "steady flight", instructs subject B to place feet in correct position and rise up. (S)he helps subject B to lean forward</li> <li>Operator 1, with laser feedback, instructs subject B to stand in correct position and to close eyes</li> </ul>

Period 1: Parabola 8	
Normal 1	<ul style="list-style-type: none"> <li>Operator 1, at "10", stops and starts the eye recording</li> <li>Operator 2, at "10", instructs subject B to place feet in correct position and lean backward and/or crouch</li> </ul>
Hyper 1	<ul style="list-style-type: none"> <li>Operator 1, at "pull-up", hits button '2': stimulation for <a href="#">exp. 1</a> is started after 1 second (manual control only)</li> </ul>
Micro	<ul style="list-style-type: none"> <li>Operator 1, at "injection", hits button '3': stimulation for <a href="#">exp. 2</a> is started after 3 seconds (manual control only)</li> <li>Operator 2, at "injection", instructs and helps subject B to stand in correct position and to close eyes</li> <li>Operator 1, at "injection", gives feedback about the angle of subject B</li> <li>Operator 2, at "pull-out", instructs subject B to lean back and crouch. If needed, the upper seat belt is released</li> </ul>
Hyper 2	<ul style="list-style-type: none"> <li>Operator 1, in second hyper-g phase, hits button '4' (manual control only).</li> </ul>
Normal 2	<ul style="list-style-type: none"> <li>Operator 1, at "steady-flight", hits button 5, stimulation for <a href="#">exp. 1 and 2</a> is started after 20 seconds (manual control only)</li> <li>Operator 2, at "steady-flight", releases tension in springs, detaches springs from harness and attaches them to baseplate with Velcro.</li> </ul>

Period 1: Parabola 9	
Normal 1	<ul style="list-style-type: none"> <li>Operator 1, at "10", stops and starts the eye recording</li> <li>Operator 2, at "10", instructs subject B to stand in correct position and to close eyes</li> <li>Operator 1, at "10", gives feedback about the angle of subject B</li> </ul>

<b>Hyper 1</b>	<ul style="list-style-type: none"> <li>Operator 1, at “pull-up”, hits button ‘2’: stimulation for <a href="#">exp. 1 and 2</a> is started after 1 second (manual control only)</li> </ul>
<b>Micro</b>	<ul style="list-style-type: none"> <li>Operator 1, in second hyper-g phase, hits button ‘3’ (manual control only)</li> </ul>
<b>Hyper 2</b>	<ul style="list-style-type: none"> <li>Operator 1, in second hyper-g phase, hits button ‘4’ (manual control only)</li> </ul>
<b>Normal 2</b>	<ul style="list-style-type: none"> <li>Operator 1, at “steady-flight”, hits button 5, stimulation for <a href="#">exp. 1 and 2</a> is started after 20 seconds (manual control only)</li> <li>Operator 2, at “steady flight”, instructs subject B to place feet in correct position and rise up. (S)he helps subject B to lean forward</li> <li>Operator 1, with laser feedback, instructs subject B to stand in correct position and to close eyes</li> </ul>

<b>Period 1: Parabola 10</b>	
<b>Normal 1</b>	<ul style="list-style-type: none"> <li>Operator 1, at “20”, tells subject A that the stimulation will occur in the first hyper-g phase</li> <li>Operator 1, at “10”, stops and starts the eye recording</li> <li>Operator 2, at “10”, instructs subject B to stand in correct position and to close eyes</li> <li>Operator 1, at “10”, gives feedback about the angle of subject B</li> </ul>
<b>Hyper 1</b>	<ul style="list-style-type: none"> <li>Operator 1, at “pull-up”, hits button ‘2’: stimulation for <a href="#">exp. 1 and 2</a> is started (manual control only)</li> </ul>
<b>Micro</b>	<ul style="list-style-type: none"> <li>Operator 1, in second hyper-g phase, hits button ‘3’ (manual control only)</li> <li>Operator 2, at “injection”, instructs subject B to lean back, relax and support themselves</li> </ul>
<b>Hyper 2</b>	<ul style="list-style-type: none"> <li>Operator 1, in second hyper-g phase, hits button ‘4’ (manual control only)</li> </ul>
<b>Normal 2</b>	<ul style="list-style-type: none"> <li>Operator 1, at “steady-flight”, hits button 5, 3 stimulation periods for <a href="#">exp. 2</a> are started after 20 seconds with 30 seconds break (manual control only)</li> <li>Operator 1, at “steady flight”, stops eye recording</li> <li>Operator 2, at “steady flight”, instructs subject B to place feet in correct position and rise up. (S)he helps subject B to lean forward</li> <li>Operator 1, with laser feedback, instructs subject B to stand in correct position and to close eyes</li> <li>Operator 1 completes 3 trials with subject B</li> <li>Operator 2, at “steady-flight”, releases subject A: remove the cover of the hole in the right eye, release seat belts, unclamp helmet and guide subject A from the mattress to the chair</li> <li>Operator 2 checks the camera position and adjusts if needed</li> <li>Operator 2, after calibration, positions subject A correctly on the chair (places extra back cushion), clamps the helmet to the beam, checks head angle and places the eye cover</li> <li>Operator 2, when finished with the subjects, secures the foam mattress to the floor by closing the seat belts</li> </ul>

<b>Period 1: Parabola 11-14</b>	
<b>Normal 1</b>	<ul style="list-style-type: none"> <li>Operator 1, at “10”, stops and starts the eye recording</li> <li>Operator 2, at “10”, instructs subject B to stand in correct position and to close eyes</li> <li>Operator 1, at “10”, gives feedback about the angle of subject B</li> </ul>
<b>Hyper 1</b>	<ul style="list-style-type: none"> <li>Operator 1, at “pull-up”, hits button ‘2’: stimulation for <a href="#">exp. 2</a> is started after 1 second (manual control only)</li> </ul>

<b>Micro</b>	<ul style="list-style-type: none"> <li>Operator 1, at <i>"injection"</i>, hits button '3': stimulation for <a href="#">exp. 1</a> is started after 3 seconds (manual control only)</li> <li>Operator 2, at <i>"injection"</i>, instructs subject B to lean back, relax and support themselves</li> </ul>
<b>Hyper 2</b>	<ul style="list-style-type: none"> <li>Operator 1, in second hyper-g phase, hits button '4' (manual control only).</li> </ul>
<b>Normal 2</b>	<ul style="list-style-type: none"> <li>Operator 1, at <i>"steady-flight"</i>, hits button 5, stimulation for <a href="#">exp. 1 and 2</a> is started after 20 seconds (manual control only)</li> <li>Operator 2, at <i>"steady flight"</i>, instructs subject B to place feet in correct position and rise up. (S)he helps subject B to lean forward</li> <li>Operator 1, with laser feedback, instructs subject B to stand in correct position and to close eyes</li> </ul>

Period 1: Parabola 15	
<b>Normal 1</b>	<ul style="list-style-type: none"> <li>Operator 1, at <i>"10"</i>, stops and starts the eye recording</li> <li>Operator 2, at <i>"10"</i>, instructs subject B to stand in correct position and to close eyes</li> <li>Operator 1, at <i>"10"</i>, gives feedback about the angle of subject B</li> </ul>
<b>Hyper 1</b>	<ul style="list-style-type: none"> <li>Operator 1, at <i>"pull-up"</i>, hits button '2': stimulation for <a href="#">exp. 2</a> is started after 1 second (manual control only)</li> </ul>
<b>Micro</b>	<ul style="list-style-type: none"> <li>Operator 1, at <i>"injection"</i>, hits button '3': stimulation for <a href="#">exp. 1</a> is started after 3 seconds (manual control only)</li> <li>Operator 2, at <i>"injection"</i>, instructs subject B to lean back, relax and support themselves</li> </ul>
<b>Hyper 2</b>	<ul style="list-style-type: none"> <li>Operator 1, in second hyper-g phase, hits button '4' (manual control only).</li> </ul>
<b>Normal 2</b>	<ul style="list-style-type: none"> <li>Operator 1, at <i>"steady-flight"</i>, hits button 5, stimulation for <a href="#">exp. 1</a> is started after 20 seconds (manual control only)</li> <li>Operator 2, at <i>"steady-flight"</i>, releases subject B: disconnect the wires at the EVS and EMG electrodes and release the seatbelts</li> <li>Operator 2 helps subject B to take off the harness and instructs subject B to move over to experiment 1</li> <li>Operator 2 stores the harness in the bag and gets other harness out</li> <li>Operator 1 waits for experiment 1 to be finished</li> <li>Operator 1, when subject B gets off the force plate, zeros the force plate</li> </ul>

**Period 2: Mid-flight break (15 min)**

- Operator 1, when stim for exp. 1 is finished, disengages the stimulators and stops eye recording
- Operator 1 will prepare the ESC software for the new measurements.
  - Assign a new participant to the eye recordings
- Operator 2 releases subject A: remove eye cover, unclamp and cover helmet, take off helmet, disconnect wires at EVS electrodes, unbuckle seatbelts, remove EyeSeeCam and earphones with microphone. Operator 2 then instructs subject A to move over to experiment 2.
- Operator 1, if needed, relocates the beams on the chair to match subject B's measures

The subjects are then prepared for their second experiment:

- Operator 2 will start with preparing subject B for experiment 1:
  - The earphones with microphone are attached to the subject.
  - The EyeSeeCam goggles are placed on the subject's head
  - The helmet is placed on the subject's head
  - The insulated wires are connected to the rubber electrodes.
  - The subject is seated in the chair to perform the calibration
  - The camera is adjusted with direct feedback from the MacBook, so that the eye is in focus.
  - Eye movements are calibrated: operator 2 spans the calibration sheet while operator 1 runs the software and tells the subject what to do
  - The subject is correctly positioned on the chair, a cushion is placed behind the subject, then the belts are tightened
  - The fin of the helmet is clamped onto the vertical beam when the subject is in the right position (head pitched up 18.8°)
  - The animations are shown and short explanations of the movement are repeated
  - The eye patch is put back in place
- Operator 1 prepares subject A for experiment 2:
  - The operator helps the subject to put on the harness and tightens it
  - EMG electrode attachment is checked
  - The subject is secured to the backboard by attaching and tightening the seatbelts
  - The insulated wires are connected from the stimulator to the rubber electrodes
  - The EMG cables are connected from the amplifier to the surface electrodes and operator 1 checks to see if EMG responses are well measured. If not, the electrode placement will be adjusted
- Operator 1, when preparation is finished, engages the stimulators and starts eye recording
- Operator 1, at "1 minute", hits button '0': stimulation for exp. 1 is started immediately

Period 3: Parabola 16-19	
Normal 1	<ul style="list-style-type: none"> <li>Operator 1, at "10", stops and starts the eye recording</li> <li>Operator 2, at "10", instructs subject A to stand in correct position and to close eyes</li> <li>Operator 1, at "10", gives feedback about the angle of subject A</li> </ul>
Hyper 1	<ul style="list-style-type: none"> <li>Operator 1, at "pull-up", hits button '2': stimulation for <u>exp. 2</u> is started after 1 second (manual control only)</li> </ul>
Micro	<ul style="list-style-type: none"> <li>Operator 1, at "injection", hits button '3': stimulation for <u>exp. 1</u> is started after 3 seconds (manual control only)</li> <li>Operator 2, at "injection", instructs subject A to lean back, relax and support themselves</li> </ul>
Hyper 2	<ul style="list-style-type: none"> <li>Operator 1, in second hyper-g phase, hits button '4' (manual control only).</li> </ul>
Normal 2	<ul style="list-style-type: none"> <li>Operator 1, at "steady-flight", hits button 5, stimulation for <u>exp. 1 and 2</u> is started after 20 seconds (manual control only)</li> <li>Operator 2, at "steady flight", instructs subject A to place feet in correct position and rise up. (S)he helps subject A to lean forward</li> <li>Operator 1, with laser feedback, instructs subject A to stand in correct position and to close eyes</li> </ul>

Period 3: Parabola 20	
Normal 1	<ul style="list-style-type: none"> <li>Operator 1, at "10", stops and starts the eye recording</li> <li>Operator 2, at "10", instructs subject A to stand in correct position and to close eyes</li> <li>Operator 1, at "10", gives feedback about the angle of subject A</li> </ul>
Hyper 1	<ul style="list-style-type: none"> <li>Operator 1, at "pull-up", hits button '2': stimulation for <u>exp. 2</u> is started after 1 second (manual control only)</li> </ul>
Micro	<ul style="list-style-type: none"> <li>Operator 1, at "injection", hits button '3': stimulation for <u>exp. 1</u> is started after 3 seconds (manual control only)</li> <li>Operator 2, at "injection", instructs subject A to lean back, relax and support themselves</li> </ul>
Hyper 2	<ul style="list-style-type: none"> <li>Operator 1, in second hyper-g phase, hits button '4' (manual control only)</li> </ul>
Normal 2	<ul style="list-style-type: none"> <li>Operator 1, at "steady-flight", hits button 5, 3 stimulation periods for <u>exp. 2</u> are started after 20 seconds with 30 seconds break (manual control only)</li> <li>Operator 1, at "steady flight", stops the eye recording</li> <li>Operator 2, at "steady flight", instructs subject A to place feet in correct position and rise up. (S)he helps subject A to lean forward</li> <li>Operator 1, with laser feedback, instructs subject A to stand in correct position and to close eyes</li> <li>Operator 1 completes 3 trials with subject A</li> <li>Operator 2, at "steady-flight", releases subject B: remove the cover of the hole in the right eye, unclamp helmet, release seat belts, and guide subject B from the chair to the mattress</li> <li>Operator 2 correctly positions the subject, clamps the helmet and checks head position</li> <li>Operator 2 places the foam on top of the subject and secures the seat belts</li> <li>Operator 2 checks the camera position and adjusts if needed</li> <li>Operator 2 shows animations and shortly repeats them for the subject</li> <li>Operator 2 places the eye cover back in place</li> <li>Operator 2, when finished, secures the foam cushions to the chair by closing the seat belts</li> </ul>

Period 3: Parabola 21	
<b>Normal 1</b>	<ul style="list-style-type: none"> <li>Operator 1, at "10", stops and starts the eye recording</li> <li>Operator 2, at "10", instructs subject A to stand in correct position and to close eyes</li> <li>Operator 1, at "10", gives feedback about the angle of subject A</li> </ul>
<b>Hyper 1</b>	<ul style="list-style-type: none"> <li>Operator 1, at "pull-up", hits button '2': stimulation for <a href="#">exp. 1 and 2</a> is started after 1 second (manual control only)</li> </ul>
<b>Micro</b>	<ul style="list-style-type: none"> <li>Operator 1, at "injection", hits button '3' (manual control only)</li> <li>Operator 2, at "injection", instructs subject A to lean back, relax and support themselves</li> </ul>
<b>Hyper 2</b>	<ul style="list-style-type: none"> <li>Operator 1, in second hyper-g phase, hits button '4' (manual control only)</li> </ul>
<b>Normal 2</b>	<ul style="list-style-type: none"> <li>Operator 1, at "steady-flight", hits button 5, stimulation for <a href="#">exp. 1 and 2</a> is started after 20 seconds (manual control only)</li> <li>Operator 2, at "steady flight", instructs subject A to place feet in correct position and rise up. (S)he helps subject A to lean forward</li> <li>Operator 1, with laser feedback, instructs subject A to stand in correct position and to close eyes</li> </ul>

Period 3: Parabola 22	
<b>Normal 1</b>	<ul style="list-style-type: none"> <li>Operator 1, at "10", stops and starts the eye recording</li> <li>Operator 2, at "10", instructs subject A to stand in correct position and to close eyes</li> <li>Operator 1, at "10", gives feedback about the angle of subject A</li> </ul>
<b>Hyper 1</b>	<ul style="list-style-type: none"> <li>Operator 1, at "pull-up", hits button '2': stimulation for <a href="#">exp. 1 and 2</a> is started after 1 second (manual control only)</li> </ul>
<b>Micro</b>	<ul style="list-style-type: none"> <li>Operator 1, at "injection", hits button '3' manual control only)</li> <li>Operator 2, at "injection", instructs subject A to lean back, relax and support themselves</li> </ul>
<b>Hyper 2</b>	<ul style="list-style-type: none"> <li>Operator 1, in second hyper-g phase, hits button '4' (manual control only).</li> </ul>
<b>Normal 2</b>	<ul style="list-style-type: none"> <li>Operator 1, at "steady-flight", hits button 5, stimulation for <a href="#">exp. 1</a> is started after 50 seconds (manual control only)</li> <li>Operator 2, at "steady-flight", attaches the springs to the harness of subject A and tensions the springs up to the marks</li> <li>Operator 1 gives feedback about Fz load</li> <li>Operator 2 tensions the springs appropriately and instructs the subject to lean into endstops and crouch</li> </ul>

Period 3: Parabola 23-25	
<b>Normal 1</b>	<ul style="list-style-type: none"> <li>Operator 1, at "10", stops and starts the eye recording</li> <li>Operator 2, at "10", instructs subject A to place feet in correct position and lean backward and/or crouch</li> </ul>
<b>Hyper 1</b>	<ul style="list-style-type: none"> <li>Operator 1, at "pull-up", hits button '2': stimulation for <a href="#">exp. 1</a> is started after 1 second (manual control only)</li> </ul>
<b>Micro</b>	<ul style="list-style-type: none"> <li>Operator 1, at "injection", hits button '3': stimulation for <a href="#">exp. 2</a> is started after 3 seconds (manual control only)</li> <li>Operator 2, at "injection", instructs and helps subject A to stand in correct position and to close eyes</li> <li>Operator 1, at "injection", gives feedback about the angle of subject A</li> <li>Operator 2, at "pull-out", instructs subject A to lean back and crouch. If needed, the upper seat belt is released</li> </ul>
<b>Hyper 2</b>	<ul style="list-style-type: none"> <li>Operator 1, in second hyper-g phase, hits button '4' (manual control only)</li> </ul>
<b>Normal 2</b>	<ul style="list-style-type: none"> <li>Operator 1, at "steady-flight", hits button 5, stimulation for <a href="#">exp. 1 and 2</a> is started after 50 seconds (manual control only)</li> <li>Operator 2, at "steady flight", instructs subject A to place feet in correct position and rise up. (S)he helps subject A to lean forward</li> <li>Operator 1, with laser feedback, instructs subject A to stand in correct position and to close eyes</li> <li>ONLY IN PARABOLA 25: Operator 1, after stim, stops the eye recording</li> <li>ONLY IN PARABOLA 25: Operator 2, after stim, releases the tension in the springs</li> <li>ONLY IN PARABOLA 25: Operator 2, at "1 minute", tensions the springs up to the mark and adjusts with feedback from operator 1</li> </ul>

Period 3: Parabola 26-30	
<b>Normal 1</b>	<ul style="list-style-type: none"> <li>Operator 1, at "10", stops and starts the eye recording</li> <li>Operator 2, at "10", instructs subject A to place feet in correct position and lean backward and/or crouch</li> </ul>
<b>Hyper 1</b>	Operator 1, in second hyper-g phase, hits button '2' (manual control only)
<b>Micro</b>	<ul style="list-style-type: none"> <li>Operator 1, at "injection", hits button '3': stimulation for <a href="#">exp. 1 and 2</a> is started after 3 seconds (manual control only)</li> <li>Operator 2, at "injection", instructs and helps subject A to stand in correct position and to close eyes</li> <li>Operator 1, at "injection", gives feedback about the angle of subject A</li> <li>Operator 2, at "pull-out", instructs subject A to lean back and crouch. If needed, the upper seat belt is released</li> </ul>
<b>Hyper 2</b>	<ul style="list-style-type: none"> <li>Operator 1, in second hyper-g phase, hits button '4' (manual control only)</li> </ul>
<b>Normal 2</b>	<ul style="list-style-type: none"> <li>Operator 1, at "steady-flight", hits button 5, stimulation for <a href="#">exp. 1 and 2</a> is started after 50 seconds (manual control only)</li> <li>Operator 2, at "steady flight", instructs subject A to place feet in correct position and rise up. (S)he helps subject A to lean forward</li> </ul>

	<ul style="list-style-type: none"> <li>Operator 1, with laser feedback, instructs subject A to stand in correct position and to close eyes</li> </ul>
--	---

<b>In flight – After last parabola</b>	
<ul style="list-style-type: none"> <li>Operator 2, when stim is ended, releases subject A: release tension in springs, detach springs from harness, disconnect EMG and EVS electrodes, take off harness</li> <li>Operator 1, when stim is ended, disengages the stimulators, stops eye recording, saves all data and shuts down all electrical equipment</li> <li>Operator 1, when finished with equipment, releases subject B: release seatbelts, take off eye cover, unclamp and cover helmet, take off helmet, disconnect wires at EVS electrodes, remove EyeSeeCam and headset with microphone.</li> <li>Operator 1 provides the subjects with their flight suits, shoes and socks</li> <li>Operator 1 clamps the helmet to the chair</li> <li>Operator 2 secures the foam mattress to the floor with seatbelts, attaches springs to the baseplate with Velcro and secures backboard in backward position with straps</li> </ul>	
<b>Time needed</b>	10 minutes

## Subject training – on ground, week before flights

Before the parabolic flight campaign all subjects will receive a video as well as a text document in which our experimental procedure is explained. In the video is shown how the subjects have to indicate their perceived motion evoked by EVS as it is important to teach the subjects how to report the perception of motion for experiment 1. In the video, we will show them animations of 4 possible illusory motions evoked by EVS in the head-down and head-straight condition and explain the types of motion to them. During the experiment, they will choose 1 of the 4 types of motion as a report of their perceived motion evoked by the stimulus. They will also be rating their choice of motion on a scale from 1 to 3, where the illusory sensation of movement evoked by the stimulation was: vague and not precise (1), moderately clear and precise (2), or perfectly clear and precise; like a real perception (3). They have to learn the words that are associated with the types of motion, as well as the scale for rating the vividness of the motion, so that they can report their perceived motion quickly during the experiment in the flights.

We will also train the subjects on the Monday before the flights (December 4) or during the afternoon the day before they fly, to familiarize them with experimental procedures and to let them experience the feeling of EVS. During the training, we will also be recording the data to establish a baseline measurement for these participants. Before the experimental training, we will let them read and sign the informed consent and give them the opportunity to ask questions. Then we will apply the anesthetizing Pliaglis cream and let it dry for 30 minutes. During that time, a small skin region of the subject's right leg (above the medical gastrocnemius and soleus muscles) will be shaved and then cleaned (i.e. scrubbed) before the self-adhesive EMG surface electrodes will be secured at these spots. During the remaining time, the subject puts on the harness and subsequently we will explain the experiments in more detail. After the 30 minutes the dried Pliaglis film is removed and then the training and baseline recording of each separate experiment begins. Note, for each subject there will be a predefined order of experimental trials during the flights. The order of experimental training will be the same as this predefined trial order.

For experiment 1, we will explain our experimental procedure once more and show them the animations with the 8 possible illusory motions (4 for the head-down condition and 4 for the head-straight condition) evoked by EVS. Then we will attach electrodes and familiarize them with the sinewave EVS. We will ask them to take a seat and sit comfortably, and to put on the eye tracking goggles (EyeSeeCam) and helmet. We will calibrate the camera and secure them in either the head-down or head-straight position (this will be predefined per subject). While securing them, we will mark the appropriate positions of the beams the helmet will be fixed to per subject. We will mention the names of the 4 types of motion they can choose from once more, and then we will apply the 20 second stimulus (with a sinusoidal wave of 0.4Hz and 4mA) with a rest period of 5 seconds before and after stimulation, and ask them to report their perception of motion afterwards. This stimulation and reporting of perception will be repeated 5 times. We will then unclamp the helmet, guide them to the either the chair or mattress and reclamp the helmet to secure them in the other head position. We will mention the names of the 4 types of motion they can choose from once more and conduct the same stimulation and report paradigm as mentioned above 3 times. When the subjects are finished in this set-up, we will ask them to release themselves as fast as possible to practise an emergency evacuation. First, we will instruct them how they can evacuate themselves in the quickest way.

For experiment 2, the subject is positioned on the force plate and secured to the backboard with the two seatbelts. Marks will be added on the force plate to indicate the right foot position for each subject. Before starting with the trials, the subjective zero angle of the subject will be determined. Therefore, the subject has to stand in a position where the activity of the plantar flexor muscles and the dorsi flexor muscles is balanced. The offset position for every trial will be the subjective zero angle plus 3 degrees forward. Then, the EVS and EMG electrodes will be connected to the stimulator and amplifier respectively, by connecting the cables to the electrodes. We will stimulate the participant for a brief period of time to familiarize the participant with the stochastic vestibular stimulus that we use for this experiment. Then, the springs will be attached to the harness and tensioned to the right amount. Depending on the predefined order of trials in the flights, the springs will be detached again before starting the training trials. During the training, the subject will perform 8 spring-loaded trials of 20 seconds to collect 160 seconds of data for comparison to data collected in this set-up during the flight and 8 non-loaded trials to also match the time of collected data during the flights. Prior to each trial, the subject will be instructed to stand in the correct posture: the ankles should align with the marking on the force plate, the feet should be 5 cm apart, the head has to be turned over the left shoulder and slightly pitched upwards, and (s)he has to lean 3 deg anterior. When the subject is ready, (s)he closes the eyes and subsequently receives 20 seconds of SVS. When the stimulation is ended, the subject can relax for 40 seconds if needed before a new trial is started. Before the next trial, the subject is instructed to stand in the right position and close the eyes before receiving the stimulation. When the subject is finished with the trials of the first set-up (i.e. with or without springs), there is a break of 1 min 40 sec to get the subject ready for the next set of trials. Depending on the subject's trial order, this either involves attaching the springs and, if needed, making minor adjustments to get the appropriate downward load, or detaching the springs.

After the second set of trials, we will train the subjects how to evacuate in an emergency situation. The quickest way to free yourself when standing in the setup with springs connected to the harness is the release the seatbelts and then take off the harness. Before starting the evacuation process, we will disconnect the EMG and EVS wires from the subject, to make sure they won't be damaged (in a real emergency situation, they may be damaged of course).

Once out of the set-up, we will ask if they are okay and if they have any questions.

## 10. Risk Assessment

### Analysis of External Component Failures

Loss of aircraft power supply	Experiments cannot be continued until power returns
Loss of cabin pressure. Pressure drop from 850 mbar to 350 mbar in 5 seconds (e.g. impact on air sealed container).	No impact on experimental set-up
Vent-line clogging or reduced flow	No impact on experimental set-up

### Summary of Hazards

Hazard Group	Hazardous conditions/Risks	Hazard classification <sup>(1)</sup>	Risk Management See §/HR#
Radiation (Ionizing, electromagnetic, laser)	<ul style="list-style-type: none"> <li>Someone might stare into the laser beam</li> </ul>	Major	§8 (tent)
Fire	<ul style="list-style-type: none"> <li>A fire might be ignited by a shorted circuit</li> </ul>	Critical	§7
Electrical Shock/Static Discharge	<ul style="list-style-type: none"> <li>Contact by personnel with voltage above 32V. Possibility of burns or death</li> </ul>	Catastrophic	HR#1
Structural failure	<ul style="list-style-type: none"> <li>Structure not able to withstand emergency landing conditions</li> </ul>	Catastrophic	HR#2
Toxic Materials/ Contamination	<ul style="list-style-type: none"> <li>Cabin contamination might occur due to the shattering of Eyeseecam lens.</li> </ul>	Major	§4.1
Collision / Impact	<ul style="list-style-type: none"> <li>n/a</li> </ul>		
Injury and/or Illness	<ul style="list-style-type: none"> <li>Personnel can be injured by sharp edges, corners or protuberances of the experiment while floating uncontrolled through the cabin</li> </ul>	Major	§9
	<ul style="list-style-type: none"> <li>Subjects can be injured when losing balance in exp2 and fall in hyper-g</li> </ul>	Major	§8 (seatbelts)
	<ul style="list-style-type: none"> <li>During exp2, subjects are subjected to hyper-g while being loaded by the springs. Combined acceleration will be 2.8g.</li> </ul>	Major	§9
	<ul style="list-style-type: none"> <li>Shattering springs during exp2</li> </ul>	Major	HR#4
	<ul style="list-style-type: none"> <li>Personnel can be injured by collision with the metal fin on the subject's helmet.</li> </ul>	Major	§8 (Rack 2)
Corrosion	<ul style="list-style-type: none"> <li>n/a</li> </ul>		
Explosion-Implosion	<ul style="list-style-type: none"> <li>n/a</li> </ul>		
Loss of Habitable Environment	<ul style="list-style-type: none"> <li>n/a</li> </ul>		
Extreme Temperature	<ul style="list-style-type: none"> <li>n/a</li> </ul>		
Any other which may not fall into the above categories	<ul style="list-style-type: none"> <li>Subject gets sick because of the parabolas</li> </ul>	Minor	HR#3
	<ul style="list-style-type: none"> <li>An inability for the subject to evacuate</li> </ul>	Catastrophic	HR#5

(1) Catastrophic/ Critical / Major / Minor

### Hazard Reports

Hazard Report #1	
Writer's name	<b>Rick van der Vliet</b>
Hazard Group	Electrical Shock/Static Discharge
Hazard Description	Electrical shock. Contact by personnel with power above 32V. Possibility of burns or death.
Hazard classification	<b>Catastrophic</b>
<b>Hazard cause</b>	Defective wires

<b># 1</b>			
<b>Hazard Control</b>	<b>A</b>	Wire routing and cable connections performed by electrician.	
Verification method(s)	1	Inspection of the whole electrical circuit after assembly and prior arrival at PFC site.	Closed
	2	Operational test of the experiment in the laboratory prior arrival at PFC site	Closed
<b>Hazard cause #2:</b>	Defective insulation of wires, terminals and/or connectors		
<b>Hazard control</b>	<b>A</b>	Equipment design ensures isolation of high voltage conductors and absence of exposed energized contacts/surfaces.	
Verification method(s)	1	Inspection of the whole electrical circuit after assembly and prior arrival at PFC site.	Closed
<b>Hazard control</b>	<b>B</b>	Equipment design implements all supply connectors of socket type.	
Verification method(s)	1	Inspection of the whole electrical circuit after assembly and prior arrival at PFC site.	Closed
<b>Hazard cause #3:</b>	Short Circuit to exposed conductive surfaces.		
<b>Hazard control</b>	<b>A</b>	Grounding of conductive equipment chassis to power supply common ground	
Verification method(s)	1	Verification of equipment and metallic structure connection to the electrical ground prior arrival at PFC site.	Closed
<b>Hazard control</b>	<b>B</b>	Connection of the common ground to the rack structure.	
Verification method(s)	1	Verification of proper rack bonding prior arrival at PFC site.	Closed
<b>Hazard control</b>	<b>C</b>	Electrical Bonding of external conductive surface to ground	
Verification method(s)	1	Verification of proper equipment bonding prior arrival at PFC site.	Closed

<b>HAZARD REPORT #2</b>			
Writer name:	<b>Rick van der Vliet</b>		
Hazard Group:	Structural failure		
Hazard Description :	Rupture of the rack. In case of hard landing the test rack could break. Causing major injury.		
Hazard Classification :	<b>Catastrophic</b>		
<b>Hazard cause #1:</b>	Under design of the rack		
<b>Hazard control</b>	<b>A</b>	The rack strength is computed according to PFC requirement.	
Verification method	1	Design review by Novespace	Closed (§8)
<b>Hazard control</b>	<b>B</b>	The computation is done following the worst load case (9g load) as other load cases are less detrimental and the strut profiles are symmetric.	
Verification method(s)	1	Design review by several team mates.	Closed (§8)
<b>Hazard cause #2:</b>	Mishap in experimental rack building		
<b>Hazard control</b>	<b>A</b>	Fixation of the structure is performed by mechanics according to manufacturer strut manufacturer and appropriate tools.	
Verification method(s)	1	Structure assembly is cross checked internally	Closed (§8)

<b>HAZARD REPORT #3</b>	
Writer name:	<b>Zeb Jonker</b>
Hazard Group:	Other
Hazard Description:	Subject gets sick during the experiment.

Hazard Classification:		<b>Minor</b>	
<b>Hazard cause #1:</b>	Subject does not make his situation clear to the operators.		
<b>Hazard control</b>	<b>A</b>	Most subjects are experienced flyers and we will train this situation with the subjects on the ground. In experiment 2 the subject has to yell stop and rest against the backboard or kneel. In experiment 1 the subject has to yell stop and stay seated.	
Verification method(s)	1	The role playing training on the ground will be supervised and commented on by the other team members.	Closed
<b>Hazard cause #2:</b>	Operators are too late terminating the experiment once the subject starts to feel sick.		
<b>Hazard control</b>	<b>A</b>	We will train this situation on the ground with a clear task description. Operator 1 sits closest to the rack and will grab a bag for the subject. Operator 2 will shut off the stimulator and comfort the subject.	
Verification method(s)	1	The role playing training on the ground will be supervised and commented on by the other team members.	Closed

HAZARD REPORT #4			
Writer name:	<b>Anne Arntz</b>		
Hazard group:	Injury		
Hazard Description:	The springs or the straps connected to the springs break during loading / while the subject is attached and standing upright. Breaking springs may cause shattering of metal.		
Hazard Classification:	<b>Major</b>		
<b>Hazard cause #1:</b>	Under design of the loading equipment		
<b>Hazard control</b>	<b>A</b>	We will use the exact equipment (straps, springs, hooks) that was used by Ritzmann et al, (2015) during parabolic flights with Novespace.	
Verification method	1	Computations are cross checked between experimenters.	Closed
<b>Hazard control</b>	<b>B</b>	We will design the attachment point of the springs to the baseplate to be similar to the attachment point used by Ritzmann et al, (2015). Calculations will be done to hold a case load of 2.8g.	
Verification method(s)	1	Design review by several team mates.	Closed (\$4.2 system 5.2)
<b>Hazard control</b>	<b>C</b>	The springs are placed into plastic tubes so that, in case the springs 'explode', metal is not flying all over the place and injuring the subject	
Verification method(s)	1	Design review by several team mates.	Closed (\$4.2 system 5.2)

HAZARD REPORT #5	
Writer name:	<b>Daphne van der Putte</b>
Hazard Group:	Other
Hazard Description :	An inability for the subject to evacuate when necessary
Hazard Classification :	<b>Catastrophic</b>
<b>Hazard cause #1:</b>	The setup of experiment 1: the (seat)belts and the helmet in the laying and the sideways position

<b>Hazard control</b>	<b>A</b>	The subjects will be given instructions on how to release themselves from the setup	
Verification method	1	The experimenters will assess if subjects can safely and swiftly release themselves.	Closed
<b>Hazard control</b>	<b>B</b>	The seatbelts used to secure the subject to the chair are quick release	
Verification method	1	Design review by several team mates.	Closed (§8)
<b>Hazard control</b>	<b>C</b>	The mechanism to release the helmet fin are knobs that handle easily	
Verification method	1	Design review by several team mates.	Closed (§8)
<b>Hazard control</b>	<b>D</b>	The seatbelts used to secure the subject to the mattress can be released quickly	
Verification method	1	Design review by several team mates.	Closed
<b>Hazard cause #2:</b>		The setup of experiment 2: the springs and the seatbelts	
<b>Hazard control</b>	<b>A</b>	The subjects will be given instructions on how to release themselves from the setup	
Verification method(s)	1	The experimenters will assess if subjects can safely and swiftly release themselves.	Closed (§9, training)

## 11. Applicable Requirements

Requirements	Yes, No, N/A, pending	If no, provide Req. Exemption Form #
GENE-01: Safety analysis	Yes (§10)	
GENE-02: Non-conformity with requirements	N/A	
GENE-03: Functional tests	Yes	
GENE-04: Supervision of running experiments	Yes	
MECA-01: Emergency landing condition loads	Yes (§8)	
MECA-02: Mechanical safety factor	Yes (§8)	
MECA-03: Primary structure materials	Yes (§8)	
MECA-04: Frangible materials	N/A	
MECA-05: Compliance with mechanical attachment limitations	Yes (§8)	
MECA-06: Restriction applicable to welded assemblies	N/A	
MECA-07: Handling of experiment racks	Yes	
MECA-08: Maximum mass of experiment racks	Yes (§8)	
MECA-09: Stacking of equipment	Yes (§8)	
MECA-10: Securing of removable equipment for take-off and landing	Yes (§8)	
MATE-01: Hazards related to materials and products, and justification of quantities	Yes (§5)	
MATE-02: Double containment of liquids, powders and particles	Yes (§5)	
MATE-03: Allowed products and quantities	Yes (§5)	
MATE-04: Labeling of products	Yes	
MATE-05: Asphyxiating gases	N/A	
MATE-06: Reserved	N/A	
MATE-07: BioSafety Level	N/A	
MATE-08: Blood sampling: protection of test subject	N/A	
MATE-09: Blood sampling: Qualification of operators	N/A	
MATE-10: GMOs: authorization for use	N/A	
MATE-11: Authorized GMO group	N/A	
PRES-01: EC compliance of pressurized systems and components	N/A	
PRES-02: MDP and safety factors determination of the pressurized systems and components	N/A	
RES-03: Protection of pressurized systems from shocks and other mechanical impacts	N/A	
PRES-04: Accessibility of controls of pressurized systems	N/A	
PRES-05: Two-failure tolerance of pressurized systems	N/A	
PRES-06: MDP of a marked component	N/A	
PRES-07: MDP of an unmarked component	N/A	
PRES-08: Cylinders with $\pi$ marking	N/A	
PRES-09: Requalification of cylinders	N/A	
PRES-10: Purchase date of cylinders	N/A	
PRES-11: Storage of cylinders	N/A	
PRES-12: Technical file of non-off-the-shelf chambers	N/A	
PRES-13: Inspection of frangible portholes and walls	N/A	
PRES-14: Protection of frangible portholes and walls	N/A	
HEAT-01: Thermal runaway prevention	N/A	
HEAT-02: Location of temperature measurement means for regulation	N/A	
HEAT-03: Heating and materials compatibility	N/A	
MOBI-01: Limited access to moving parts	N/A	
MOBI-02: Securing of access to moving parts	N/A	
MOBI-03: Integrity of systems containing moving parts	N/A	
FREE-01: Mass of free-floating systems	N/A	

FREE-02: Limitation of deflection of free-floating systems	N/A	
FREE-03: Fall-protection of free-floating systems	N/A	
FREE-04: Shock-protection of free-floating systems	N/A	
ELEC-01: Electrical design of experiments powered from the aircraft	Yes (§7)	
ELEC-02: Accessibility of controls and status indicators	Yes	
ELEC-03: Marking of electrical equipment	N/A	
ELEC-04: Electrical power consumption measurement	Yes (§7)	
ELEC-05: Grounding	Yes (§7)	
BATT-01: Charge of batteries	N/A	
BATT-02: Liquid electrolyte batteries	N/A	
BATT-03: Date of purchase of batteries	N/A	
BATT-04: Battery cut-off and protection device	N/A	
BATT-05: Li-Ion Polymer batteries	N/A	
UPS-01: UPS system	N/A	
UPS-02: Date of purchase of UPSs	N/A	
UPS-03: Indication of operation of an UPS from the battery	N/A	
POWE-01: Protection of power supplies by fuses	N/A	
LASER-01: Design of lasers	No	1
LASER-02: Removal of laser protection covers or opening of access doors	Yes	
LASER-03: Removal of laser protection covers in flight (Class 4 laser)	N/A	
EM-01: Limit values of exposure to electromagnetic fields	N/A	
EM-02: Electromagnetic field protection covers	N/A	
IONI-01: Authorization for use of radioactive sources	N/A	
PUMP-01: Authorized pumps	N/A	
MEDI-01: Authorization to conduct biomedical research on human subjects	Yes	
MEDI-02: Emergency evacuation of experiment subjects	Yes	
ANIM-01: Animal research: legal provisions	N/A	
ANIM-02: Animal research: Containment of animals	N/A	
SERV-01: Loss of aircraft utilities	Yes	
SERV-02: Cabin depressurization	Yes	
SERV-03: Compliance with aircraft interfaces	Yes	
MISC-01: Extreme temperatures	N/A	
MISC-02: Padding of experiment racks	Yes (§6)	
ITF-01: Experiment dimensions vs Aircraft access door dimensions	Yes (§8)	
ITF-02: Experiment installation and performance inside the experiment area only	Yes	
ITF-03: Experiment dimensions Vs. cabin dimensions	Yes	
CAB-01: Total mass of complete experiments limited at 4 t	Yes	
CAB-03: Allowed seat tracks for experiment attachment	Yes	
CAB-05: Aisle width for evacuation	Yes	
CAB-06: EMI interference with aircraft	N/A	
ITF-04: Aircraft rail linear loading limitation	Yes (§8)	
ITF-05: Maximum current limit on power distribution panels	Yes (§6/7)	
ITF-06: Suitable 230 V-AC plug	Yes	
ITF-07: Maximum temperature of products vented through vent line	N/A	
ITF-08: Vent line flow rate	N/A	
ITF-09: Allowed vented products	N/A	
ITF-10: Vent line maximum pressure	N/A	

## APPENDIX A.A – Reference Documents

<b>Document description</b>	<b>Filename</b>
Safety recommendations Porti (page 5-9)	1_Porti_Manual
Paper of Ritzmann et al. (2015) about harness	2_Ritzmann_2015
MSDS NuPrep Skin Prep Gel	MSDS_Nuprep
SDS Spectra360 electrode gel	SDS_Spectra_Electrode_Gel
MSDS Durapore adhesive tape	MSDS_Durapore_Tape
MSDS Lidocaine (Pliaglis cream)	MSDS_Lidocaine
MSDS Tetracaine (Pliaglis cream)	MSDS_Tetracaine
MSDS Loctite	MSDS_Loctite
MSDS Skin cleaning swabs	Msd_s_medi-swab
MSDS Fixomull adhesive tape	MSDS_Fixomull
MSDS EMLA crème	MSDS_EMLA
Calculations backboard structure	Calculations backboard structure updated
Specs laser sensor	technical_specification_optoNCDT_lasersensor
SDS Silica packets	SDS_Silica_Packets

## APPENDIX A.B – Information Related to Ground Activities

### A.B1. Products Used on Ground

Products Used for Ground Operations					
Name of pure products and/or solution <sup>(1)</sup>	Existing MSDS (Yes/No)	IATA class/Division <sup>(2)</sup>	IATA Group <sup>(2)</sup>	Total Quantity	Product containment means
NuPrep Skin Prep Gel (Weaver, Aurora, Colorado)	Yes	Not regulated	n/a	2 tubes	Tube
Spectra 360 electrode gel (Parker Laboratories, Fairfield, NJ)	Yes	Not regulated	n/a	2 tubes	Tube
Carbon rubber electrodes (Uni-Patch, Wabasha, USA)	No			4	Backpack
Self-adhesive Ag/AgCl Ambu Blue Sensor M surface EMG electrodes (Ambu, Ballerup, Denmark)	No			50	Backpack
Adhesive tape (Durapore)	Yes	Not regulated	n/a	4 roll	Backpack
Tissues					Backpack
Pliaglis topical anesthetic cream (Galderma, Lausanne, Switzerland)	No			2 tubes	Tube
Lidocaine	Yes	Not regulated		7%	
Tetracaine	Yes	Not regulated		7%	
EMLA crème, topical anaesthetic	Yes	Not regulated	n/a	1 tube	Tube
Contact lens solution (brand has to be determined)		Not regulated			
Loctite 243	Yes	Not regulated	n/a	1 bottle	Bottle
Skin Cleansing Swabs, saturated with 70% v/v Isopropyl Alcohol (Medi-Swab)	Yes	Not regulated	n/a	4 swabs	Backpack
Fixomull stretch adhesive tape (BSN medical)	Yes	Not regulated	n/a	1 roll	Backback
Elastofix (BSN medical)	No			1 box	Box

(1) If you use solutions based upon the pure chemicals above, please mention them and mention the concentrations

(2) Information available in chapter 14 of MSDS

## A.B2. Ground Auxiliary Procedures

Period 0: preparation of subjects on ground as detailed in Chapter 9

Subject training as explained in Chapter 9

## A.B3. Description of the ground based hardware

### *Description of Ground-Based Experimental Equipment*

We will not use experimental equipment on the ground which is different than the in-flight equipment.

Components	Purpose
...	...

### *Configuration of the Experiment Upon Arrival at Novespace*

...

### *Configuration of the Experiment for Transportation to the Aircraft*

...

### *Configuration of the Experiment Upon Arrival On-Board the Aircraft*

...

## A.B4. Specific Requirements for Ground Operations

...

## APPENDIX A.C – Requirement Exemption Form

<b>Exemption form #:</b>	<b>1</b>
<b>Requirement # :</b>	LASER-01 Design of lasers
<b>Identification of the hardware/system/product/procedure subjected to exemption:</b> OptoNCDT 1401 – 100mm (Micro Epsilon)	
<b>Rationales for exemption acceptance:</b> The laser is attached to our backboard set-up and can only emit its laser beam directing towards the floor (baseplate). The distance from the floor and the laser will maximally be 130mm, making it impossible to stare directly in the laser beam.	
<b>Safety means in place to ensure the experiment safety :</b> In Figure 15, the design of the laser can be seen. The laser has a switch to turn the laser beam on and off. A light on top of the laser box indicates whether the laser is on (red light means laser is off, green light means laser is on). The laser has a warning plate at the cover. To protect people from staring into the laser beam, we made some sort of tent of light blocking. The fabric is spanned at all four sides of the laser.	
	
<p><b>Figure 15:</b> Laser protection tent</p>	
More information about this laser can be found in the attached document 'technical_specification_optoNCDT_lasersensor.pdf'	